Surface modification of mesenchymal stromal cell derived - extracellular vesicles with peptides for targeted cancer therapy

Pedro Espirito Santo Prates Gonçalves

Thesis to obtain the Master of Science Degree in

Biomedical Engineering

Supervisors: Prof. Cláudia Alexandra Martins Lobato da Silva

Dr. Nuno Filipe Santos Bernardes

Examination Committee

Chairperson: Prof. Maria Margarida Fonseca Rodrigues Diogo

Supervisor: Dr. Nuno Filipe Santos Bernardes

Members of the Committee: Prof. Fábio Monteiro Fernandes

October 2022

Declaration

I declare that this document is an original work of my own authorship and that it fulfills all the requirements of the Code of Conduct and Good Practices of the Universidade de Lisboa.

Declaração

Declaro que o presente documento é um trabalho original da minha autoria e que cumpre todos os requisitos do Código de Conduta e Boas Práticas da Universidade de Lisboa.

Acknowledgments

I want to sincerely thank everyone who contributed to this work.

To Doctor Nuno Bernardes, I would like to express my gratitude for his attentive supervision, consistent availability to respond to my questions, and for including me in this project, which I found so interesting. Furthermore, many thanks for the encouragement.

My gratitude also goes to Professor Claudia Lobato da Silva for informing me about this project and for her important orientation.

To Doctor Miguel Fuzeta, I wish to express my appreciation, especially for teaching me so much about this work, and for being willing to help me with any scientific matters.

Additionally, I appreciate everyone in Laboratory 3 for always being in a good mood. And I want to especially thank Marilia, Cristiana, and Teresa for their help, both for guiding me during experiments and for the ideas shared.

To my friends, I would like to thank them for their support and for making the past five years a lot more enjoyable.

Finally, I am deeply grateful to my family, especially my parents for their unconditional support.

Abstract

Conventional systemic cancer therapies are responsible to induce severe side effects. This limits the efficacy of the current therapeutic strategies and this challenge needs to be addressed by novel approaches.

In the last decade, extracellular vesicles (EVs), phospholipid bilayer membrane structures released by all cells, have emerged as promising nano drug delivery systems (NDDS). These display amenability for loading with multiple anticancer therapeutics as well as for engineering aimed to improve their accumulation at the target tissues.

In order to develop an EV-based NDDS for targeted cancer therapy, in this work, EVs derived from mesenchymal stromal cells and MDA-MB-231 derived EVs were isolated through a scalable and selective protocol comprising tangential flow filtration (TFF) and size exclusion chromatography (SEC). Here, the adjustment of upstream and downstream processing such as the cell confluence reached during expansion as well as the MWCO of amicons used for the EV ultrafiltration, were identified to be crucial parameters for increased batch yields.

Moreover, the EVs were decorated with a targeting moiety that includes p28, a peptide that displays a preferential penetration into cancer cells. The anchoring to EVs was achieved through the use of a novel fusion peptide combining p28 with CP05, which anchors itself in the surface of EVs by interacting with CD63. Incubation of breast cancer cells with EVs-p28 led to an increased cell uptake of EVs by 1,4-fold, showing their superiority as a NDDS.

Future work targeting the evaluation of the drug delivery efficiency of this system is important as it will allow a greater understanding of the potential application of the proposed NDDS.

Keywords: extracellular vesicles, mesenchymal stromal cells, p28, anti-cancer therapy, drug delivery systems, scalable production

Resumo

As terapias sistémicas convencionais aplicadas em oncologia podem causar efeitos secundários severos, o que limita gravemente a eficiência dos tratamentos e requer novas abordagens para procurar novas soluções terapêuticas.

Na última década, as vesiculas extracelulares (EVs), estruturas limitadas por membrana, têm emergido como veículos promissores para entrega de fármacos, apresentando não só flexibilidade para serem carregados com agentes anticancerígenos bem como para serem modificados com o objetivo de melhorar a sua acumulação em tecidos alvo.

Neste trabalho, com o intuito de desenvolver um nanossistema baseado em EVs para terapias para o cancro, estas vesículas foram isoladas de células mesenquimais do estroma e de cancro de mama (MDA-MB-231) através de um protocolo escalável e seletivo que inclui filtração tangencial de fluxo e cromatografia de exclusão por tamanho. Demonstra-se que ajustes no processo a montante e a jusante, como nas confluências celulares atingidas durante a expansão, assim como o peso molecular de corte dos amicons usados na ultrafiltração de EVs poderão ser fundamentais para o aumento da produtividade em cada lote.

Adicionalmente, as EVs foram decoradas com o p28, um péptido que apresenta uma penetração preferencial em células cancerígenas. A ancoragem às EVs foi conseguida através do uso de um novo péptido que combina o p28 com o CP05. Este último ancora-se à superfície das EVs através de interações com CD63. A exposição de células de cancro da mama com EVs-p28 levou a um aumento na captação de EVs de 1,4x, mostrando a sua superioridade como veículo dirigido para entrega de fármacos. Assim, futuros estudos que investiguem a eficiência da entrega de fármacos com este sistema serão importantes pois permitirão um melhor entendimento do seu potencial em aplicações terapêuticas.

Palavras-chave: vesiculas extracelulares, células mesenquimais do estroma, p28, terapia anti-cancro, produção escalável

Table of Contents

List of Figures

in each batch. **C)** Quantity of particles produced by each cell, quantified at the final of isolation protocol. MWCO - molecular weight cut off.

Figure 9- Characteristics of MSC-EVs. **A)** Variations in the filtrate flow of the TFF through all the assays performed. **B)** Representative fractionation of the TFF concentrated cell conditioning medium (BM EVs SEC 7). The ultraviolet light of wavelength 280 nm (UV280) (blue line) was measured in the eluent. The fractions of the first peak area contain EVs, whereas smaller constituents of the cell conditioning medium, such as contaminating proteins are contained in later fractions. The y-axis represents the UV280 absorbance in milli-absorbance units and the x-axis represents the volume eluted through the column since the start of the sample elution. **C)** Comparison of the MSC-EV recovery through the various operation units of the EV isolation protocol. **D)** Comparison between the particle-to-protein ratio (PPR) of batch BM EVs SEC 7 and previous work [188] developed with a similar experimental setup (UMC-Utrecht (n=3)). **E)** EV average size and mode of size (n=5, technical replicates). **F)** Representative NTA size distribution curves of MSC-EVs, obtained from BM EVs SEC 7. PPR - particle to protein ratio. TFF- Tangential Flow Filtration. SEC – Size Exclusion Chromatography NTA - Nanoparticle Tracking Analysis. UMC Utrecht - University Medical Center Utrecht.

Figure 10 - EV staining with Alexa Fluor™ 647 NHS Ester. A) Representative fractionation of the labelled EVs (BM EVs SEC 7). The ultraviolet light of wavelength 280 nm (UV280) (blue line) was measured in the eluent. The fractions of the first peak area contain EVs, whereas the second peak signals the fractions where the unbound dye (Alexa Fluor™ 647 NHS Ester) is being eluted. The y-axis represents the UV280 absorbance in milli-absorbance units and the x-axis represents the volume eluted through the column since the start of the sample elution. **B)** Comparison of MSC-EV yields in UF operation unit applied to labelled EVs. **C)** Comparison of the emission spectra of labelled MSC-EVs (excitation Wavelength of 620 nm) of the different batches of MSC-EVs.

Figure 11 - Design of the EV anchoring conjugated peptide CP05-p28. A) A diagram depicting the surface modification of EVs with a CP05-p28. A peptide sequence (CP05) that anchors to CD63 on the EV surface, a $(GGGGS)_2$ linker, a Myc-tag reporter, and the p28 peptide (i.e., the 28 amino acid sequence Leu50-Asp77 from the protein azurin) comprise the final peptide design. From de Almeida Fuzeta M. et al. (2021) [188]. **B)** Description of the sequences that are present in the design of CP05-p28. The sequences of the peptides are presented from the N-terminal (left) to the C-terminal (right).

Figure 12 - Detection of CP05-p28 and functionalization of EVs with CP05-p28. A) Detection of CP05-p28 conjugation peptide through Myc-tag immunodetection in a dot blot. The peptide was loaded into the dot blot apparatus at different quantities, 10, 5, 2, 1, and 0.3 µg. PBS was utilized as a negative control and an already developed fusion protein, R2-C1C2, containing the same Myc-tag was used as a positive control. An equivalent amount of peptide molecules of R2-C1C2 as 0.3 µg of CP05-p28 conjugated peptide was loaded into the dot blot apparatus. The R2-C1C2 was generously provided by Sander Kooijmans (UMC Utrecht). **B)** Relative percentage of the signal intensity generated by the peptides loaded onto the dot blotting apparatus, considering the signal generated by R2-C1C2 as 100%. **C)** Scheme of the workflow employed for the labelling of each batch of EVs, as well as its functionalization and usage into assays of cell uptake. **D)** Emission spectrum (excitation wavelength of 620 nm) of functionalized and non-functionalized EVs. **i)** Batch where labelled functionalized and non-functionalized EVs did not display significant fluorescence in comparison with the negative control, PBS. **ii)** Batch where labelled, functionalized and non-functionalized, EVs displayed significant fluorescence in comparison with the negative control, PBS.

Figure 13 - Decoration of MSC-EVs with CP05-p28 increased the uptake of EVs by triple negative and metastatic breast cancer cells, MDA-MB-231. **A) i)** Flow Cytometry analysis of the EV uptake by breast cancer cells, where EVs functionalized with CP05-p28 display an increase in the EV uptake into cells, the x-axis represents the EV florescence height and the y-axis represents the side scatter (n= 2 technical replicates). **ii)** median fluorescence intensity (MFI) of flow cytometry (n= 2 technical replicates). **iii)** Relative EV uptake based on the MFI values. (n= 2 technical replicates). **iv)** Comparison between

the quantity of EVs administered to breast cancer cells and their fluorescence intensity, in the different conditions tested, i.e. non-functionalized EVs (EVs) and CP05-p28 conjugation peptide-functionalized EVs (EVs-p28). **C)** Comparison between the Median fluorescence intensity (MFI) of flow cytometry when EVs are administered in different dosages to breast cancer cells (n=1, EVs-p28, low dose, and n=2 technical replicates, EVs-p28, high dose). MFI - median intensity fluorescence.

Figure 14- Production of MDA-MB-231 derived EVs and their characteristics. **A)** Number of TFF, SEC, and UF isolated particles per T-175 culture flask. **B)** Quantity of particles produced by each cell, quantified after CM was processed through TFF, SEC, and ultrafiltrated in amicons ultra centrifugal units. **C)** Comparison between batches considering the number of cells per T-culture flask at the end of the conditioning period, the size of each batch, i.e., the number of T-Flasks (20 mL of cell culture medium each), the total number of particles isolated through TFF, SEC and UF, and the MWCO of the amicons ultra centrifugal units used in UF of each batch. **D)** NTA size distribution curves of MDA-MB-231 derived EVs. **E)** Average size and mode of the size of MDA-MB-231 derived EVs.. **F)** Comparison between the quantity of EVs obtained in MDA EVs SEC 1, produced in DMEM, MDA EVs SEC 3, OptiMEM, produced in OptiMEM, and OptiMEM that was processed through the whole isolation protocol, i.e., TFF, SEC, and UF in amicon ultracentrifugal units.TFF- Tangential Flow Filtration. SEC - Size Exclusion Chromatography. UF - Ultrafiltration MWCO - molecular weight cut off. NTA - Nanoparticle Tracking Analysis.

Figure 15 - **EV staining with Alexa Fluor™ 647 NHS Ester. A)** Comparison of EV yields in UF operation unit performed for stained MDA-MB-231 derived EVs. **B)** Comparison between the emission spectra (excitation wavelength of 620 nm) of the different batches of MDA-MB-231 derived EVs. **C)** Representative emission spectrum (excitation wavelength of 620 nm) of a batch where labelled functionalized and non-functionalized EVs did not display significant fluorescence in comparison with the negative control, PBS.

Figure 16 - **Uptake assay with CP05-p28 functionalized MDA-MB-231 derived EVs**. **A)** Representative flow cytometry analysis of the MDA-MB-231 derived EV uptake by breast cancer cells, MDA-MB-231. The x-axis represents the EV florescence height, and the y-axis represents the side scatter. **B)** Median fluorescence intensity (MFI) of flow cytometry measurements. (n=2 technical replicates for no EVs, and n=1 for EVs and EVs-p28). MFI - Median Fluorescence Intensity.

Figure 17 – Suggestions for future studies A) Suggestions on how to navigate the EV manipulation protocols according to the quantity of EVs isolated and the fluorescence of EVs in each batch. The quantity of EVs suggested is aimed for the performance of assay uptakes comprising one technical replicate in each condition, i.e., functionalized, and non-functionalized EVs, with approximately $2x10^9$ EVs. **B)** Contrast of the MWCO of amicon ultra centrifugal units necessary for EV UF at the different stages of the study. The “After” column comprises the suggestions made for future work following a similar workflow.

Figure 18 - Important aspects for the translation of extracellular vesicle (EV) - based therapies into clinical settings.

List of Tables

List of Acronyms

A/A	Antibiotic-Antimycotic
ACE2	Angiotensin Converting Enzyme 2
AFM	Atomic Force Micros
AKT	Protein Kinase B
Alix	ALG-2-interacting protein X
ALS	Amyotrophic Lateral Sclerosis
ALS	Amyotrophic Lateral Sclerosis
AT	Adipose Tissue
BBB	Blood Brain Barrier
BCA	Bicinchoninic Acid
BM	Bone Marrow
BSA	Bovine Serum Albumin
CD	Cluster of Differentiation
CDK2	Cyclin Dependent Kinase 2
CM	Conditioned Medium
CMV	Cytomegalovirus
CNS	Central Nervous System
Cop1	Constitutional Morphogenic Protein 1
COVID-19	Coronavirus Disease-19
COX-2	Cyclooxygenase-2
CRISPR	Clustered Regularly Interspaced Short Palindromic Repeats
CROSS-FIRE	CRISPR Operated Stoplight System for Functional Intercellular RNA Exchange
DC	Dendritic Cells
DLS	Dynamic Light Scattering
DMEM	Dulbecco's Modified Eagle Medium
DMSO	Dimethyl Sulfoxide
EBV	Epstein-Barr Virus
ECM	Extracellular Matrix
EDTA	Ethylenediaminetetraacetic Acid
EGF(R)	Epidermal Growth Factor (Receptor)
ESCRT	Endosomal Sorting Complex Required for Transport
EV	Extracellular Vesicle
EVs-p28	Extracellular Vesicles Functionalized with p28
FACS	fluorescence activated cell sorting
FAK	Focal Adhesion Kinase
FasL	Fas Ligand

FBS	Fetal Bovine Serum
FDA	Food and Drug Administration
FoxM1	Forkhead Box M1 protein
GM-1	Gangliosidosis-1
GMP	Good Manufacturing Practice
GPI	glycosylphosphatidylinositol
GTPases	Guanosine Triphosphatase
GvHD	Graft Versus Host Disease
HAV	Hepatovirus A
HBV	Hepatovirus B
HCV	Hepatovirus C
HEK	Human embryonic kidney
HER2	Human Epidermal Growth Factor receptor 2
HIV-1	Human Immunodeficiency Virus 1
HLA-DR	Human Leukocyte Antigen – DR isotype
hpL	Human Platelet Lysate
HRS	Hepatocyte Growth Factor-Regulated Tyrosine Kinase Substrate
ICG	Indocyanine Green
IL	Interleukin
ILV	Intraluminal Vesicle(s)
ISCT	International Society of Cellular Therapies
kRasG12D	Kirsten Rat Sarcoma Virus
Lamp2b	Lysosome-Associated Membrane Protein
LDL	Low Density Lipoprotein
mAu	milli-absorbance unit
MFI	Median Fluorescence Intensity
MHC	Major Histocompatibility Complex
miRNA	micro RNA
MISEV 2018	Minimal Information for Studies of Extracellular Vesicles 2018
MMP2	Matrix-Metalloproteinase-2
mRNA	messenger RNA
MSC	Mesenchymal Stromal Cells
MSC-EVs	Mesenchymal Stromal Cell derived Extracellular Vesicles
mTOR	Mechanistic Target Of Rapamycin Kinase
MV	Microvesicle
MVB	Multivesicular Body
MVE	Multivesicular Endosome
MW	Molecular Weight
MWCO	Molecular Weight Cut-Off
NDDS	Nano Drug Delivery System

Nrf2	Nuclear Factor Erythroid 2 – Related Ractor 2
NTA	Nanoparticle Tracking Analysis
OA	Osteoarthritis
PB	Peripheral Blood
PBS	Phosphate-buffered saline
PD-L1	Programmed Death-Ligand 1
PE	Phosphatidylinositol
PEG	Polyethylene Glycol
PEG	Polyethylene Glycol
PGLA	Poly Lactic-co-Glycolic Acid
PI3K	Phosphoinositide 3-Kinase
PPR	Protein to Particle Analysis
PrP	Prion Protein
PS	Phosphatidylserine
PS	Phosphatidylserine
Rab	Ras-associated binding
RGV	Rabies Viral Glycoprotein
RIPA	radioimmunoprecipitation assay
RT	Room Temperature
S/X-F	Serum/Xenogeneic-Free
SCERG	Stem Cell Engineering Research Group
SEC	Size Exclusion Chromatography
SEC	Size Exclusion Chromatography
siRNA	Small Iterfering RNA
SNARE	Soluble-N-ethylmaleimide- Sensitive Fusion Attachment Protein Receptor
TBS	tris-buffered saline
TEM	Transmission Electron Microscopy
TFF	Tangential Flow Cytometry
TGF-β1	Transforming Growth Factor Beta 1
TSG101	Tumor Susceptibility Gene 101
UF	Ultrafiltration
UMC Utrecht	University Medical Center Utrecht
UV280	Ultraviolet light of wavelength 280 nm
VEGFR	Vascular Endothelial Growth Factor
WJ	Wharton's Jelly

1. Introduction

1.1. Cancer

Cancer is a generic term created to describe a family of more than two hundred pathologies that can occur in any part of the human body [1]. The process that leads to tumorigenesis, *i.e.*, the formation of a tumor, is the sequential accumulation of genetic mutations in genes that regulate cell growth. These mutations result in a loss of function in the tumor suppressor genes and/or a gain of function in oncogenes [1]. In addition, epigenetic alterations also play a role in the transformation of normal cells into their cancerous derivatives [1]. These processes lead to the disruption of normal cell physiology and allow the arise of malignant characteristics such as uncontrollable cell growth and invasion of adjacent and distant tissues in a phenomenon called metastasis, which is the primary cause of death by cancer [2].

The alterations in cell physiology that dictate malignant growth were summarized by Hanahan, D. and R.A. Weinberg. These are self-sufficiency in growth signals, insensitivity to anti-growth signals, tissue invasion, and metastasis, limitless replicative potential, sustained angiogenesis, evading apoptosis, and self-sufficiency in growth signals [3]. Later the addition of two cancer hallmarks, the deregulated cellular energetics and avoidance of immune destruction, and two enabling characteristics, genome instability, and mutation as well as the tumor-promoting inflammation were added to complete the cancer hallmark list [4]. And finally, a recent update annexed two novel hallmark capabilities, phenotypic plasticity and disrupted differentiation, as well as two enabling characteristics, polymorphic microbiomes and nonmutational epigenetic reprograming to the list [5]. This provides a valuable theoretical framework to understand cancer and for the creation of therapeutic options that to be effective should aim to target these characteristics.

There are many people affected by this pathology. In 2020, 18,1 M cancer cases and almost 10 M deaths caused by cancer were reported, making this disease the second leading cause of death worldwide [2]. These numbers reflect the harsh reality that the treatment of malignancies still is, and has always been, considered one of the most arduous challenges faced by the scientific community [6] despite the long decades that it has been investigated.

Surgery, radiotherapy, and chemotherapy are still the main conventional treatments. However, they are characterized by a lack of selectivity, which can lead to significant side effects [7], [8]. It is, thus, mandatory to develop more effective strategies to reduce the lethality of cancer as well as to reduce the major side effects that can completely disrupt the wellbeing of patients undergoing cancer treatment.

Through the encapsulation of chemotherapeutic drugs into nano drug delivery systems (NDDS), these can reduce non-specific delivery, preventing the major side effects [9] associated with the low selectivity of free drugs. Extracellular vesicles are signalosomes that play a major role in cell-to-cell communication being capable of triggering phenotypical responses in cells through the delivery of their cargo. As such, EVs constitute a promising option to be used as NDDS, presenting a high biocompatible and low immunogenicity since they occur naturally in the organism [10]. Additionally, a substantial flexibility is

added by their surface engineering through various methods, as well as encapsulation of cargoes, such as chemical and biological cancer therapeutics. Finally, an efficient crossing of biological barriers such as cellular membranes is also an hallmark of EVs [11], [12].

1.2. Extracelular Vesicles (EV)

1.2.1. EV biology

Extracellular vesicles (EVs) are spherical entities covered by a phospholipid bilayer that are released by cells across all three domains of life, archaea, bacteria, and eukarya [13]. Their discovery dates back to 1946 when they were identified as procoagulant particles in the plasma [14], which was followed by their classification as platelet dust in 1967 [15]. With time, these entities became known as EVs, and in 1996, a paradigm-shifting study revealed that EVs displayed antigen-presenting capabilities. REFERENCE

EVs are mediators of intercellular communication, being vehicles capable of both close-range communication, in a paracrine manner, and long-range communication. Having this fundamental mission of being signalosomes, EVs trigger phenotypic responses in their receiver cells as they deliver the messages delegated to them by their parent cells. These delegated messages assume the form of enriched molecules present in EVs' membrane and their lumen. Relative to their lumen, EVs can carry various biomolecules such as proteins, lipids, and most surprisingly nucleic acids [16] (Figure 1), including mRNAs and small-noncoding RNAs, and mainly microRNAs that when efficiently delivered to recipient cells trigger functional responses [17]. Anchored to their membrane, EVs carry molecules such as proteins, glycans, and lipids, some of them being more enriched in EVs than in the plasma membrane of cells, such as cholesterol phosphatidylserine, glycosphingolipids, sphingomyelin, and unsaturated lipids [9] (Figure 1). These groups of molecules can act in cellular uptake and/or elicit the trigger of signaling pathways through surface interactions with the recipient cells [18], [19].

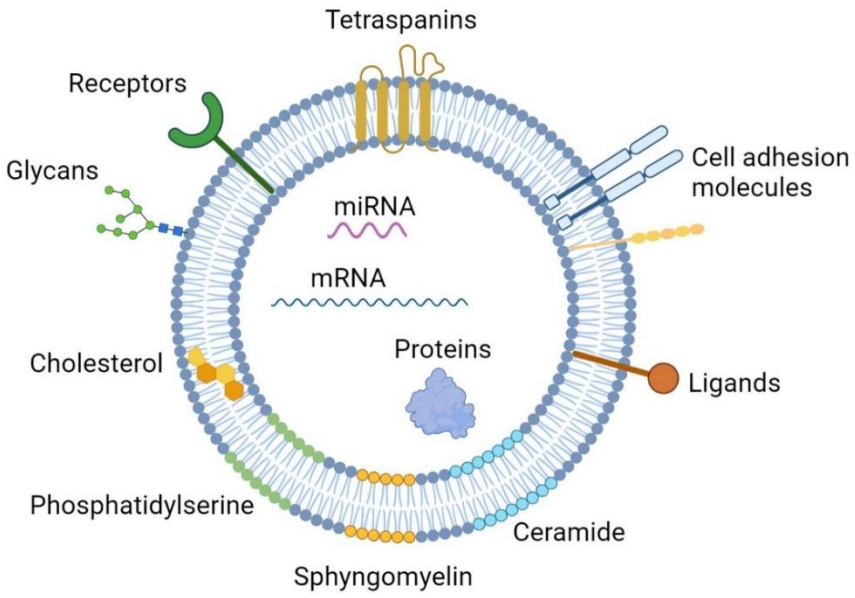

Figure 1 – Schematic representation of the composition of an EV. EVs are phospholipid-bound spherical structures enclosing a portion of the cytoplasm of their cell of origin. Such structures carry cargoes in their lumen or in their limiting membrane. These include proteins such as tetraspanins that

are involved in cellular uptake and adhesion and integrins that also participate in cellular adhesion. Besides, EVs can also carry lipids, namely cholesterol, phosphatidylserine, and ceramide, glycans, which are involved in cellular uptake, as well as other ligands and cell-specific receptors that are involved in cell-specific responses. Additionally, nucleic acids such as miRNA and mRNA can also be transported in EV lumen.

EVs comprise a heterogenous population, where different subpopulations are distinguished based on their mechanism of biogenesis. The most prevalent EV subpopulations are exosomes, microvesicles (MV), also called ectosomes, and apoptotic bodies. Exosomes are small EVs, with 50 nm - 150 nm in size [20], which are characterized by specific markers, such as CD63, CD81, CD9, TSG101, and Alix [21], and the mechanism through which their genesis stems is the endocytic pathway [22]. Microvesicles are a group of EVs characterized by having 100 -1000 nm in size [20], and by being formed through direct budding with the cellular membrane. Their specific markers encompass matrix-metalloproteinase-2 (MMP2) [21] and CD40 [23]. The third category of EVs are the apoptotic bodies, which are cellular debris with sizes of 500 - 2000 nm that are being cleared out of the system [23], formed when the cells undergo apoptosis and can have as their cargo cell organelles, for instance. However, their surface markers remain unknown.

As possible to observe exosomes and microvesicles present an overlapping interval of sizes, and additionally, other properties such as their density and molecular composition are also overlapped [24]. This is a well-documented problem that prevents the attribution of specific functional roles to sub-populations of EVs and needs further research.

1.2.2. Biogenesis, cargo sorting, and release of EVs

As mentioned before each of the identified sub-populations of EVs undergoes a different biogenic pathway. Exosome formation follows the endocytic pathway, where an early endosome matures and gives rise to a mature endosome. Through the maturation of an endosome inward budding of intraluminal vesicles (ILV) occurs at the limiting membrane [25], giving rise to a multivesicular endosome (MVE), also called a multivesicular body (MVB) [26] which can then either undergo the lysosomal pathway, where the MVB fuses with a lysosome or it can also fuse with an autophagosome, both leading to the degradation of ILVs [20] (Figure 2). Additionally, the MVB can fuse with the cell plasma membrane releasing the ILVs into the extracellular space, where they will start to be called exosomes [20] (Figure 2). Post-translational modifications, such as ISGylation of membrane proteins of the MVB, such as TSG101 and HRS as well as MVB pH are some of the factors recognized to have an impact on the fate of MVB [27]–[30]. However, the mechanisms that determine the route to be followed by the MVB are not yet fully understood

In exosome biogenesis the endosomal sorting complex required for transport (ESCRT) that consists of four protein complexes, ESCRT-0,-I,-II,-III, and associated proteins (VPS4, VTA1, ALIX) [31] is the cellular machinery that orchestrates the formation of exosomes in a stepwise manner [20]. Initially, ESCRT-0, comprised of HRS and ESCRT-I, containing the tumor susceptibility protein 101 (TSG101) cluster ubiquitylated transmembrane cargoes, proteins, and lipids, in the MVB limiting membrane forming discrete membrane microdomains [31]. Afterward, ESCRT-I will recruit ESCRT-III mediated by

ESCRT-II, which will finally induce budding at the MVB membrane and fission towards the lumen of MVBs [31].

Exosome biogenesis can also occur in an ESCRT - independent manner [20]. Although ESCRT-III is indispensable for membrane fission, the mechanisms involved in cargo clustering and membrane budding are not necessarily ESCRT-dependent. For this synthenin is required as well as the ESCRT accessory protein ALG-2 interacting protein (ALIX) that will bridge the exosome cargoes to the ESCRT-III [32]. In addition, a certain lipid, ceramide, which is formed by the hydrolysis of sphingomyelin into ceramide through neutral sphingomyelinase can impose a curvature in lipid raft microdomains of the endosomal membrane, ultimately leading to the formation of ILVs [33]. Furthermore, ILVs loaded with CD63 are still formed after depletion of ESCRT [34], showing the role of this tetraspanin in exosome biogenesis. And other proteins of the tetraspanin family (CD9 and CD81) [35] can also be involved in the ESCRT-independent biogenesis of exosomes, through the formation of membrane microdomains and inducement of MVB membrane budding.

Next, if the degenerative route is not followed, the MVB is transported along microtubules until reaching the plasma membrane where it will undergo docking and fusion mediated by GTPases, such as Rab27a and Rab27b, Rab35, actin, and SNARE (soluble-N-ethylmaleimide- sensitive fusion attachment protein receptor) proteins [20], [36]–[38].

On the other hand, MV formation consists of the outward budding at the level of the plasma membrane of the cell, where fission must happen [39] (Figure 2). In this process, some of the mechanisms overlap with the ones needed for exosome formation such as the formation of membrane microdomains. The role of ceramide and of the ESCRT machinery is also maintained in MV genesis with the alteration that in this case, it acts in the plasma membrane instead of the MVB limiting membrane [20]. However, in MV genesis there are nuances comprised by rearrangements of the cellular membrane, specifically of protein and lipids, for instance, the exposition of phosphatidylserine (PS) and phosphatidylinositol (PE) from the inner leaflet to the outward leaflet, causes physical bending at the level of the plasma membrane, which favors membrane budding [20]. This is a process that is regulated by Ca^{2+}-dependent enzymes, namely aminophospholipid translocases, scramblases, and calpain.

Cargo Sorting

Cargoes are the first regulators of EV formation [20], and the ESCRT subunits are also involved in its recruitment. Moreover, it is known that the exosomal cargoes can be sorted into endosomes through the Golgi apparatus or be internalized at the level of the plasma membrane [20]. These processes are regulated through multiple Rab GTPases [20]. And there is a regulatory pathway involving syndecan and synthenin, that in conjunction with ALIX helps the segregation of signaling cargoes to EVs as well as it helps the biogenesis of ILVs [32]. MicroRNA, however, is sorted into exosomes differently, being regulated by the presence of specific motifs in these molecules, suggesting that microRNAs are sorted into exosomes in a regulated manner [20]. The mechanisms involved in this process are still not completely identified. Possible candidates that can sequester RNA cargoes are for instance ESCRT-II sub-complexes, and tetraspanin-enriched microdomains [40]. A technique that may be suitable to shed light on the key players of EV cargo sorting is proximity labelling. Recently, a CD63 fused APEX was

explored to investigate exosome cargo and this approach may also provide insight into the proteins involved in important intracellular exosome processes, namely in cargo sorting [41].

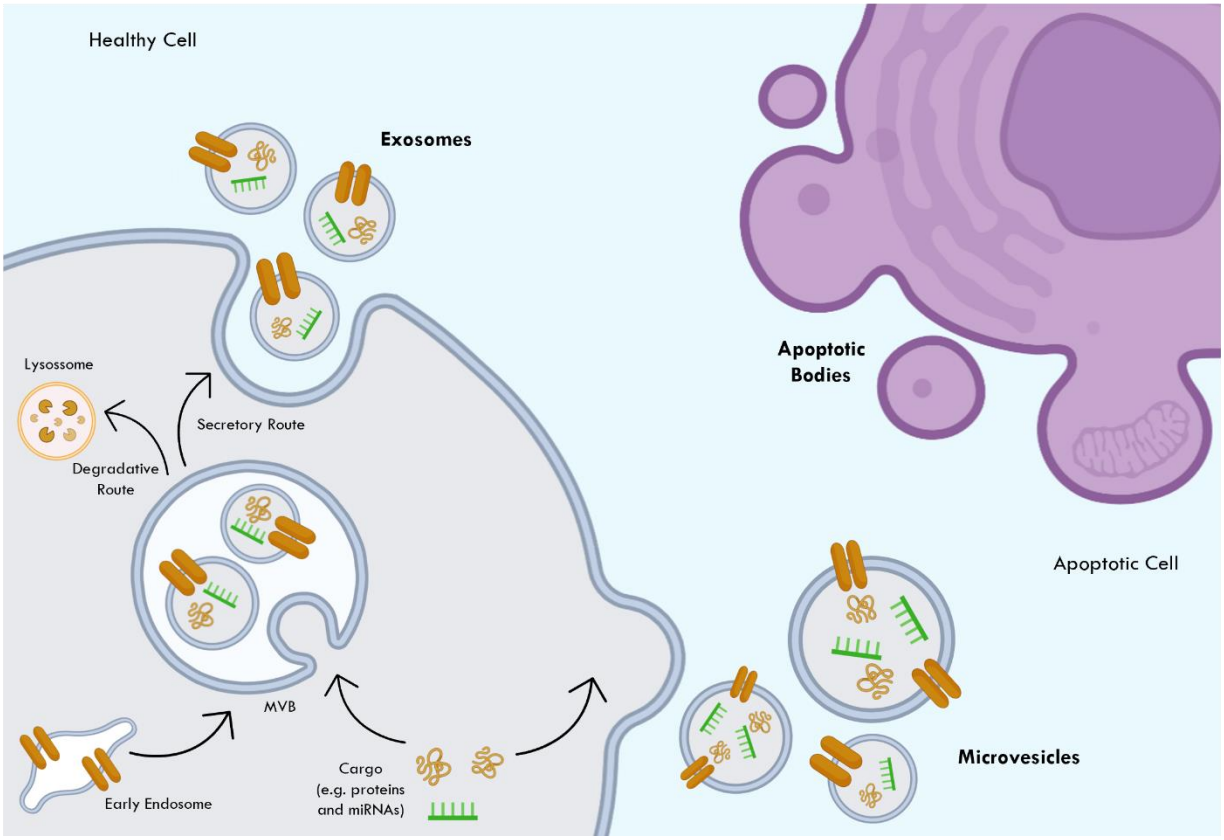

Figure 2 - **Main subpopulations of EVs**. Exosomes are generated through the endocytic pathway, where an early endosome matures into late endosomes that will suffer inward budding of intraluminal vesicles forming the multivesicular body, which upon fusion with the cellular membrane releases exosomes into the extracellular space. In contrast, microvesicles are formed through the outward budding of the plasma membrane. And apoptotic bodies formation happens through the bleeding of the plasma membrane.

1.2.3. Uptake of EVs by recipient cells

Once in the extracellular space, EVs can be targeted to recipient cells either at a close or long distance [42], where they may release their cargo and trigger functional responses and phenotypic changes in the cell or simply activate cell signaling pathways through surface interactions.

Firstly, EV binding to the plasma membrane of recipient cells occurs mediated by the interaction of specific molecules enriched in the surface of EVs such as integrins [43], tetraspanins, lectins [44], bioactive lipids, and heparan sulfate proteoglycans with receptors present in the cell membrane of the recipient cell [20]. This binding can lead to the internalization of EVs or to the trigger of a signaling pathway that promotes functional changes in the cell, even without the transfer of cargo [20]. Additionally, extracellular matrix (ECM) proteins, such as fibronectins and laminin, also play an important role in the binding of EVs to recipient cells [20], [45].

Internalization of EVs can happen through the endocytic pathway by several mechanisms, that seem to be undergone by EVs depending on proteins and glycoprotein present at their surface and on the surface of recipient cells [46]. One of the mechanisms of uptake happens in a clathrin-dependent manner (Figure 3). Here, firstly the essential components to the formation of the clathrin pit are assembled, which include clathrin itself [47]. This will induce curvature in the membrane and will lead to the internalization of EVs localized in that domain [47]. After the fission of the formed vesicle, the clathrin will finally be uncoated from the internalized vesicle [47]. On the other hand, EV endocytosis can also be clathrin-independent [46]. It can be caveolin-mediated (Figure 3), where invaginations in the plasma membrane enriched in caveolins, cholesterol, and sphingolipids are formed, called caveolae [46]. EVs localized in this membrane microdomain will be internalized upon pinching off of this invagination. Endocytosis mediated through lipid rafts can also happen (Figure 3). These membrane microdomains are characterized by the presence of higher levels of cholesterol and sphingolipids in comparison to normal membrane sites, and they are more densely packed floating freely in the membrane bilayer. Less specific endocytic routes also occur such as phagocytosis and macropinocytosis [46] (Figure 3). Phagocytosis consists of invaginations surrounding the extracellular material to be internalized. And macropinocytosis consists of the internalization of EVs through the formation of membrane protrusions surrounding extracellular liquid that fuse back with the cell internalizing the extracellular material [46], [48].

When EVs are internalized through the endocytic pathway they will end up in an MVB and one of three paths can be followed (Figure 3). Firstly, the MVB can fuse with lysosomes or autophagosomes and be degraded [20]. And the proteins and lipids degraded will then provide metabolites to the recipient cell. Alternatively, EVs contained in the MVB can escape through back fusion with the MVB limiting membrane releasing their cargo in the cytoplasm and possibly eliciting functional changes in the cell. This is a crucial route when it comes to the delivery of EVs cargo to cells, which appears to be associated with an acidic pH of the MVB however the factors that influence the fate of MVB are yet poorly understood [49]. Thirdly, another route that avoids EV degradation is the fusion of MVBs with the plasma membrane of the cell, recycling the EV into the extracellular space [20].

Additionally, EVs can fuse with the plasma membrane of recipient cells and release their cargo into the cytoplasm of the cell [20], [46] (Figure 3). Of note, is that this mechanism permits the distribution of transmembrane molecules present in EVs into the cell membrane of the cell. The determination of which routes of uptake result in higher functional delivery levels is of great benefit for the successful development of EVs as therapeutics because it will permit the steering of EVs towards those uptake routes.

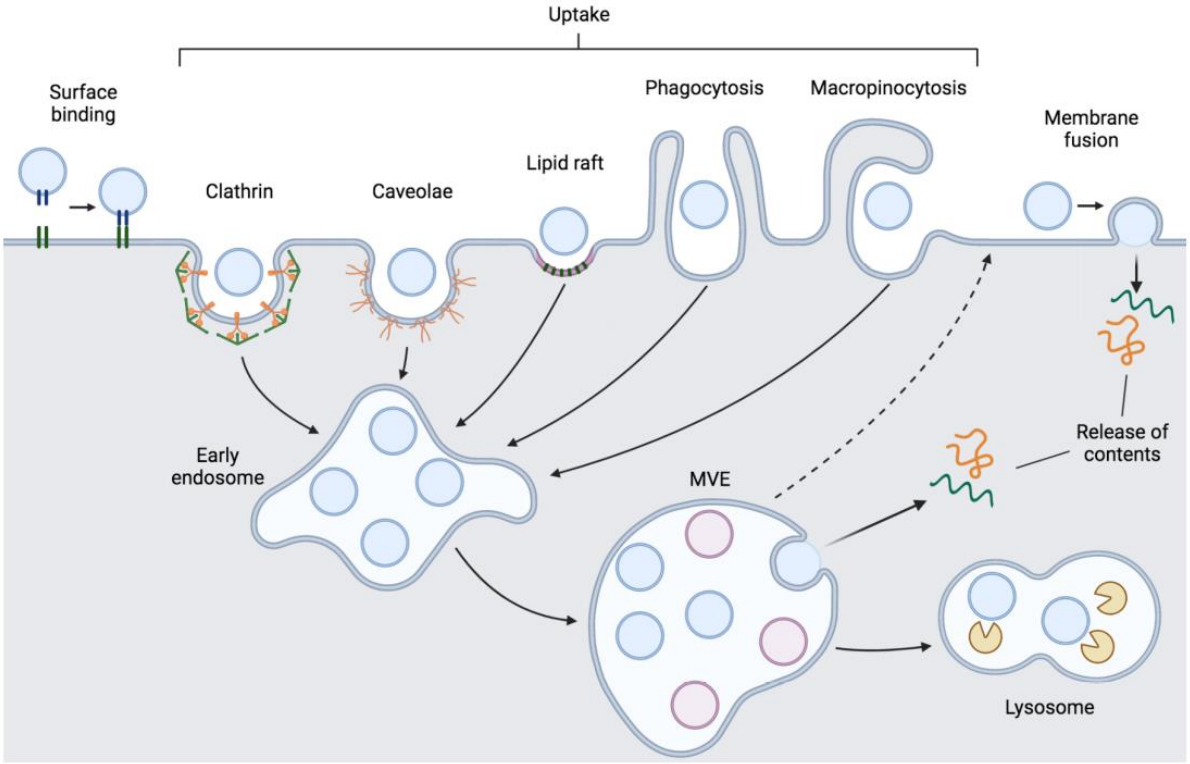

Figure 3 - Interaction of EVs with recipient cells. EVs can trigger intercellular signaling pathways without entering the recipient cell through binding to the surface of these cells in a process that can be mediated by various molecules, for example, it can consist of ligand-receptor interaction. EVs can also penetrate into cells. This can occur in various manners, which include clathrin-mediated endocytosis and caveolin-mediated endocytosis, endocytosis mediated by lipid rafts, phagocytosis, and macropinocytosis. Once internalized EVs will end in the lumen of MVBs, where they can fuse back with the limiting membrane of the MVB and release their cargo into the cytoplasm of recipient cells, possibly triggering a functional response. Moreover, MVB containing the internalized EVs can fuse with lysosomes in which case the EVs will be degraded. Alternatively, the MVB can travel back to the cellular membrane leading to the recycling of EVs into the extracellular space. Another possible route to deliver EV cargo is comprised of the direct fusion of EVs with the plasma membrane of the recipient cell. MVB multivesicular bodies. From de Almeida Fuzeta, M. (2022) [50].

1.2.4. Physiological role of EVs

EVs play a role in several physiological processes in a pleiotropic manner, being crucial for the maintenance of a homeostatic state. [51]. For example, the increase in the load of immune cell-derived EVs that occurs in patients with a wide range of infectious and inflammatory pathologies is postulated to possibly constitute a way to restore homeostasis [52]. Overall, the immune cell-derived EVs participate both in the innate and adaptive immune systems, being involved in immune suppressive mechanisms and immune stimulatory pathways [52].

The discovery of the physiological functions that EVs partake in has its beginning in a groundbreaking study by Raposo et al., 1996, where it was demonstrated that B cells infected with the Epstein-Barr Virus (EBV), release EVs that can induce T cell proliferation and antigen-specific responses [53]. Moreover, dendritic cells (DC) were discovered to secrete EVs containing major histocompatibility complexes II that can stimulate naive CD4+ T cells [54]. And T cells are known to be able to transfer EVs containing miRNA to antigen-presenting cells (APC), regulating the expression levels of those RNAs. Additionally, in immune suppression, T cells can induce DC apoptosis through FASL. And EVs derived from immature

DC cells that carry IL-10 and TGF-Beta1 can reduce inflammation levels by inhibiting T-cell proliferation [55].

The involvement of EVs in functions associated with other organismal systems is also described. Platelet-derived EVs play an important role in the circulatory system being involved in blood coagulation [56], [57]. In the renal system, urinary exosomes transporting aquaporin-2 molecules are involved in fluid balance control [58]. And in the cardiac system, endothelial cell-derived EVs carrying multiple miRNAs can have an atheroprotective role [59]. Considering the nervous system EVs are crucial for CNS development, contributing in functions such as maintenance of synapses, and the development of the CNS. In fact, EVs carrying the Sonic HedgeHog molecule, which is known to play a role in Sonic hedgehog signaling which regulates cortical development, contribute to the lateralization of the central nervous system (CNS) in mouse embryos [60]. EVs are also important vehicles of communication across the blood brain barrier (BBB) [52]. Shawn cell-derived EVs are involved in axon regeneration in the peripheral nervous system [61]. Besides, bacteria-derived EVs in the gut can maintain the integrity of the intestinal epithelium and its paracellular permeability through the regulation of the tight junctions, being important to prevent inflammatory and metabolic diseases. [62], [63]. In the reproductive system, sperm fusion to the egg, in mice, is dependent upon the secretion of unfertilized egg-derived EVs in a CD9-dependent manner and on the interaction of these EVs with the sperm [64]. In addition, sperm motility is also highly impacted by the stimulation of prostate gland-derived EVs, prostatosomes [65]. Moreover, in the musculoskeletal system, one of the most abundant microRNAs in muscle-derived EVs is miR-206 which is involved in the development and differentiation of tissue, especially after injury [66] and this payload in EVs derived from myogenic progenitor cells may modulate the expression of muscle extracellular matrix collagen [67].

1.2.5. Pathological role of EVs

When there is a disruption in the cellular communication that sustains the homeostatic state of an organism, including the trafficking routes associated with EVs certain systems can fall into a state of disease. In such situations, cargo (being luminal or transmembranar) and oftentimes a certain group of other EV characteristics can be altered. There is a kind of chicken and the egg conundrum concerning the role of EVs in pathology, where in certain conditions it is not certain if EVs are the ones that trigger the pathological processes and environments along their trafficking pathways, or if EVs are neutral entities merely being a byproduct of the environment they are inserted in.

In the immune system, EVs are associated with autoimmune and inflammatory diseases, such as type 1 and 2 diabetes, multiple sclerosis, and transplant rejection depending on the cargo of such immune cell-derived EVs and their cell of origin [52]. Moreover, EVs also play a role in neurodegenerative diseases, such as Parkinson's, Alzheimer's, and amyotrophic lateral sclerosis (ALS), Here EVs act as a shuttle of misfolded proteins which leads to pathogenicity, in the case of Parkinson transferring α-synuclein, and in Alzheimer’s β-amyloid proteins, whereas in ALS EVs transfer superoxidase dismutase 1 [68], [69]. In addition, EVs can also transfer prion protein (PrP) abnormal isoform, in cases of prion disease. However, there is counterevidence for such an effect where EVs are described as helping in the clearance of such pathological proteins [70].

EVs released from cardiovascular system-related cells such as cardiomyocytes, fibroblasts, and smooth muscle cells, to name a few can be involved in pathological processes in this system. Studies indicate that these EVs and their microRNA cargoes are involved in inflammation and coagulative reactions contributing to the development of atherosclerosis [71]. In addition, EVs mediate the cross-talk between cardiomyocytes and fibroblasts, being able to lead to situations of heart hypertrophy [72], in such cases a known microRNA EV cargo that plays a role in this phenomenon is the miR-21-3p [73]. Moreover, the transfer of genetic material from viruses, such as HIV-1, EBV [70], and influenza [75] from infected to uninfected cells can be mediated through EVs, and exosomes may be involved in the promotion of infection of the virus COVID-19 [76], having COVID-19 virus receptors, CD9 and ACE2, that may be associated with the spread of this virus.

In tumors, cancer-derived EVs are deeply involved in cancer pathophysiology because they are involved in communication routes with other tumorous cells and non-tumorous cells in the microenvironment, such as immune cells, fibroblasts, and endothelial cells amongst others, which leads to an overall microenvironment modulation that ends up supporting tumor growth [4]. A few examples of said processes are the capability of glioblastoma-derived EVs to stimulate endothelial sprouting enhancing angiogenesis [77], a hallmark of cancer. Additionally, it was demonstrated in several reports such as one concerning gastric cancer patients that tumor-derived EVs can lead to the induction of regulatory T cells, modulating immune surveillance [78]. EVs are also related to the establishment of pre-metastatic niches, a phenomenon that is dependent upon the integrin patterns expressed on EVs' surface, which can determine their organotropism, α6β4 and α6β1 are related to lung metastasis, whereas integrin αvβ5 is associated with liver metastasis [79]. This establishment requires the modulation of certain factors in the new cancer niche, such as angiogenesis, matrix remodeling, and immune suppression. Besides that, EVs can be a mechanism for clearing chemotherapeutic drugs from cancer cells, helping in the resistance of tumor cells to these anticancer agents [80]. Moreover, the triggering of a cancerous phenotype in normal cells can be mediated through the transfer of oncogenic proteins transferred in EVs derived from tumor cells [52].

1.2.6. EVs as intrinsic therapeutic agents, targets, and biomarkers

EVs can also have intrinsic therapeutic properties depending on the cell type from which they are produced and the physiological conditions of the parental cell. Such EVs with associated beneficial properties can be used as therapeutic agents, especially in tissue regeneration and immune modulation [23]. This therapeutic ability is associated with the delivery of functional molecules, including proteins, lipids, and nucleic acids to the recipient cells which trigger functional responses, or simply through their surface interaction with cells activating signaling pathways, in this case not needing to deliver the cargo into the cytoplasm of the cell to have functional activity.

As a cell-free therapeutic option, EVs circumvent or reduce the possibility of a considerable part of the drawbacks encountered in cell therapies, such as neoplasia formation as they are non-mutagenic and non-replicative [9], as well as immunogenicity, since EVs may be less immunogenic than their parent cells, due to a reduced transmembrane protein content, namely a decreased quantity of MHC-II complexes on their surface [81], [82]. EVs achieve these benefits while maintaining some of the

therapeutic effects of cell therapies [83], [84], such as the capability of inducing angiogenesis, and were already shown to be a therapeutic viable option to this end [9].

Specifically, mesenchymal stromal cells (MSC) receive great attention in research for their applications in regenerative medicine, and although initially thought to exert these beneficial effects through cell differentiation there is now a growing body of knowledge that asserts that their beneficial properties are achieved in a paracrine manner [85]. MSC-EVs are capable of decreasing inflammation, as was demonstrated in clinical cases of osteoarthritis (OA) where MSC(BM)-EVs down-regulated gene expression of the proinflammatory pro-cytokines, IL-1, IL-6, IL-7. IL-17 and COX-2 upregulated the levels of aggrecan and type II collagen [86]. They are also capable of immunomodulation, for instance, an abundantly present miRNA, miR-100-5p in exosomes derived from MSC of the infrapatellar fat pad can protect articular cartilage from damage in mice with OA and ameliorate their gait irregularities through the inhibition of the mTOR autophagy pathway [87]. Focus is also placed on the ability of MSC-EVs to stimulate tissue regeneration. It was demonstrated by Nakamura Y. *et al.* that MSC-derived exosomes enhanced angiogenic and myogenic processes *in vitro* and muscle regeneration in an *in vivo* model, which was mediated in part by the transference of certain miRNAs, namely miR-494 [88]. In addition, in a rat model with acute kidney injury, the administration of human MSC(BM)-EVs improved renal function through stimulation of tubular epithelial cell proliferation and inhibition of apoptosis [89], showing their role in tissue regeneration.

Evidencing their properties as antioxidant agents, Luo Q. et al. demonstrated the antioxidant activities of MSC-EVs in hippocampal neurons stimulated with H_2O_2 *in vitro* and in a mice model with seizure damage. Notably, MSC-EVs were enriched in antioxidant miRNA, being able to promote the reconstruction of hippocampal neuronal structures and reduce associated cognitive impairments through acting in the Nrf2 defense system [90]. MSC-EVs are also able to decrease infarct size and increase myocardial viability in a mouse model of myocardial ischemia/reperfusion injury through the activation of the PI3K/Akt signaling pathway [91]. Additionally, EVs also proved their value as therapeutic tools in a multiple sclerosis mouse model, where an injection of placental MSC-EVs was able to induce the differentiation of oligodendrocyte precursor cells into mature myelinating oligodendrocytes, leading to increased myelination in the spinal cord of the treated mice and reduced DNA damage in oligodendrocytes [92].

A different therapeutic related to EVs can also be their targeting in order to inhibit their pathological activity in a given biological context [93], [94]. For that, an in-depth understanding of EV biology and of the disease-specific mechanisms in which EVs participate is necessary. The steps that can be targeted to stop EV trafficking in pathological processes include inhibition of EV synthesis, release, and uptake. For example, the discovery of cancer cell-derived EVs as important systems for the establishment of the pre-metastatic niche as well as for cancer cell communication within the tumor microenvironment [95] renders the disruption of their trafficking a possible manner in which tumor progression can be prevented. In fact, in a breast cancer xenograft model, it was discovered that the attenuation of neutral sphingomyelinase 2, reduces EV secretion and consequently lessens the extent of angiogenesis and metastasis [96].

As EVs provide a snapshot of the circumstances of their parent cells, whether they are normal or stressed, and are involved in many of the pathological processes in an organism, they can also be used as biomarkers [94], [97]–[99] to evaluate the presence and severity of the pathology, as well as the effectiveness of treatment. An explored application of this feature of EVs is their use as cancer biomarkers [98] where tumor cells secrete EVs into body fluids such as blood or urine. For instance, in glioblastoma patients, tumor-derived microvesicles are found in the serum and these microvesicles are depleted upon tumor removal [100]. Moreover, since EVs can be collected in liquid biopsies they are an alternative to the invasive, painful, and often risky [101] conventional tissue biopsies used in the context of disease diagnosis, which can be more easily performed with minimal risk of complications for the patient while generating less discomfort. Additionally, another application where EVs may bring benefit is in the development of EV-based vaccines [102], [103].

1.2.7. Extracellular vesicles as delivery vehicles

NDDS are a valuable tool when it comes to the improvement of the targeting abilities of free drugs, the decrease of off-target effects which results in fewer side effects and to attain a controlled drug release. Through the improvement of such parameters, NDDS are able to confer a more favorable pharmacokinetic and pharmacodynamic profile to a free drug, providing an overall enhanced efficacy and minimizing toxicity [9]. These upgrades are useful considering free drug characteristics such as poor bioavailability, fluctuations in available quantity in plasma and non-observable sustained release, which are in themselves sufficient to render a therapeutic process ineffective [104].

In the last few years, EVs emerged as promising candidates for NDDS because they can trigger phenotypical and functional responses in recipient cells functioning as a system of cell-to-cell communication. Notably, as EVs naturally occur in the organism they present high biocompatibility and do not show significant cytotoxic and immunogenic effects [10]. These systems are also explored for their high bioavailability and organotropic properties which can render them especially effective in cell specific targeting [105]. As well, EVs may also present an increased stability in circulation because of their negatively charged surface and ability to avoid the mononuclear phagocytic system through the exposition of the CD47 surface protein [106]. Additionally, EVs can also cross biological barriers, namely the blood-brain barrier [23], [107]. With these characteristics, EVs come up as promising options to be applied as NDDSs. And apart from such advantages, EVs also have the potential to improve the development of RNA and DNA-based therapies, which have their development hindered by the lack of an appropriate delivery system. RNA and DNA are susceptible to blood RNases and DNases, respectively, being unstable in circulation, and their negative charges render them inefficient in penetrating membranes to target cells [108], [109]. The encapsulation of these molecules within EVs comes up as a possible viable solution, facilitating penetration of RNA and DNA molecules into cells and conferring protection.

In the field of NDDS, other viable options are available, namely, synthetic nanocarriers, which started to be researched much earlier than EVs to improve the efficacy and therapeutic index of drugs while reducing off-target effects and drug toxicity. For instance, liposomes, a prominent option in this field have already been extensively studied in the last 30 years [110]. Therefore, alongside other synthetic

options, liposomes are yet considered the state-of-art option when it comes to the usage of NDDS. Nonetheless, despite the advantages, the usage of synthetic formulations for the delivery of therapeutic molecules failed to meet the expectations as they can present considerable immunogenicity, a short half-life [111], an inefficient crossing of biological barriers, and a poor biodistribution, with most liposomes ending up accumulating in the liver and the spleen after intravenous injection [110], [112]. Additionally, to achieve better targeting properties, the surface engineering of these systems may often have to resort to harsh reagents that are not compatible with biological conditions, which may render them a concern in terms of safety and can interfere with the integrity and functionality of the systems and the respective cargoes.

However, even though EVs are recognized for their stability in circulation, studies have already shown that the biodistribution profile of EVs is similar to that of liposomes upon intravenous injection [112] where most of the EVs end up in the liver and spleen within hours or minutes [110], [113]. The utilization of different cellular sources, and downstream processing methods, which impact the functionality and biophysical properties of EVs may explain the contrasting findings. Another factor that can impact the biodistribution of EVs is the protein and lipid profiles displayed on their surface. Additionally, even though the expression patterns of surface molecules such as tetraspanins [44] and integrins [79] in EVs' surface, endows them with organotropic ability, upon systemic administration, naive EVs rarely achieve relevant clinical numbers in the targeted tissue. It is imperative to learn about the biodistribution profiles of EVs, as well as how bioprocess parameters affect them, in order to develop a safe and effective EV-based NDDS.

To improve EVs' targeting capabilities, surface engineering can be used to anchor targeting moieties into the EV's surface. This has the potential to solve the off-target accumulation, which could consequently lead to insufficient EV accumulation in desired sites. In addition, EV surface modifications can also be used to confer stealth properties to EVs to avoid non-specific phagocytic uptake, which will possibly also improve their accumulation in targeted sites. This can be accomplished through the addition of polyethylene glycol (PEG) to the EV surface or by including CD47 in their membrane, which acts in an opposite mechanism than PS that promotes phagocytosis, acting as a “do not eat me” signal to macrophages leading to an increase in EV circulation time [12]. Anchoring cargo on the surface of EVs is also a possibility that can be particularly useful for large and polar molecules. However, the cargo anchored in this manner is more susceptible to being damaged [12]. Fluorescent labeling that takes advantage of the membrane properties of EVs can also be a valuable tool when it comes to employing EVs as theranostic tools and in studying their uptake and trafficking routes.

The strategies implemented for EV surface modifications vary according to the intended therapeutic application. Generally, two kinds of approaches may be considered, before isolation and post isolation. Prior to isolation techniques have the objective of engineering the producer cells. This strategy comprises approaches such as genetic and metabolic engineering as well as the alteration of the plasma membrane of the parent cell [105]. These approaches were already successfully applied to develop systems with enhanced therapeutic efficacy, such as in a study where dendritic cells were engineered to express lysosome-associated membrane protein (Lamp2b) fused with the rabies viral glycoprotein peptide (RGV), a peptide that is neuron-specific. This fusion peptide endowed exosomes with enhanced

targeting abilities to neurons, the microglia, and oligodendrocytes after systemic intravenous injection [107].

On the flip side, post-isolation techniques focus directly on the EV surface and encompass physical methods, for instance, fusion with liposomes, lipid post-insertion [105], and surface adsorption, for example, Gao X. et al. already created a surface adsorption mechanism through a CD63 specific peptide, CP05, that was fused to a muscle targeting peptide and also to an antisense oligonucleotide [114]. This system leads to enhanced targeting abilities of the modified exosomes to the muscles leading to a functional improvement through an increased muscle dystrophin expression in the quadriceps of dystrophin-deficient mdx mice without any detectable toxicity. Additionally, chemical modifications can also be used for surface engineering strategies [105]. One example is the bio-orthogonal copper-free azyde alkyne cycloaddition, which was already employed for the addition of a cyclic peptide, Arg - Gly - Asp - D - Tyr - Lys to the surface of MSC-derived EVs. These engineered EVs were targeted to ischemic regions of the brain in a murine artery occlusion model, being able to reduce inflammation through the delivery of curcumin [115]. The molecules amenable to be used with each technique differ, but overall antibodies, fragments of antibodies, antibody mimetics, proteins, aptamers, polysaccharides [116], and glycans are possible candidates [105].

Although plenty of examples exist where EVs are targeted to certain cells and tissues, fewer are the ones where EVs are targeted to a specific uptake route or sub-cellular locations. Nonetheless, studies have already shown it to be possible to fine-tune the routes of uptake and subcellular destination of EVs, which can be useful for therapeutic applications since it can lead to enhanced therapeutic efficacy and potency [117].

EVs can be loaded with several therapeutic cargoes, namely nucleic acids (e.g., RNA molecules, such as coding RNAs, like mRNA, and non-coding RNAs, like miRNA and siRNA), proteins, small molecules (e.g., curcumin a naturally occurring substance, and paclitaxel or doxorubicin, two chemotherapeutic drugs) as well as nanoparticles. And multiple techniques can be utilized for cargo encapsulation, either directly loading the cargo into EVs, or loading them into parent cells, which will then produce EVs enriched in such cargo [11], a strategy that requires the compatibility of such cargo with the cell culture viability. This comprises an interesting option unique to EVs that allows taking advantage of the cellular machinery for cargo sorting [11]. Of note is that these drug loading techniques should aim to maintain the structural integrity of EVs and their cargo as well as their biological properties and immunogenicity while having high efficiency.

At the level of the EVs, the techniques that can be used are electroporation, sonication, extrusion, saponin-assisted loading, freeze-thaw cycles, thermal shock, pH gradient method, extrusion, direct incubation, and hypotonic dialysis. Indirectly at the level of the parent cells, EVs can be loaded through indirect incubation and transfection, such as demonstrated by Kosaka et al. that transfected HEK293 and COS-7 with a vector for the expression of multiple miRNAs, resulting in the overexpression of these miRNA in cells, and gene silencing upon treatment of COS-7 cells with the microRNA containing EVs [118]. However, lack of efficiency in drug loading is one of the main bottlenecks delaying the therapeutic applications that use EVs as NDDS [119].

Parent cell selection is also a crucial step for the successful development of an NDDS. This selection can have an impact on the qualities of the isolated EVs, in terms of the biological activity, cargo, tissue homing abilities, immunogenicity as well as carcinogenicity. Moreover, the selected cell type must be evaluated in terms of its usability for large-scale production. Options such as immortalized cell lines, e.g., MDA-MB-231 and HeLa, lead to the generation of higher quantities of EVs being produced due to an almost indefinite time of culture [120]. However, these EVs are less well characterized and may present oncogenic potential [120]. Moreover, primary cells can also be utilized for EV production, with the disadvantage that lower amounts of EVs are produced and that the number of passages is limited but presenting the benefit of extended characterization [120].

In terms of cell source, until today, studies have utilized multiple cell sources, including MSC, dendritic cells, macrophages, cancer cell lines, and autologous tumor cells. For example, cancer cells provide attractive advantages for EV production, such as ease of acquisition, high abundance, and the high number of EVs produced [121]. These EVs present tumor homing abilities to their parent cells, and it is even hypothesized that they may be specifically effective in traveling back to their parent cells [121]. If this is the case, tumor-derived EVs can be utilized as a Trojan horse allowing the encapsulation of chemotherapeutic drugs and delivery to their parent cells. This can constitute a major advantage when considering autologous therapies application. Considering such a possibility, Guo M. et al. loaded autologous cancer-derived microparticles loaded with a chemotherapeutic drug, MTX, and observed that this system was safe and led to enhanced survival in a mice model inoculated with a pleural tumor, and demonstrated promising positive clinical responses [122]. Such an approach constitutes a promising strategy to treat advanced lung cancers with malignant pleural effusion through the harnessing of the potential of autologous drug-loaded microparticles. In addition, Qiao L. et al. encapsulated Doxil, a chemotherapeutic drug, into cancer cell-derived exosomes and systemically delivered them to mice bearing subcutaneous tumors, showing that exosomes migrate to their original tumor tissue and, ultimately, that drug-loaded cancer-derived exosomes can be used for targeted cancer therapies [121]. Notably, in another study using exosomes sheathed doxorubicin-loaded porous silicon nanoparticles to encapsulate doxorubicin, the drug levels were enriched in total tumor cells following intravenous injection, because of the system enhanced tumor accumulation, extravasation from blood vessels, and deep penetration in tumor parenchyma [123].

Another advantage worth to be noted is that cancer cell-derived EVs loaded with a chemotherapeutic drug can overcome the drug resistance usually faced in cancer stem cells upon free drug delivery [124], which constitutes a major mechanism of cancer cell resistance to chemotherapy. This is a feature that can also occur in EVs from other cell sources. Moreover, despite the advantages and promising applications, cancer-derived EVs contain intercellular signaling messengers, including nucleic acids, proteins, enzymes, and lipids that are associated with tumor development, progression, and metastasis [121]. As such, these EVs may trigger oncogenic responses and need to be further studied to confirm their safety. Cancer cell-derived EVs' interaction with the immune system is also not well understood yet, with their role as immune system inhibitors or activators not being clear, nonetheless, it is reported that such characteristics may vary according to the kind of tumor considered as well as its progression stage [125].

MSC-EVs can also be employed in the development of NDDS. Similar to their parent cells, MSC-EVs present low immunogenicity [126], being promising candidates for heterologous off-the-shelf NDDS products. And, because clinical-grade MSC are already cultured for years in the context of cell therapy applications, complying with the GMP practices, the use of MSC as EV producers may be facilitated. Moreover, MSC-EVs possess high modification flexibility and may also present tumor homing properties as their parent cells [127] which are important features for their application as NDDS in targeted cancer therapies. Apart from the endogenous therapeutic benefits of MSC-EVs, these systems were already shown to be amenable for loading with a spectrum of therapeutic components, namely non-coding RNAs such as siRNAs and miRNAs, as well as chemotherapeutic drugs. Pre-clinical studies describing the anti-tumor effects of MSC-EVs are plentiful, with several cell sources, cargoes, and tumor models being explored. For instance, Zhou et al. already showed that upon MSC(AT)-EV loading with miR424-5p EVs exerted anti-tumor cytotoxicity in human triple-negative breast cancers cells, both *in vitro* and *in vivo*, through the down-regulation of the PD-L1 pathway [128]. And, in another study, exosomes derived from MSC transfected with miR-584 led to the reduction of malignant glioma progression *in vivo* [129].

1.2.8. Upstream Processing

One of the main challenges faced in the field of EVs is the low yield obtained during manufacturing[130]. This renders basic scientific research, pre-clinical studies and clinical trials more challenging, leading to a significant delay in the progress of the field in order to harness the full potential of EVs in clinical settings[131]. The whole bioprocessing pipeline, from upstream to downstream processing, needs to be considered for EV manufacturing optimization. Upstream processing comprises cell culture leading to EV production, thus requiring appropriate choice of both the cell culture medium used and the culture vessel, which can range from small vessels such as T-flasks up to 500 L bioreactors, depending on the chosen approach. This step influences the characteristics of the final product and therefore should be carefully selected while having in mind a specific application.

Progress is already being made towards optimizing the upstream conditions of EV production through the adaptation of already well-established technologies in other fields to produce functional and safe EVs in a cost-effective way. Scaling-up or scaling-out of such platforms is expected to decrease the associated costs with EV manufacturing[132]. The simplest scaling option is to adopt the use of multi-layer flasks (e.g. hyperflasks, Cellstacks, Cell Factories) instead of the use of conventional T-flasks[132]. These systems present several layers for cell growth, decreasing the manipulation time needed in comparison to conventional T-flasks and reducing lab footprint. For example, hyperflasks were used for the cultivation of bone marrow-derived MSC and the EVs isolated from the conditioned medium (i.e. containing EVs) were shown to significantly suppress the symptoms of graft *versus* host disease (GvHD) in a murine model[133]. However, culture monitoring is challenging when using these planar systems, which do not lead to cost savings in the whole process, namely in what concerns the quantity of cell culture medium used [134].

Bioreactors represent promising scale-up or scale-out options for EV manufacturing, which under optimized conditions can generate higher cell and EV yields, in a more cost-effective way (e.g. lower

need for consumables such as culture medium), compared to static systems[132]. In fact, some bioreactor systems were already explored for EV production (Figure 4).

Hollow-fiber bioreactors allow adherent cells to grow attached to fibers composed of a permeable membrane, while the cell culture medium flows across the membrane. In a recent study, it was observed that Wharton's Jelly (WJ) MSC-EVs produced in a hollow-fiber system displayed enhanced osteochondral regeneration activity when compared to 2D culture flasks, leading to superior repair activity of cartilage defects *in vivo*[134]. Another study revealed that MSC(WJ) expanded in hollow-fiber bioreactors produced EVs with enhanced renoprotective effects in comparison to EVs produced by cells grown in conventional 2D cultures [135].

Stirred-tank bioreactors can be used as a scalable option that provides homogenization of the cell culture medium through mechanical stirring. Microcarrier technology can be used in combination with these bioreactors for expanding adherent cells and providing a high surface-area-to-volume ratio [130]. These bioreactors can enhance EV productivity as high as 100-fold in comparison to conventional 2D culture flasks[136].

In the context of scalable platforms available for EV production, our group recently employed a single-use Vertical-Wheel^{TM} bioreactor for the production of human MSC-EVs[137]. This system provides a gentler and more homogenous mixing in comparison to the stirred-tank configuration, while also making use of microcarriers for adherent cell culture[138]. Our work revealed an average yield improvement of 6-fold referred to the final EV concentration in the culture medium, in comparison to culture flasks[137].

The use of different culture media during conditioning periods for EV obtention also impacts EV productivity and can potentially render the process more efficient. For instance, the use of non-supplemented OptiMEM (i.e. optimized formulation of Eagle's Minimal Essential Medium (MEM)) led to an increase in the production of HEK293T-derived EVs, in comparison to OptiMEM supplemented with 10% Fetal bovine serum (FBS), DMEM (i.e. Dulbecco's Modified Eagle's Medium) supplemented with 10% FBS, or DMEM supplemented with 10% EV-depleted FBS, among others[139].

In order to circumvent the low yields associated with EV production from cell culture supernatants (i.e. conditioned media), production of EV-like particles has also been employed. This is achieved through complete disruption of the cellular membrane leading to the release of self-assembled particles, reaching production yields that can be as high as 100-fold compared to normal EV release[140]. The most common approach to achieve this is extrusion, whereby cells are filtered through sequentially smaller pores[132].

Growing adherent cells as 3D cell aggregates instead of monolayers is another viable option to increase EV production yields. The formation of 3D MSC aggregates provides a microenvironment that better mimics *in vivo* conditions leading to the maintenance of MSC phenotype and innate MSC properties, which could explain the higher yields attained with this strategy. Moreover, 3D scaffolds into which cells can adhere and proliferate can also be used to promote the production of EVs and even to enhance their functional activity. This was demonstrated using bone marrow-derived MSC seeded into collagen scaffolds, which produced 2-fold more EVs compared to 2D culture conditions and enhanced the regenerative capacity of these EVs in traumatic brain injury mouse models[141].

Importantly, clinical trials employing bioreactors for EV production are already ongoing. Recently, Codiak Biosciences developed exoSTING, a therapeutic EV-based product in which EVs are loaded with stimulators of the interferon gene for the treatment of multiple cancers[142]. This strategy is currently under clinical testing in a phase 1/2 trial (NCT04592484).

Of notice, there is still a gap in our knowledge concerning how the upstream conditions influence the characteristics and the quantity of produced EVs. For instances, in the context of the manufacturing of monoclonal antibodies, the optimization of upstream conditions was able to lead to improvements of 10 - 100-fold in product titers over the years [130]. Therefore, by adjusting operational parameters variables in the process such as the composition of culture media, oxygen concentration, materials used, as well as the cell passage, level of confluency and viability, one can expect substantial improvements in EV yields.

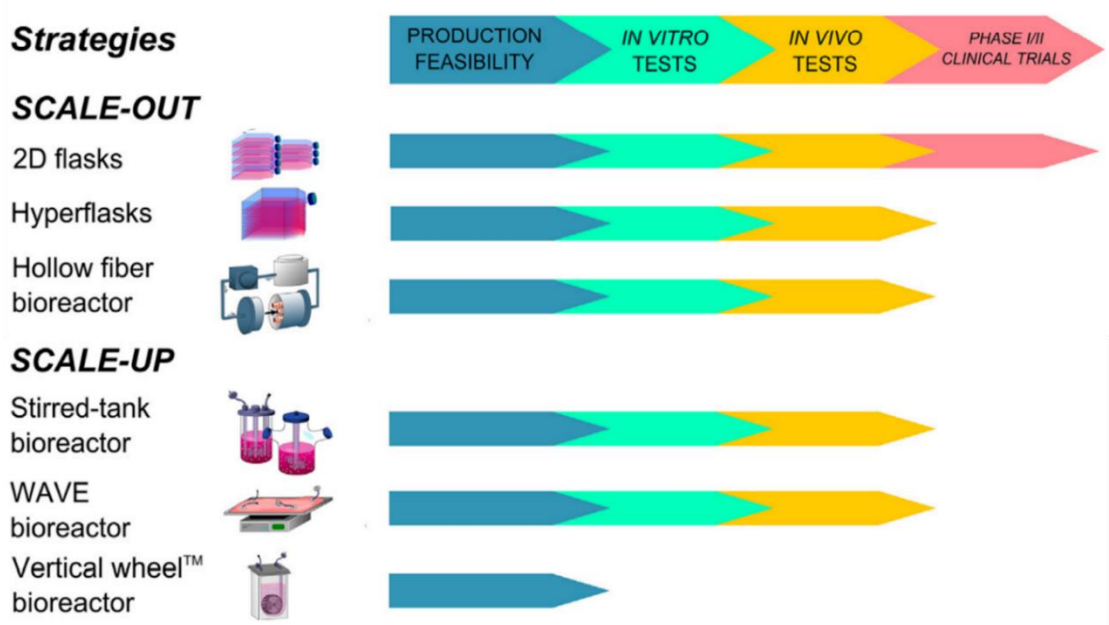

Figure 4 - Cell expansion platforms for EV production and the respective research phases. Adapted from Grangier A et al. (2021) [143]

1.2.9. Downstream Processing

The downstream processing of EVs, which comprises all the steps following upstream processing to recover and isolate EVs from cell culture conditioned medium and eventually purify them, also deserves a special attention considering the particular characteristics of EVs. Over the last years, the emergence of EVs as promising tools for the development of new therapeutic options as well as valuable structures to understand organismal pathophysiological mechanisms has prompted the development of EV isolation methods.

However, currently available isolation methods still present considerable limitations, including poor standardization, alteration of physicochemical properties of the isolated EV population and the modification of EV cargo profiles. For instance, the miRNA profile in exosomes obtained from blood

serum was reported to be different depending on the isolation method used, when comparing a precipitation-based isolation method with ultracentrifugation[144]. Likewise, the purity of EV samples largely depends on the isolation method used and a compromise between the purity of a given sample and the amount of recovered EVs must be made[145], [146].

The isolation methods available can be categorized based on the principle used for the isolation of EVs from other particles present in a body fluid or cell culture conditioned medium. These methods can be generally divided into ultracentrifugation-based methods, precipitation, size-based and microfluidics, among others.

Ultracentrifugation-based methods

Ultracentrifugation methods can be divided into two distinct techniques: differential ultracentrifugation and density gradient centrifugation. Differential ultracentrifugation is based on differences in the size and density of particles. It subjects the samples to multiple low-speed centrifugations to remove dead cells and debris, which correspond to the larger biological particles present in the sample. The low centrifugation speed periods are followed by high-speed centrifugations of 100 000 x g (or more) in order to pellet the smaller EVs and allow the collection of these particles[147], [148]. Differential ultracentrifugation is the most employed primary method of EV isolation, with more than 75% of participants reporting its use in a worldwide survey performed by the International Society for Extracellular Vesicles (ISEV) in 2020 [149]. It can be considered a method with intermediates recovery and specificity[150] and capable of processing large volumes of fluid [151], however, it is highly laborious and time-consuming, presenting the possibility of causing damage to EV structure, which can affect their performance for a specific application[148]. This method also presents low reproducibility and may lead to protein aggregation[147], [148]. Nonetheless, numerous pathological conditions were already shown to benefit from interventions based on the administration of MSC-EVs isolated through differential ultracentrifugation. These include bone disorders[152], skeletal muscle[153] and spinal cord injuries[154], [155], as well as cardiac[156] and liver[157] pathologies.

Density gradient ultracentrifugation is a low recovery, high specificity method[150] that consists in the ultracentrifugation of particles in a biocompatible medium, sucrose or iodixanol, with a gradient of concentrations that allows the isolation of EVs based on their density[147]. Although this method provides higher purities than differential ultracentrifugation [147], [148], it is also time-consuming and the duration and force of the centrifugation can affect the quality of EVs. In addition, the media used may negatively impact the therapeutic activity of the isolated EVs[158]. Furthermore, this method is largely instrument-dependent, and residual contaminants are often co-isolated with EVs, requiring highly trained technicians to be performed well[147], [148].

Precipitation-based methods

Precipitation-based methods aim to lower the hydration levels of EVs using polymers such as polyethylene glycol (PEG) or other synthetic hydrophilic polymers prone to interact with water molecules[148]. This is a high recovery and cost-effective method that is instrument-independent and can be used for large samples[147]. This method uses lower-speed centrifugation cycles in comparison

to differential ultracentrifugation [148], thus not being as mechanically harsh. In fact, precipitation-based methods, in opposition to ultracentrifugation techniques, may preserve the proteins naturally bound to the surface of EVs, which is important for the downstream analysis of EV function[159]. However, this approach lacks specificity, providing high contamination of the sample and leading to precipitation of non-vesicular components such as lipids, nucleic acids and proteins[148]. Additionally, the precipitation reagents also influence the biological activity of the isolated EVs [160].

Size-based methods

Size-based methods consist mainly of filtration-based separation methods and size exclusion chromatography (SEC). Ultrafiltration uses a filter membrane with a defined size exclusion limit to filtrate the particles present in a sample. It is less costly and faster than ultracentrifugation, and it is easy to operate presenting good portability, and providing high purity of the isolated particles[148]. MSC-EVs isolated through this method have shown angiogenic stimulatory activity[161], a property that can be harnessed for the treatment of a wide spectrum of conditions, as well as therapeutic activity in other diseases such as osteoarthritis[162]. However, low recovery, membrane clogging, and EV trapping are disadvantages usually associated to this method[147]. Tangential flow filtration (TFF) is another filtration-based technique that attenuates the membrane clogging faced in ultrafiltration due to the tangential flow of fluid across the membrane surface instead of cross-flow. TFF is more efficient and gentler than differential centrifugation, providing a higher recovery and isolation of fewer single macromolecules and aggregates[163]. Additionally, it allows the processing of large volumes of fluid and is a time-efficient, scalable, reproducible, and robust technique [163]. This method has already been used to isolate human adipose tissue MSC-EVs that upon intra-articular injection attenuated osteoarthritis progression and prevented cartilage degeneration in mouse models[164]. Additionally, MSC-EVs isolated through TFF displayed the ability to improve alveolarization and vascularization in animal models of bronchopulmonary dysplasia, reducing the damage induced by hypoxia[165]. This further demonstrates that EVs isolated through TFF can maintain their biological therapeutic activity.

Size exclusion chromatography (SEC) allows the separation of particles based on their interaction with the pores present in the stationary phase. Sample particles with higher dimensions will not be retained within such pores and, as a result, will be eluted first (i.e. before smaller particles). This represents a gentle separation method of EVs that maintains the structural integrity and biological activity of the vesicles, which can be illustrated by the fact that SEC isolated MSC-EVs, but not ultracentrifugation isolated MSC-EVs, maintained their immunomodulatory activity, impairing T cell proliferation [166]. Moreover, this technique is easy to operate and provides a higher purity than differential ultracentrifugation[148]. Despite of these advantages, SEC may suffer from pore blockage, it is a time-consuming method and presents high equipment costs. Additionally, SEC involves sample dilution, thus usually requiring a concentration step afterward, which can further impose yield losses on the process.

Microfluidic-based methods

Microfluidic-based methods utilize microscale devices to isolate EVs. These methods can be based on EV-specific surface markers, such as microfluidic-based immunoaffinity, which rely on surfaces coated with antibodies for isolation. For example, a microfluidic device functionalized with antibodies against the tetraspanin protein CD63 was able to efficiently isolate circulating EVs, being well suited for exosome-based diagnostics[167]. Beads coated with capture antibodies can also be employed, allowing to obtain higher EV yields [168]. In the future, this methodology may even allow isolating MSC-EV subpopulations showing increased therapeutic effects; however the identification of such subsets is still challenging [169]. Microfluidic devices for EV isolation can also be based on EV size and density including approaches such as membrane filtration, nano-wire-based traps, nano-sized deterministic lateral displacement, and acoustic isolations [170]. Overall, these methods are simple and efficient as well as easy to automate and they provide higher sensitivity than differential centrifugation.

Other methods

Other relevant methods based on different EV properties are available. For instance, anion exchange chromatography is a method that takes advantage of EV negative surface charge for their isolation. This method presents a similar yield, morphology, and size in comparison to differential ultracentrifugation[171]. MSC-EVs purified through this technique demonstrated the ability to prevent the onset of type 1 diabetes and uveoretinitis[172], showing the maintenance of the biological activity of the isolated MSC-EVs. Nevertheless, anion exchange chromatography may co-isolate particles with a negative net charge such as proteins. Thus, combining it with another technique such as SEC may provide greater specificity.

Apart from the microfluidic approach to the immunoaffinity isolation principle, other approaches based on chromatography are available. This method is based on the interaction of the EV surface proteins, such as CD9 or CD63 with antibodies present in the chromatography column. This provides a high sensitivity and high specificity towards specific EV subpopulations. Additionally, it is a gentle approach that conserves EV morphology [148]. Nevertheless, this is associated with low EV recovery and high costs, not being suitable for processing large volumes[148].

Combination of EV isolation methods

More than 45% of researchers included in a worldwide ISEV survey in 2020 reported the use of not a single method for the isolation of EVs, but a combination of techniques [149]. This approach is particularly beneficial because it allows obtaining higher purities than single isolation methods and certain combinations of methods were already applied in studies with different applications for EVs.

TFF combined with SEC is becoming the preferred approach in comparison to the typically used ultracentrifugation. TFF and SEC, which feature easy scalability and are able to comply with good manufacturing practices (GMP), were already studied in the context of an EV-based strategy that intends to utilize HEK293-derived engineered EVs carrying an immunostimulatory cytokine fusion protein, the heterodimeric IL-15/lactadherin, for a targeted cancer immunotherapy approach[173]. Importantly, such strategy can be combined with bioreactor cultivation at upstream as a scalable and efficient method to

produce purified bioactive EVs, which has the potential to be translated into industrial EV production, allowing the processing of large volumes (in the scale of liters of conditioned medium), without significant changes in size and morphology. A combined TFF and SEC approach was already employed in the isolation of MDA-MB-231-derived EVs to demonstrate the function of an innovative platform that permits the study of EV-mediated RNA delivery, the CRISPR-operated stoplight system for functional intercellular RNA exchange[174]. Additionally, SEC may also be combined with ultracentrifugation to improve the separation of EVs from lipoproteins, providing an increased purity [175].

Currently, in the field of EVs, there is still no isolation method that can provide a high recovery of EVs combined with a high specificity [150]. As such, a compromise is always required between these two variables when choosing a suitable downstream strategy. This compromise between purity and yield is one of the main challenges faced in the field, and together with the overall unsatisfactory efficiencies and high costs associated are still the main bottlenecks that undermine large-scale EV production [148]. Other factors such as the type of biological raw materials from where EVs are isolated, the starting volume to be processed, as well as the quantity of EVs desired and their attributes must also be considered when choosing an isolation method or a combination thereof which should aim to be highly efficient, scalable and GMP compliant.

1.2.10. Technical Challenges

Until today, several discoveries and technical advances in the field of EVs paved the way for them to be considered promising therapeutic tools [176]. In fact, harnessing the EV's full potential may lead to an impactful change in the landscape of treatments for certain diseases such as cancer and neurodegenerative pathologies. This potential is reflected in the interest of biotechnology and pharmaceutical companies in creating EV-based therapeutic strategies [177]. However, for clinical translation to happen there are still many limitations that need to be conquered to make the best use of the features of these complex signalosomes.

One of the main problems to be overcome is the low yields of EVs usually obtained in studies. Overcoming this problem is important because clinical trials and further clinical applications demand large amounts of EVs [119]. To achieve this end bioprocesses that must comply with GMP must be optimized to maintain EV potency and safety while increasing EV production in a cost-effective, reproducible, and standardized manner [178]. The upstream and downstream processes still lack the reproducibility that is crucial to ensure batch-to-batch uniformity [179] and the standardization [179], [180] needed to achieve multicenter integrated analysis which permits an understanding of how certain protocols affect the final characteristics of EVs, which is currently widely unknown. The scale-up or scale-out necessary to increase yields is challenging to achieve in a reliable manner considering this heterogeneous landscape, leading to a lack of consensus on the best approaches [181]. Ensuring the development of high throughput isolation and standardized characterization techniques will also allow a faster expansion of the field towards clinical applications [182].

Another major challenge is to understand the specific characteristics of EV subpopulations, which may lead to discovering that certain subtypes of EVs, for instance, exosomes or microvesicles, have enhanced therapeutic properties. By focusing on that specific EV subtype, more effective treatments

can be developed [183]. The task at hand was not yet completed because there is not a complete consensus on specific EV subtype markers that assign them to a specific biogenesis pathway [20]. Additionally, isolation techniques that can reliably separate these subpopulations do not yet exist which makes comprehensive comparison impossible [183], as such researchers are urged, in MISEV 2018 guidelines, to not use terms such as exosomes or microvesicles which carry with them the expectation of a specific mechanism of biogenesis that cannot be proved but are instead advised to use operational terms for EV subtypes that are based on physical characteristics, biochemical characteristics or description of conditions, e.g. hypoxic EVs, or cell origin [150].

The lack of definition of the best storage conditions for EVs is, currently, also a limitation in the field. Inappropriate conditions can lead to alterations in the chemical and physical properties of EVs affecting their biological activity. For instance, a temperature of 4ºC is inadequate for EV storage as it leads to aggregation and disruption of the EV structure [130]. And, overall, the ideal storage conditions to maintain EVs intact remain to be defined. However, studies point out that temperatures around -80ºC or less may be appropriate [130], [184], which may render the transportation of EVs burdensome in terms of costs. Additionally, to maintain EV properties the freeze-thaw cycles should be minimized even though EVs can maintain stability during multiple cycles [130]. Furthermore, there is a lack of studies that assess the impact of storage on EV omics profile, which is an important parameter to be accessed for safety reasons as well as for certain applications.

Freeze drying is another strategy that may be viable for EV storage and can be useful for the creation of off-the-shelf products based on EVs. This technique did not impact the size and the number of MSC-EVs, nor the activity of enzymes encapsulated into these EVs that were freeze-dried [185]. Nonetheless, further assessment of the impact of this technique in EVs must be done

Apart from technical issues, the EV complexity places this biological product in an ambiguous regulatory scenario because it renders the clear identification of the active substances and the mechanisms of action involved in their therapeutic activity a difficult challenge [177]. Such incapacity of clearly stating these parameters prevents the categorization of EVs into a specific subtype of biologic drugs. And the field is overall far from having defined quality control criteria. This is caused by the lack of standardization and validation at several levels of EV production, such as the lack of definition of appropriate solvents and buffers, storage conditions, and quantification and characterization techniques [182]. Because of this panorama of uncertainty, the EV market is moving at a faster pace than the regulatory framework since the number of EV products near commercialization is increasing [177].

Lastly, guaranteeing the safety of EV products is a must. EVs can easily be decontaminated from bacteria through aseptic filtration. However, the virus decontamination is not as straightforward because several viruses, such as HAV, HBV, HCV, HIV, and CMV to name a few display similar properties in comparison to EVs such as size, comprehended between 20 -200 nm, hydrophobic coating, and electric charge [186]. This creates a high likelihood of isolation techniques such as ultracentrifugation, filtration-based techniques, and SEC to co-isolate the virus. And although immunoaffinity-based methods may partially prevent EV contamination they do not guarantee consistent decontamination. The utilization of inactivating virus agents could be a solution, but it may lead to an alteration of the EV properties. Screening through next-generation sequencing techniques may alleviate some of these concerns,

however, currently, the best strategy to avoid virus contamination is to comply with GMP practices. Other measures such as the inactivation of FBS and hPL are also important to attain virus sterility. And epidemiological surveillance and appliance of screening procedures on donors can also be important measures to be adopted [186]. Nonetheless, the probability of allogeneic virus contamination in EVs is expected to not be greater than the one encountered in the cellular sources [186].

The lack of understanding of EV biology [176], [179], as well as the inefficient EV cargo loading, which is a hallmark of the field [179], are other challenges that need to be conquered if EVs are to move forward to clinical applications. To conquer the present limitations of this multidisciplinary field it will be of great importance to integrate cell biologists, physicians, engineers, and regulatory bodies to arrive at comprehensive solutions and understanding of EVs to permit their translation from bench top to the bedside [176], [182].

1.3. Mesenchymal Stromal Cells (MSC)

Mesenchymal Stem Cells were first identified by Caplan, in 1991 [187], within the bone marrow. Since then, the term "stem" has become a source of controversy in the name of mesenchymal stem cells because the stemness of these plastic adherent adult marrow-derived multipotent mesenchymal cells is not, currently, supported by sufficient data [188]. Hence, it is now established by the International Society of Cellular Therapies (ISCT) that the previously termed Mesenchymal Stem Cells should be addressed as multipotent Mesenchymal Stromal Cells (MSC) unless stemness is demonstrated *in vitro* and *in vivo* [189].

Mesenchymal Stromal Cells possess immune-modulatory and trophic properties that comprise the ability to prevent fibrosis (scarring), and angiogenesis, enhance cell growth and differentiation of stem and progenitor cells and display chemoattractive properties [190]. These effects are exerted through the secretion of bioactive factors, such as chemokines, cytokines, EVs, and growth factors, that can act both in an autocrine and paracrine manner [85].

To characterize MSC, a set of minimal criteria was established, it includes plastic adherence, the presence of the markers CD73, CD90, and CD105, and the absence of hematopoietic and endothelial markers CD14, CD11b, CD79α or CD19, CD34, CD45 and HLA-DR, as well as the *in vitro* osteogenic, adipogenic and chondrogenic differentiation potential [189].

Concerning the sources of isolation, MSC can be derived from multiple tissues, including the bone marrow (BM), WJ, adipose tissue (AT), peripheral blood (PB), dental pulp, endometrium, tendons, synovial fluid, placenta, amniotic fluid, dermis, salivary gland, and cartilage [191]. Comparing the different sources several characteristics are similar, however, MSC biological activity, as well as the expression of some markers, can differ between them [192]. Additionally, other characteristics such as availability and ease of access also vary among different sources and may render some more beneficial to be used in clinical applications.

Comparing, likely, the two sources that are most studied and used in clinical practices, AT and BM, to which safety was already widely established, MSC(AT), presents a considerable advantage over MSC(BM) because these are available in higher quantities, up to 500-fold, and AT is more accessible for harvesting, being associated with less time of morbidity [193]. However, treatment of certain

pathologies may favor the use of one source over the other, a knowledge that will tend to emerge from the future clinical investigation. The bottom line is that some of the therapeutic properties change among different sources, being enhanced or less prevalent depending on the cell source [194].

Clinical trials involving MSC started in 1995 [195], and their number has risen at a striking rate since then because of the wide range of their therapeutic properties. On 15th June 2022, searching for the terms mesenchymal stem cells OR mesenchymal stromal cells, on the ClinicalTrials.gov website, 1534 clinical trials, worldwide, were found to be taking place, with most of them occurring in the USA, China, and Europe. Several pathological conditions, including categories such as Neoplasms, Musculoskeletal diseases, Wounds and Injuries, the Digestive System, and Mental Disorders are aimed to be treated with the use of MSC.

1.3.1. Mesenchymal Stromal Cell-Derived Extracellular Vesicles

EVs are one of the bioactive factors released by MSC responsible for the trophic and immunomodulatory properties of these cells. MSC-EVs were already described to exert similar therapeutic effects as MSC in animal models and humans [196]. And, since MSC are immune evasive, i.e., they do not trigger the immune system, MSC-EVs, because of their reduced transmembrane content, are also not expected to trigger the immune system, being considered safer than their parent cells. In fact, MSC-EVs have been shown to have immune-suppressive properties. This opens the possibility for the creation of off-the-shelf products for allogeneic therapies based on MSC-EVs. And considering such characteristics and other inherently related to EVs such as the fact that they are non-mutagenic and do not replicate, MSC-EVs represent a promising alternative to MSC-based cell therapies [23].

Although not numerous, MSC-EVs are already at the stage of clinical trials. On 30th June, 19 clinical trials involving MSC-EVs are taking place (acquired on clinicaltrials.gov using the search term ((extracellular vesicles OR exosomes OR microvesicles) AND (mesenchymal stromal cells OR mesenchymal stem cells). Several pathological conditions are aimed to be treated with the use of MSC-EVs. In the field of oncology, for instance, a phase 1 clinical trial for the treatment of metastatic prostate cancer in patients bearing the kRasG12D mutation is being performed. The strategy employed consists of the loading of EVs with certain siRNA, generating what authors denominate as iExosomes. (NCT03608631). Additionally, as previously mentioned an MSC-EVs based product denominated exoSTING, an MSC-EV product for the treatment of solid tumors is also undergoing phase 1/2 clinical trials for the treatment of advanced solid tumors (NCT04592484). And MSC-EVs are also being utilized for the treatment of respiratory tract conditions such as acute respiratory distress syndrome (NCT04602104), or COVID-19-associated pneumonia (NCT04602442). Moreover, among others, pathologies such as stroke, musculoskeletal diseases such as rheumatic diseases, as well as digestive diseases, including Crohn's disease are the aim of this collection of clinical trials using MSC-EVs.

1.4. Azurin and the Cell Penetrating Peptide p28 as Anticancer Agents

Azurin is a protein with 128 amino acids (14 kDa), derived from the bacteria *Pseudomonas aeruginosa*. It integrates the cuprexidon superfamily, which is comprised of copper-binding proteins that participate in the electron transport chain of prokaryotes. In terms of structure, azurin is composed of a greek key

beta-barrel, which comprises parallel and antiparallel strands, and outside of the barrel, one alpha-helix can be found [197]. Because azurin preferentially enters cancer cells, while showing no apparent effect on normal cells, its use has been explored as an anticancer agent [198]–[201].

In recent years, a small peptide, with 28 amino acids (2.8 KDa), extracted from azurin, p28 (Leu^{50}-Asp^{77}), has been the center of attention, as p28 is the protein transduction domain of azurin [202] holding the same anticancer properties, pro-apoptotic and anti-angiogenic, and preferential entrance in tumor cells observed in azurin [203]–[206]. In its constitution, it holds the alpha helix domain as well as a partial beta-sheet structure [207], [208] (Figure 5), and in terms of its physicochemical properties, it is an amphipathic peptide with a negative net charge [197].

However, the mechanisms that endow p28 with the capacity to preferentially penetrate cancer cells are not yet fully known, but the entrance within cells may happen through interactions with enriched components of caveolae, including gangliosidosis-1 (GM-1) and caveolin-1 [207]. This is a specific type of lipid raft where small membrane invaginations, 50 - 100 nm, are formed. The levels of cholesterol also modulate the entry of p28 into the cells [207], and it is possible that aberrant N-glycosylation of membrane proteins can also contribute to its uptake, however, p28 penetration in cells is independent of the presence of membrane glycosaminoglycans, unlike what is observed for cationic cell-penetrating peptides [207].

Upon preferential penetration into cancer cells, p28 can exert its anti-cancer properties. Specifically, the 10 -12 C-terminal amino acid residues are responsible for the cell growth inhibitory properties and pro-apoptotic activity of p28. This peptide prevents the ubiquitination of the wild-type or mutant tumor suppressor protein p53 (Figure 5) by the constitutional morphogenic protein 1 (Cop1), an E3 ubiquitin ligase, through binding to the DNA binding domain of p53, which prevents its degradation [209], [210]. This mechanism leads to an increase in the post-translational levels of p53, which cause the activation of cell-cycle inhibitors, p21, and p27, that downregulate FoxM1, ultimately leading to cell-cycle arrest in the G2-M phase. An additional mechanism through which p53 elicits its anticancer properties is by selective inhibiting the expression of cyclin-dependent kinase 2 (CDK2) and cyclin A expression [211], which can also lead to cell cycle arrest and apoptosis.

In terms of anti-angiogenic properties, p28 is also able to preferentially penetrate endothelial cells, co-localized with caveolin-1 and the Vascular Endothelial Growth Factor Receptor 2 (VEGFR2), inhibiting the activity of VEGFR2 which inhibits the phosphorylation of the downstream targets, focal adhesion kinase (FAK) and protein kinase B (AKT) leading to the inhibition of endothelial cell motility and migration and ultimately reducing angiogenesis [212] (Figure 5).

Moreover, a synergistic effect, in terms of the anti-cancer properties, is observed when DNA damaging or anti-mitotic chemotherapeutic drugs and p28 are administered in combination [213]. The effect may be caused due to the response of the cancer cell membrane to p28, which is able to change the cancer cell membrane properties, making it less stiff [214], which favors the permeabilization of chemotherapeutic drugs. Such alteration is particularly significant because cancer drug-resistant cells present an altered biophysical status, including increased stiffness which renders chemotherapeutic drugs less effective. Thus, p28 may favor an increased permeabilization of drugs into cancer cells enhancing their effectiveness.

In fact, p28 already participated in two phase 1 clinical trials for the treatment of pediatric patients with recurrent or progressive central nervous system tumors (NCT01975116) and adult patients with advanced solid tumors (NCT00914914), and has achieved promising results, not presenting toxicity nor immunogenicity, and not showing adverse effects, being approved by the FDA as an orphan drug for the treatment of brain tumor glioma [204], [206].

Apart from p28 use as a therapeutic agent, other applications can be found in the literature where the tumor-targeting ability of p28 is taken advantage of. For instance, a non-invasive Near Infrared (NIR) probe was developed, conjugating the clinically non-toxic p28 with the FDA-approved NIR dye Indocyanine Green (ICG). This probe was created for usage in intraoperative settings making it possible to identify positive tumor margins more easily and correctly in a real-time 3D fashion during breast cancer conservative surgery where the rate of positive tumor margins after surgery is high [215]. Moreover, an NDDSs was also developed, where PGLA nanoparticles, loaded with the chemotherapeutic drug Gefitinib, an EGFR inhibitor, were functionalized with p28, intending to improve the targeting abilities of the NDDS toward A549 lung cancer cells. The system was demonstrated to reduce primary and metastatic tumor burden, showing that PGLA nanoparticles functionalized with p28 provide a new strategy for cancer therapy [216].

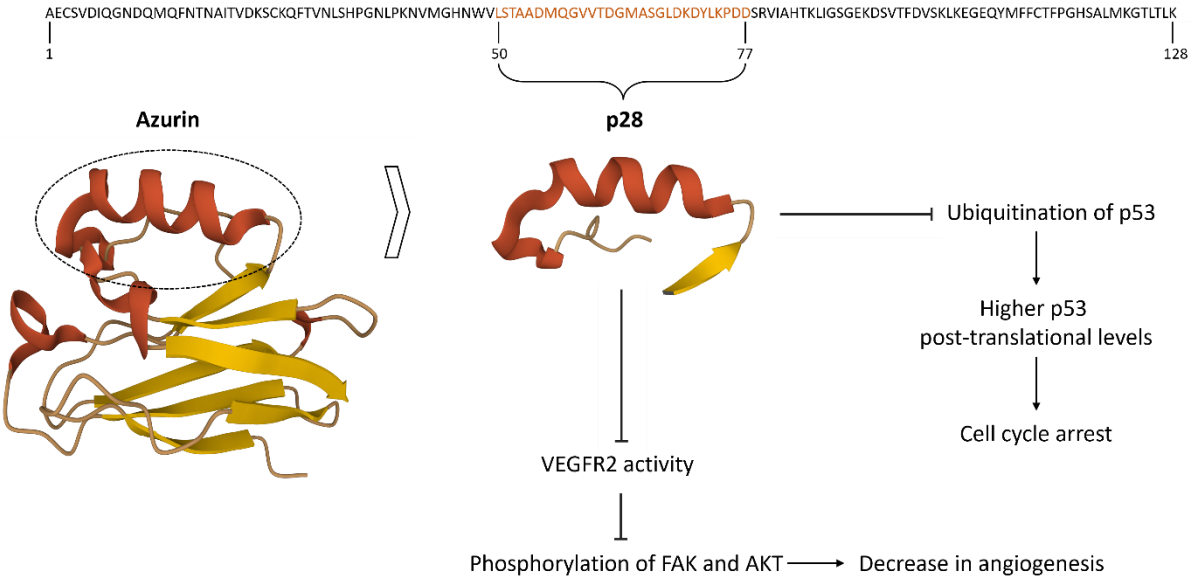

Figure 5 - Structure of azurin from *Pseudomonas aeruginosa* and of p28. The primary structure of azurin and of p28 (dark orange) are shown. The ribbon drawing of azurin is color-coded based on the secondary structure, the beta sheets are represented by yellow, and the alpha helix is represented by dark orange. The ribbon drawing of azurin (1jzg) and of p28 were generated using the structure available at Protein Data Bank. Additionally, the mechanism by which p28 can exert its anti-cancer properties, anti-proliferative, through the increase of the post-translational levels of p53, and anti-angiogenic, through the inhibition of the VEGFR2 activity are shown. FAK - Focal Adhesion Kinase, AKT - Protein Kinase B.

1.5. Aims and Motivation

A total of 18,1 million new cancer cases were reported in 2020 [2]. And one of the main causes of worldwide mortality is cancer [2]. Unfortunately, current treatments do not efficiently address this pathology, resulting in poor success rates and a lack of selectivity that can lead to serious side effects as well as damage and loss of healthy tissue [7], [8].

By encapsulating current chemotherapeutic drugs in NDDS, it is possible to improve the overall effectiveness and specificity of these medicines [9]. However, nowadays most widely used solutions are of synthetic nature, which do not fully capture the complexity of the cellular membrane, and may present some drawbacks such as substantial toxicity, rapid clearance from the body, and poor biological barrier crossing [111], [217].

These problems can be overcome by EVs, which naturally occur in biological organisms and have high biocompatibility [10]. Additionally, they are more efficient at crossing biological barriers [11] such as the BBB, and at delivering miRNAs [218], which can be used as effective therapeutics for a variety of pathologies [219], including cancer [220].

Particularly, EVs derived from MSC are the carriers of some therapeutic properties of these cells and as a result, should exhibit low immunogenicity [126] and high safety. Therefore, it may be possible to develop off-the-shelf products for allogeneic therapies based on MSC-EVs. Moreover, there are already reliable platforms available for MSC expansion due to the widespread use of these cells in cellular therapies, which can also be taken advantage of for EV production.

This work aims to produce and isolate EVs, from primary human MSC, through a process that is closely translatable to clinical practice. Recently, during a collaborative partnership developed for Doctor Miguel Fuzeta PhD studies [188] with the University Medical Center Utrecht (UMC Utrecht), our group aimed to produce MSC-EVs using serum/xenogeneic-free (S/X-F) cell culture conditions and then isolated using a GMP-compatible scalable and selective isolation technique that combines TFF and SEC. Thus, one aim of this thesis was to introduce and establish these methodologies in our facilities, envisaging also its optimization. Additionally, apart from the utilization of this methodology for isolating EVs from primary cells, we also aimed to employ the method, for immortalized cell lines, since it may be useful for several therapeutic purposes. With that objective, MDA-MB-231, a triple negative, metastatic breast cancer cell line was used for EV production.

Subsequently, as this work is part of a project that aims at developing a NDDS using MSC-EVs functionalized with p28 for targeted cancer therapy, we will investigate the influence of this functionalization on MSC-EV uptake by cancer cells, hoping that p28 will facilitate greater cancer cell penetration. It is, in fact, essential to develop a NDDS with improved targeting capabilities since naive EVs cannot accumulate at clinically relevant numbers in the targeted tissues after systemic exogenous administration [110], [221].

And as part of the partnership with UMC Utrecht, we also aim at testing the functionalization of EVs derived from MDA-MB-231 with p28 to, in the future, assess the effect of this surface modification on the effectiveness of EVs-p28 in functionally delivering RNAs. The CRISPR-operated stoplight system for functional intercellular RNA exchange (CROSS-FIRE) [174], a recently developed innovative system developed in this cell line, will be used to accomplish this aim. Moreover, this cancer cell line exhibits

significant robustness in cell culture conditions and rapid proliferation, making it a viable option for EV production when envisaging scalability, for the manufacturing of EV-based NDDS for targeted cancer therapy. However, more research is necessary to determine the safety of EVs derived from cancer cells.

2. Materials and Methods

2.1. MSC(BM) isolation from human samples

The human MSC(BM) used in this study are part of the cell bank available at the Stem Cell Engineering Research Group (SCERG), iBB - Institute for Bioengineering and Biosciences. MSC(BM) were isolated following an adapted version of the cell isolation protocol described by Santos et al. using human platelet lysate (hPL) - supplemented medium instead of fetal bovine serum (FBS) [222]. Human tissue utilized to isolate cells was obtained under a collaboration agreement of iBB-IST and Instituto Português de Oncologia, Francisco Gentil, Lisboa. These human samples were collected from healthy donors after informed written consent according to the Directive 2004/23/EC of the European Parliament and of the Council of 31 March 2004 on setting standards of quality and safety for the donation, procurement, testing, and processing, preservation, storage and distribution of human tissues and cells (Portuguese Law 22/2007, June 29) with the approval of the Ethics Committee of the clinical institution. Human MSC(BM) were cryopreserved in cryovials (ABDOS) in culture medium containing 10% (v/v) dimethyl sulfoxide (DMSO) (Sigma Aldrich), in a liquid/vapor-phase nitrogen container.

2.2. Cell thawing

Both MSC(BM) and the cell line MDA-MB-231 kindly provided by Dr Pieter Vader (UMC Utrecht) were utilized for EV production. Cryovials containing cells were retrieved from the cryostorage to be thawed. MDA-MB-231 were cryopreserved in cryovials (ABDOS) in culture medium containing 10% (v/v) DMSO (Sigma Aldrich), in a liquid/vapor-phase nitrogen container. MSC(BM) were thawed at P2, P3, or P4. And MDA-MB-231 were thawed at P13 and P19. After depressurizing the cryovial inside the flow hood and partially thawing the material in a 37ºC water bath, 5 mL of warm supplemented medium was used to fully thaw the cells.

For MSC(BM) DMEM low glucose (1 g/L) medium was supplemented with 5% (v/v) of hPL UltraGRO™ PURE (AventaCell Biomedical) and 1% Antibiotic-Antimycotic (Thermo Fisher Scientific). For MDA-MB-231 DMEM high glucose (4,5 g/L) was supplemented with 10% FBS, qualified (Gibco) and 1% Antibiotic-Antimycotic (Thermo Fisher Scientific). Centrifugation (ThermoFisher Scientific, Heraus Multifuge X1R Centrifuge) at 1250 rpm was performed for 7 minutes. And afterward, the supernatant was discarded, and the pellet resuspended in the same culture medium where cells were initially thawed. Cells were counted using the Trypan Blue (Gibco) exclusion method and, finally, MSC(BM) were inoculated in T-flasks at a seeding density of 3000 - 4000 cells/cm^2, whereas one vial containing 1 million cells of the cell line MDA-MB-231 was inoculated in a T-25 flask. Culture conditions were maintained at 37ºC, and with 5% CO_2 in a humidified atmosphere.

The culture medium was changed every 3 - 4 days until MSC(BM) reached a 70 - 80 % confluency (qualitatively assessed) and until MDA-MB-231 reached an 80 - 90 % confluency.

2.3. Cell passage and expansion

At 70 - 80% cell confluency Tryple™ Select (Gibco), a xeno-free detaching solution was applied to MSC(BM) for 7 minutes, at 37ºC. For MDA-MB-231 when a confluency of 80-90% was reached 0,05% (v/v) trypsin (Thermo Fisher Scientific) with 0,1 mM ethylenediaminetetraacetic acid (EDTA) (Sigma Aldrich) was applied for 4 minutes at 37ºC. After thawing MSC(BM) were passaged at least once before final inoculation into T-flasks for EV production at a seeding density of 3000 - 4000 cells/cm^2. MDA-MB-231 were maintained in culture from P13 to P37 and expanded when intended to be utilized for EV production. These cells were seeded at 15 000 cells/cm^2 - 39 000 cells/cm^2.

2.4. EV production

After final inoculation for EV production in T-175 flasks cells were cultured in the same conditions described before. When maximum cell confluency, 90 - 100% was achieved, MSC(BM) and MDA-MB-231 were washed with DMEM low glucose basal medium (i.e. only supplemented with 1% Antibiotic-Antimycotic) and DMEM high glucose basal medium, respectively. These basal culture mediums were used during the 48 hours conditioning period for MSC(BM) and the 24 hours conditioning period for MDA-MB-231. Additionally, for MDA-MB-231, OptiMEM™ I Reduced Serum Medium (Gibco) was also used as a conditioned medium

2.5. EV isolation from cell culture

After the conditioning period, the conditioned medium was collected and always maintained at 4ºC from this procedure onward. A 2000 x g, 15 minutes centrifugation was performed, and the supernatant underwent a bottle top filtration with a 0.45 um filter (Thermo Fisher Scientific, Nalgene)**.** For tangential flow filtration (TFF) the Minimate EVO system (PALL) is equipped with the Minimate 100 KDa MWCO Omega Membrane (PALL). And afterward, the sample undergoes size exclusion chromatography (SEC) using a HiPrep 16/60 S-400 Sephacryl column (GE Healthcare) connected to an AKTA start system (GE Healthcare). The selected EV fractions eluted from SEC are filtered through a syringe 0.45 µm filter (Corning) and concentrated with Amicons^R Ultra - 15 Centrifugal Filter Unit with a molecular weight cut-off (MWCO) of 100 kDa (Merck MilliPore) or 30 kDa, or alternativelly Amicons^R Ultra - 4 Centrifugal Filter Unit with a MWCO of 50 kDa (Merck MilliPore)

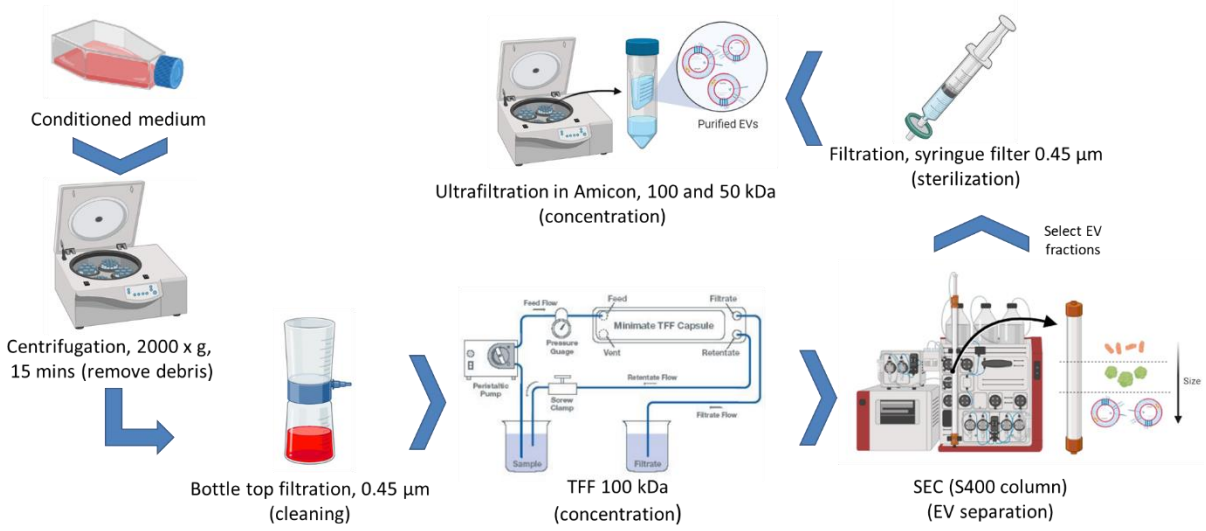

Figure 6- Workflow of the EV isolation process.

2.6. Charactherization of EVs

2.6.1. Protein Quantification

The Micro BCA™ Protein Assay Kit (Thermo Fisher Scientific) was used for the quantification of the total amount of protein in EV samples, following the guidelines for the microplate procedure provided by the manufacturer. EVs were lysed in 1x RIPA buffer (Thermo Fisher Scientific) for 10 minutes at room temperature before the quantification. Additionally, the equation obtained through the application of a linear fit to bovine serum albumin (BSA) standards was used to determine the protein concentration of each sample by measuring its absorbance. For each sample, two replicate measurements were performed. An equal final RIPA buffer concentration was used to prepare all standards and samples.

2.6.2. Nanoparticle tracking analysis (NTA)

Based on the light scattering properties and the Brownian motion of a particle, Nanoparticle Tracking Analysis (NTA) allows the quantification and determination of the size distribution of the particles present in a liquid suspension. This is achieved by focusing a laser beam on the liquid suspension, which the particles in the sample will scatter. The scattered light can be then visualized in a microscope with a 20x magnification and allows the analysis of the particle movement which is used to estimate the diffusion coefficient. Knowing the diffusion coefficient of the particles, their size can be determined through the Stokes-Einstein equation (1).

$$D = \frac{kT}{6\pi\mu R} \quad (1)$$

D: Diffusion coefficient (m^2/s);

k: Boltzman constant (1.38 x 10^{-23} m^2 kg s^{-2} K^{-1});

T: Temperature (K);

μ: Viscosity (Pa.s);

R: Radius (m)

NTA measurements were performed with a NanoSight LM10 instrument (Malvern) equipped with a sample chamber and a 405 nm laser. The NTA 3.1 software was utilized for capture and analysis. Before measurements, samples were diluted in PBS to obtain a final concentration in the range of 5 x10^8 to 2 x10^9 particles/mL. Each sample was recorded 10 times for 30 seconds using a scripted function for control and each new acquisition was achieved by pushing new sample to the detection chamber. The acquisition and post-acquisition settings were kept constant for all similar samples.
A detection threshold of 5 was set for all samples measured. The Camera level settings were set to 15 for measurements of the processed sample of EVs, the TFF filtrate, and TFF concentrate as well as for the SEC filtered fractions. Whereas, for the centrifuged and filtered conditioned medium and OptiMEM the camera level was set to 14.

2.7. Peptide synthesis

The CP05-p28 peptide was synthesized with a >95% purity by DG Peptides Co., Ltd. The peptides were dissolved in PBS to a final concentration of 4 mg/mL and stored at -20ºC until further use. The detailed peptide sequence and the molecular weight are shown in table 1.

Table 1 - Name, amino acid sequence, and molecular weight of the peptide used in the study

Name	Amino acid sequence	Molecular Weight (g/mol)
CP05-$(GGGGS)_2$-Myc-p28	CRHSQMTVTSRL-GGGGSGGGGS-EQKLISEEDL-DDPKLYDKDLGSAMGDTVVGQMDAATSL	6130.77

2.8. Peptide detection (dot blots)

EV samples are lysed in Triton X - 100, 0.01% (v/v) for 10 minutes at room temperature. Afterward, EV samples and the free peptide are heated at 95ºC, for 10 minutes. The samples were spotted on a nitrocellulose membrane using a dot blot apparatus (Bio-Rad). And blocking of the membrane was performed with 5% BSA (Thermo Fisher Scientific**)** in TBS-Tween (Thermo Fisher Scientific) for 1 hour at room temperature, followed by overnight incubation at 4ºC with a mouse anti-Myc primary antibody (Sigma Aldrich) (1:5000 dilution) and incubation with the HRP anti-mouse secondary antibody (Sigma

Aldrich) diluted in blocking buffer (1:1000 dilution) for 1 hour at room temperature. Membranes were visualized using iBright™ CL1500 Imaging System (ThermoFisher) after treatment with SuperSignal™ West Pico PLUS Chemiluminescent Substrate (ThermoFisher). The signal intensity was quantified in ImageJ using the “Gels" analysis tools.

2.9. EV uptake studies

MSC(BM) derived EVs and MDA-MB-231 derived EVs were labelled with the fluorescent dye AlexaFluor 647 NHS Ester (Invitrogen™) This lyophilized dye was dissolved at a concentration of 10 mg/mL DMSO (Sigma Aldrich). The EVs were mixed with sodium bicarbonate (Sigma Aldrich) (pH 8.3m 100 mM final concentration) and 0,625% (v/v) of Alexa Fluor 647 NHS ester (Thermo Fisher Scientific) (10 mg/mL in DMSO), and the mixture was incubated for 1 hour at 37 ºC in a shaker incubator at 450 rpm, followed by a dilution in PBS and quenching of the reaction with 100 mM Tris-HCl (Invitrogen) for 20 minutes at room temperature, where agitation was performed every 5 minutes, for the whole 20 minutes in a final volume of 1 mL.

Through SEC, using an XK-16/20 column (GE Healthcare) packed with Sepharose CL-4B (Sigma Aldrich), the unbound dye was separated from labelled EVs. The fractions containing EVs were pooled and filtered through a syringe filter, 0.45 um, as well as concentrated using Amicons^{R} Ultra - 4 Centrifugal Filter Unit with an MWCO of 100 kDa (Merck MilliPore), 10 kDa (Merck MilliPore) or 3 kDa (Merck MilliPore).

Finally, the stained EVs are characterized through NTA, and the fluorescence of the sample is measured in a plate reader (Tecan, infinite M200 PRO).

Labeled EVs were incubated with the peptide ata ratio of 50 ug of peptide / 10^{10} particles, for 2 hours at room temperature (RT). After incubation, the unbound peptide was washed out using a 100 kDa or 50 kDa MWCO Amicon^{R} Ultra-15 centrifugal filter unit (Merck MilliPore). The centrifugation conditions were 3000 x g, at 4ºC for c.a. 3 minutes for 100 kDa Amicons and c.a. 5 minutes when using 50 kDa Amicons. Washing was performed 3 times with 4 mL of PBS filtering until a final volume of c.a. 100 uL.

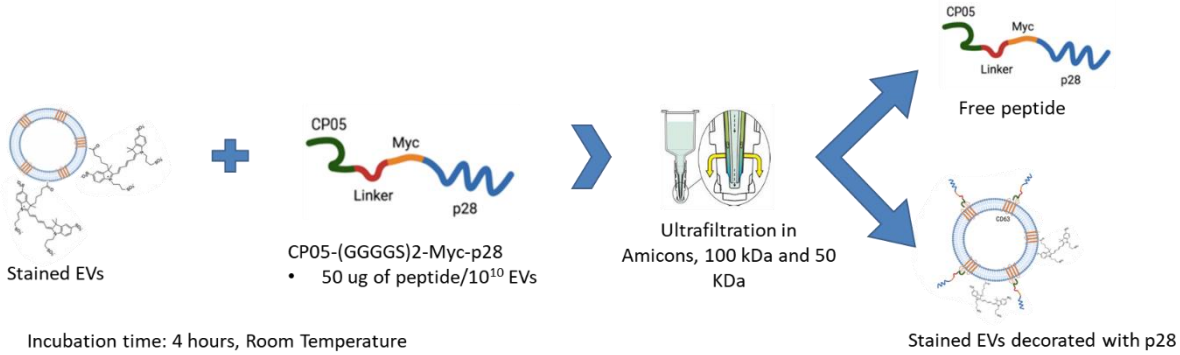

Figure 7 – Diagram of the workflow utilized for the functionalization of EVs with CP05-p28 (not to scale)**.**

MDA-MB-231 cells were seeded at 50,000 per well (156 250 cells/cm^2) in a flat bottom 96 well plate in DMEM high glucose supplemented with 10% FBS, qualified (Gibco) and 1% Antibiotic-Antimycotic

(Thermo Fisher Scientific). After 24 hours, the labeled EVs decorated with the peptide were added to the cells, and the mixture was incubated for 4 hours in a humidified atmosphere at 37ºC, with 5% CO_2. After the incubation period, cells were washed once with PBS, detached from the wells using 0,05% (v/v) trypsin (Thermo Fisher Scientific) with 1 mM EDTA (Sigma Aldrich), resuspended in culture medium, and transferred to FACS tubes. The tubes were centrifuged for 5 minutes at 350 x g, and the pellet was resuspended in FACS buffer (1 mM EDTA (Sigma Aldrich) with 2% of heat inactivated FBS, qualified (Gibco) in PBS). Lastly, cells were analysed on a Flow Cytometer (Becton Dickinson, FACSCalibur), and the results were further analysed with FlowJo software.

3. Results and Discussion

3.1. Isolation of Mesenchymal stromal cell – derived extracellular vesicles

3.1.1. Cell confluence and heterogeneity in tissue flasks' surface distribution impact MSC-EV yield

The quantity of EVs produced in each of the batches performed in the context of this work (BM EVs SEC 3, BM EVs SEC 4, BM EVs SEC 5, BM EVs SEC 6, and BM EVs SEC 7) substantially oscillated, comprising values between 1.13 x 10^9 and 1.87 x 10^{10} MSC-EVs per T-175 culture flask (Figure 8A), or 3.06 x 10^{10} to 9.06 x 10^{11} EVs per batch. These differences can be attributed to changes in upstream or downstream processing conditions that can significantly modulate the quantity of EVs produced and isolated. Additionally, the degree of the scale-out also varied greatly, ranging from 25 to 48 T-flasks (Figure 8B)**.**

The homogeneity in the distribution on the T-flask surface during expansion and the cell confluency at the beginning of the periods of cell conditioning fluctuated greatly among batches. Having a homogenous layer and high confluency (90-100%) of growing MSC during expansion is crucial for their survival during conditioning, where cells are cultured in a non-supplemented cell culture medium and hence do not have at their disposal the growth factors that are vital to sustain cell survival. When heterogeneity is high, the cells located at the lower confluency zones lose their viability significantly during the period of conditioning, detaching from the flask. This was the case of batch BM EVs SEC 6, and it may account for the fact that this batch, among all others, presents a lower quantity of cells at the end of the conditioning period (Figure 8B). In such a situation it is challenging to achieve a homogenous cell layer. This is the case because cell proliferation at, a certain stage, results in over confluence in some areas, possibly leading to the detachment of these cells while, at the same time, in zones of decreased cell density cells reach normal confluence. Of note, larger surfaces, such as in T-175 culture flasks, are generally associated with higher heterogeneity that needs to be controlled so that it does not impact greatly the conditioning period.

A

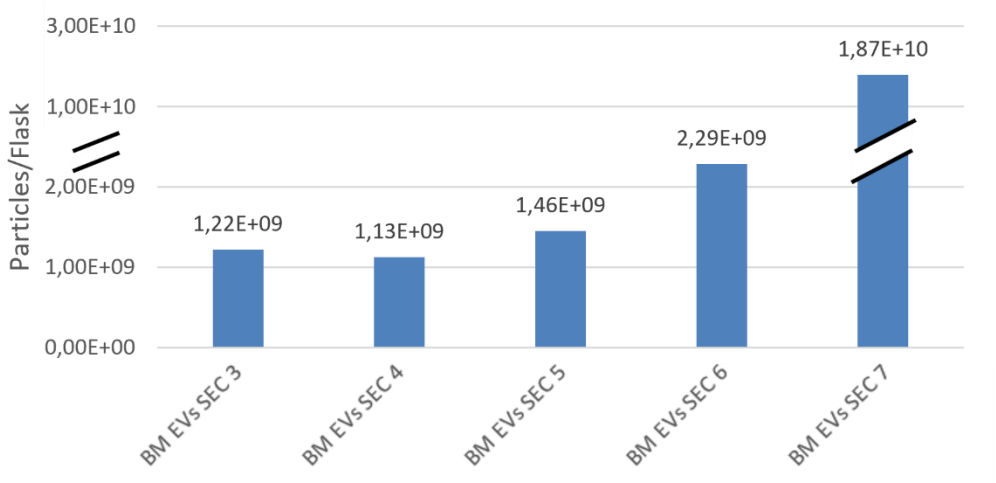

B

Assay No.	No. Cells/T-175	No. of T-175	Total No. Of EVs	MWCO of Amicons (kDa)
BM EVs SEC 3	3,28 x 10^6	25	3,06 x 10^{10}	100
BM EVs SEC 4	1,08 x 10^6	35	3,96 x 10^{10}	100
BM EVs SEC 5	1,73 x 10^6	40	5,83 x 10^{10}	50
BM EVs SEC 6	9,93 x 10^5	29	8,85 x 10^{10}	50
BM EVs SEC 7	2,75 x 10^6	48 (+1 x T-75)	9,06 x 10^{11}	30

C

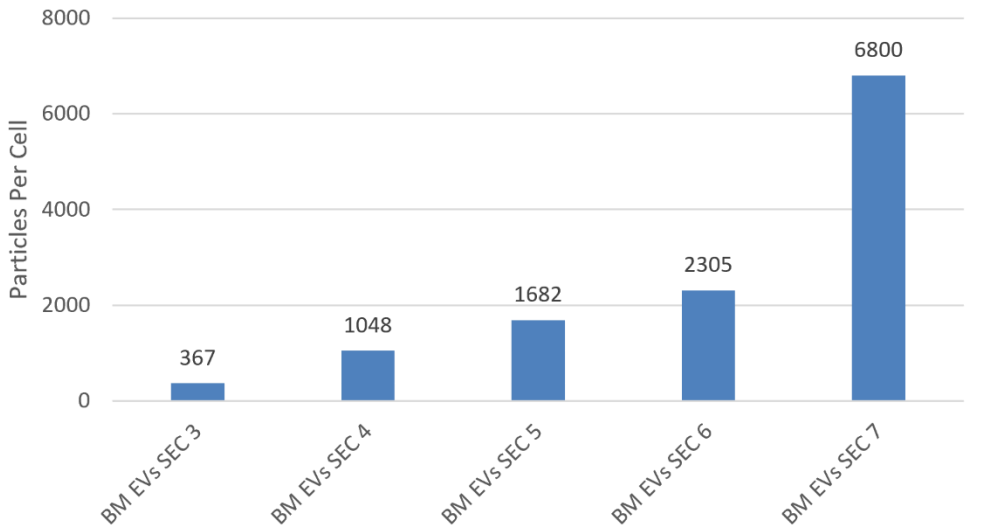

Figure 8 – **Production of MSC-EVs. A)** Number of particles isolated per T-175 culture flask. **B)** Comparison between batches considering the number of cells per T-175 flask at the end of the conditioning period, the size of each batch, i.e., the number of T-175 flasks (20 mL of cell culture medium each), the total number of particles isolated and the MWCO of the amicons ultra centrifugal units used in each batch. **C)** Quantity of particles produced by each cell, quantified at the final of the isolation protocol. MWCO - molecular weight cut off.

In batches BM EVs SEC 3, BM EVs SEC 4, and BM EVs SEC 5 even though moderate homogeneity was observed, the moderate confluence of cells (60% to 70%) led to losses in cell viability, during the conditioning period and as a result, fewer cells producing EVs leading to an overall decreased efficiency in terms of EV production. It is thus concluded that when confluences lower than 60% to 70% are present, it is not appropriate to switch to basal DMEM medium, because it will result in substantial cell death during the long 48 hours conditioning period. However, even though considerable losses of cell viability along with cell detachment were observed during these 48 hours, the cellular viability, of plastic-attached cells, was determined to be above 97% in all the assays, possibly because most of the dead cells detached from the plastic. This is an important parameter that should be captured at the end of conditioning periods since even a small percentage of cell death can release cell membranes to the cell-conditioned medium, which can outnumber the quantity of EVs released [150].

Only cells in T-flasks that reach high confluence (85 - 100%) were found to be robust enough to maintain viability and thrive under periods of conditioning, which was the case for BM EVs SEC 7. This may be associated with factors released by MSC to the extracellular space as well as the secretion of ECM, which may lead to higher gradients of concentration of these beneficial factors in high confluence areas that result in a boost in the cell robustness in such areas. However, these conclusions were reached only by observations at the phenotypic level. A more in-depth experience concerning cell stress, accessed for instance through the levels of lactate dehydrogenase (LDH) release or about cell metabolism when these are maintained in basal medium are required to obtain more quantitative data.

In the present work, the fine tuning of some procedures associated with the upstream processing was achieved, as can be observed by the increase of the EVs isolated per T-175 culture flask in the batch BM EVs SEC 7 in comparison to other MSC-EV batches, this was a substantial challenge as limited number of EVs were obtained through several of the batches. As such the application of additional strategies to increase EV production may be necessary.

For example, the use of 3D dynamic upstream, e.g., hollow-fiber, Vertical-Wheel^{TM} bioreactor , and stirred tank conditions may lead to obtaining higher yields of EVs [223]–[225]. Moreover, as bioreactors add options for a dynamic monitoring of cell culture conditions, these may be beneficial for productions under GMP conditions. However, their implementation is not straightforward demanding extensive work and technical expertise to be handled, in comparison to 2D static approaches. Additionally, other modalities of MSC cultures, such as growth as suspended spheroids were already demonstrated to lead to increased EV production. The use of environmental, chemical or mechanical stimuli to induce EV production can also be applied. The stimulation conditions may comprise hypoxia, shear stress, ultrasounds, the addition of anti-inflammatory drugs, or the addition of cytokines. However, those can also induce unpredictable changes in the characteristics of EVs which may affect their functional properties, and as such should be carefully analyzed. Moreover, the use of an MSC cell source that is more productive in terms of EV release than the BM can also be adopted. MSC(WJ) were already reported to fit in that category [224], [226].

In sum, the production of EVs was conducted under S/X-F conditions, and we concluded that high levels of cell confluence and homogeneity in the distribution on the T-flask surface should be maintained during periods of conditioning to maximize both cell viability and EV production.

3.1.2. Protocol optimization for isolating MSC-EVs comprising tangential flow filtration (TFF) and size exclusion chromatography (SEC)

TFF is the first operation unit used to concentrate the large conditioned media volumes to a final volume that is suitable to proceed through SEC. Figure 9A displays the decay in the TFF filtrate flow throughout its use in different batches of EVs. This may suggest a cumulative clogging of the TFF membrane and can account for substantial losses of EVs during their processing in this operation unit as well as a decrease in the time efficiency of the procedure. The filtrate flows started to be replenished (in Filtration 6) after the use of a more concentrated sodium hydroxide solution in the typical wash and store routine of the membrane. As such the use of this concentrated solution is suggested for future experiments.

The TFF-concentrated cell culture-conditioned medium will then be processed through SEC. The task of selecting the appropriate fractions where EVs were eluted through the interpretation of the SEC chromatogram is crucial. Those are essentially selected considering the ultraviolet light of wavelength 280 nm (UV280) absorbance measured in the eluent displayed in the chromatogram. In Figure 9B**,** a representative chromatogram of the TFF-concentrated conditioned medium is shown. The EV fractions are selected from the first UV280 absorbance peak placement, usually between the 7^{th} and 18^{th} fractions, because these are the higher dimension particles present in the sample, that as a result are the first to be eluted.

The amplitude of the EV elution correspondent peaks, obtained by subtracting the maximum milli-absorbance unit (mAu) value of the peak and the mAu at the base of the UV peak, oscillated substantially among the assays. This value usually correlates to the quantity of biological material in the sample, however, intrinsic variations of SEC procedure, such as slight alterations in the volume eluted in each SEC fraction were also observed. As such the amplitude values may not be directly indicative of the amount of EVs isolated and a more quantitative approach such as determining the area under the curve may be adopted in the future to quantify the total amount of EVs per batch.

Two pools of elution fractions were collected when no peak or lower peaks of UV280 absorbance intensity were displayed in the chromatogram (Supplementary Figure 1). The objective of collecting an additional pool outside the range of fractions expected is to assess whether a significant number of particles was being eluted in those fractions. However, most of those uncommon fractions did not contain a significant number of particles, except for the batch BM EVs SEC 5 pool B, in which the not common pool to be collected since it is very close to the peak that is more correlated to soluble proteins contained a substantial number of particles. It was hypothesized that such a number of particles could be because of a high level of protein aggregates. Since the quantification of the protein present through MicroBCA, was not possible, this pool was also discarded.

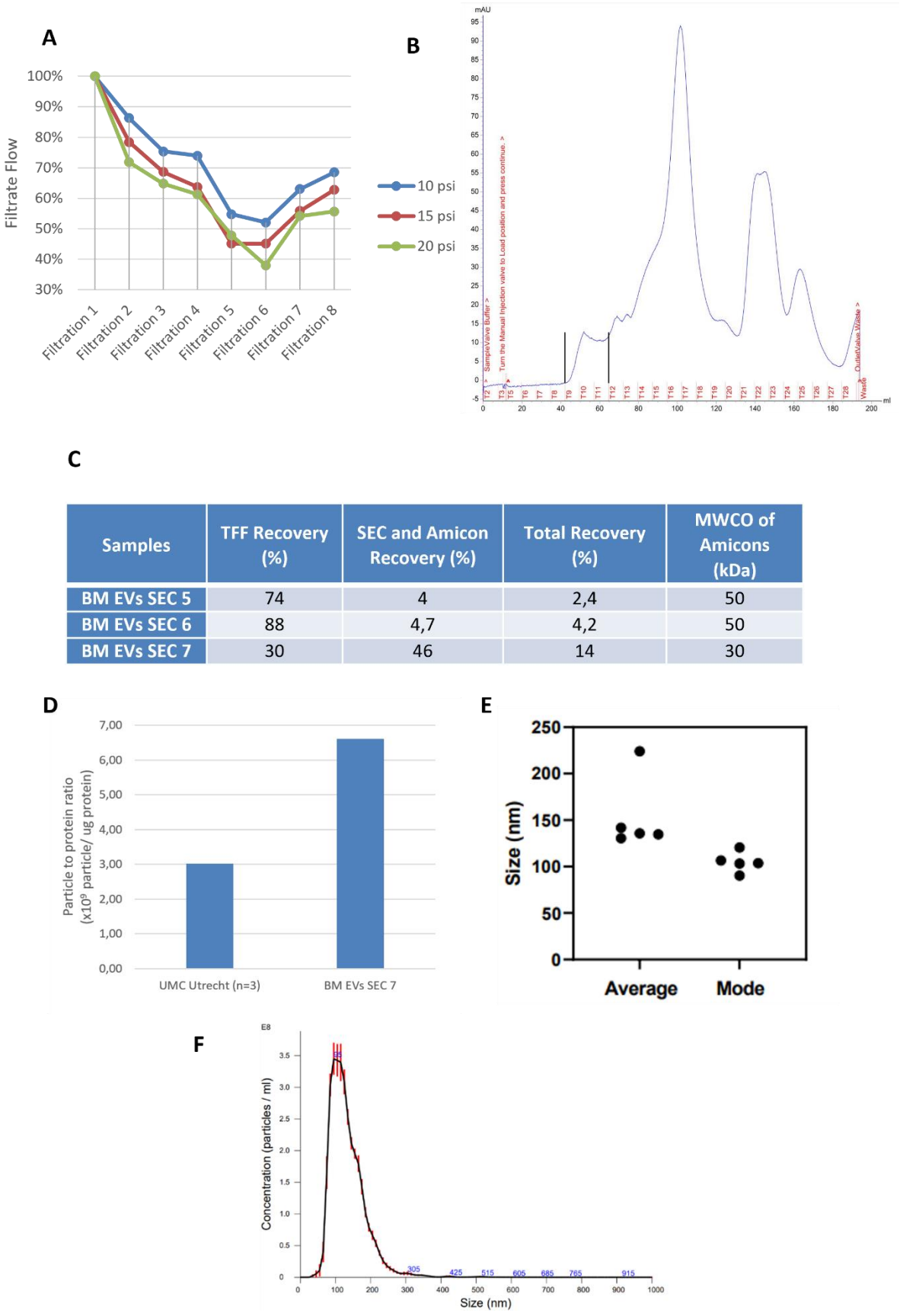

Samples	TFF Recovery (%)	SEC and Amicon Recovery (%)	Total Recovery (%)	MWCO of Amicons (kDa)
BM EVs SEC 5	74	4	2,4	50
BM EVs SEC 6	88	4,7	4,2	50
BM EVs SEC 7	30	46	14	30

Figure 9- Characteristics of MSC-EVs. **A)** Variations in the filtrate flow of the TFF through all the assays performed. **B)** Representative fractionation of the TFF concentrated cell conditioning medium (BM EVs SEC 7). The ultraviolet light of wavelength 280 nm (UV280) (blue line) was measured in the

eluent. The fractions of the first peak area contain EVs, whereas smaller constituents of the cell conditioning medium, such as contaminating proteins are contained in later fractions. The y-axis represents the UV280 absorbance in milli-absorbance units and the x-axis represents the volume eluted through the column since the start of the sample elution. **C)** Comparison of the MSC-EV recovery through the various operation units of the EV isolation protocol. **D)** Comparison between the particle-to-protein ratio (PPR) of batch BM EVs SEC 7 and previous work [188] developed with a similar experimental setup (UMC-Utrecht (n=3)). **E)** EV average size and mode of size (n=5, technical replicates). **F)** Representative NTA size distribution curves of MSC-EVs, obtained from BM EVs SEC 7. PPR - particle to protein ratio. TFF- Tangential Flow Filtration. SEC – Size Exclusion Chromatography NTA - Nanoparticle Tracking Analysis. UMC Utrecht - University Medical Center Utrecht. (Filtration 1 - BM EVs SEC 4, Filtration 2 – MDA EVs SEC 1, Filtration 3 – MDA EVs SEC 2, Filtration 4 – BM EVs SEC 5, Filtration 5 - MDA EVs SEC 3, Filtration 6 - OptiMEM, Filtration 7 – BM EVs SEC 6, Filtration 8 - BM EVs SEC 7)**.**

Impact of the MWCO of amicons ultra centrifugal units in EV recovery

In this work, we tested different molecular weight cut-offs (MWCO) of the amicon ultra centrifugal units during the ultrafiltration (UF) applied to EVs after SEC separation. The objective was to evaluate how this factor influences the loss of EVs in the UF operation unit. In fact, it was noticed that a decrease in the MWCO leads to an increase in the EV yield (Figure 9C). This was evaluated through the SEC and amicon recoveries and assumes that the SEC recoveries remained constant among the assays.

Evidence that points out to similar conclusions reported that the utilization of MWCO amicons of 10 kDa yielded significantly higher particle recoveries in comparison to 100 kDa MWCO amicons [227], [228]. Additionally, the volume of amicons here utilized (15 mL) was demonstrated to be more efficient in terms of particle recovery in comparison to lower volume amicons (4mL) [226].

Moreover, it is well known that during these concentration steps many of the EVs are lost because of adhesion, aggregation as well as destruction [227] and additional strategies aimed at further improving EV recoveries may encompass the pre-treatment of the membranes of amicons ultra centrifugal units to decrease non-specific adsorption of the EVs, which leads to their loss. Detergents such as 5% Tween 80 were already shown to decrease the unspecific membrane binding of compounds [229], however, possible remnant detergent can pose challenges to the isolation of EVs, and possibly leads to alterations in EV structure, something that may be worth to investigate. Additionally, the problems of non-specific membrane binding render the UF process more time inefficient since it leads to a decreased filtrate flux.

In addition, similarly to the quantity of EVs isolated in each batch, the MSC-EV productivity also oscillated substantially, being comprehended in between 367 and 6800 EVs released per cell (Figure 8C). This is possibly associated with batch variability in terms of cell homogeneity, viability, and heterogeneity, however, the MWCO of amicon ultra centrifugal units used for SEC-isolated EVs UF also impacted the total number of EVs isolated from each batch.

EV characteristics and remarks concerning EV isolation

The average size of MSC-EVs did not change substantially through the assays, except for BM EVs SEC 4 where EVs present a higher mean (Figure 9E). This batch appears to be an outlier among the rest. Thus, excluding this batch, both the average size and mode of MSC-EVs are below 200 nm, in which is in the interval of sizes characteristics of small EVs (up to 200 nm). However, the NTA size distribution

curves of MSC-EVs obtained with NTA (Figure 9F, Supplementary figure 3) show populations of EVs with sizes above 200 nm, demonstrating that both small EVs, in much higher proportions, and larger EVs are isolated.

In the field of EVs it is not yet well established how the upstream and downstream processing conditions affect the characteristics and quantities of EVs produced and parameters such as cell productivity. The establishment of clear causal associations between the EV production conditions and their physicochemical and functional characteristics as well as the quantity of the EV produced could take EV investigation to the next level. It will allow for the fine tune of these parameters to obtain higher quantities of a standardized EV product, in a more efficient and reproducible manner.

In this work, regarding the characteristics of the isolated EV-based product, in batch BM EVs SEC 7 the particle-to-protein ratio (PPR), a parameter used to evaluate the purity of isolated EVs, was 6,60 x 10^9 particles / µg of protein which is more than twice the value that was obtained in preliminary work performed in UMC Utrecht (Figure 9D), showing that our optimizations in upstream and downstream processes can be leading to the co-isolation of a decreased quantity of protein content, increasing the purity of the sample. Overall, this parameter can indicate the reliability of the quantification of particle measure, as these can also detect protein aggregates.

This PPR was also higher in comparison to a study that isolated MSC-EVs through TFF (4 x 10^9 particles / µg of protein) [136], which is expectable since SEC separates a significant quantity of the protein present at the TFF concentrated cell culture conditioned medium.

Additionally, figure 9C, displays, that the particle recovery was substantially variable, especially when comparing BM EVs SEC 7 with other assays. It may be the case that the significantly higher quantities of particles that were present in this batch in comparison to others, may have impacted EV recovery and therefore significantly altered these recovery values.

All things considered, the method of EV isolation here employed, TFF combined with SEC provides high specificity of the particles isolated, i.e., recovery of lower quantities of non-vesicular material, but provides a low yield. In fact, in the field of EVs, there is still no method that presents a high purity and high specificity, which would be the ideal situation, and prevent the compromise that must be made when employing an isolation strategy since the relationship between purity and yield is inversely proportional. However, SEC may present several advantages in comparison to other techniques. Firstly, precipitation kits, which are commercially available, present a high EV yield but a low purity, causing the isolation of vesicular and non-vesicular material (i.e., almost the entire secretome), being considered far from ideal when aiming to study and attribute specific functional characteristics to EVs. Ultracentrifugation techniques are the golden standard, providing EVs with higher purity, and as such, are more suitable when aiming to study EV functional properties. This is also the case for SEC. However, ultracentrifugation-based methods, unlike SEC, present the possibility of leading to protein aggregation as well as EV damage caused by the high forces applied. In contrast, SEC is a gentle method that is more reproducible because it is not operator-dependent, allowing for a more reliable and scalable EV isolation compatible with functional studies of EVs. In addition, scalability, a feature that is provided by SEC and TFF, but not by ultracentrifugation, is important to produce EVs aimed at the

treatment of patients, since this requires large doses of EVs [230], for example between 1 x 10^{11} to 4 x 10^{11} (total number of EVs necessary for a 10-day treatment) (NCT04602442)

Furthermore, the limitations of the production of MSC-EVs under clinically relevant conditions, employed by using S/X-F conditions and a scalable and selective isolation method combining SEC and TFF include the fact that the particles isolated were exclusively characterized in terms of size distribution, quantity, and PPR. Positive EV protein markers were not detected in the isolation of EVs during this research as suggested in MISEV 2018 [150]. Nonetheless, preliminary work [188] using the same MSC donor and experimental setup permitted the confirmation of important surface markers such as CD9, CD63, CD81, TSG101, and Alix, by Western blot providing evidence of the identity of the EV nature of the TFF-SEC isolated particles here obtained. Further characterization of isolated EV morphology can be attained through TEM, as well as AFM. Additionally, dynamic light scattering (DLS) would characterize EVs regarding their zeta potential. Such extensive EV characterization will allow for the evaluation of the reproducibility of the EV batches produced by the protocol here described that will be used for functional assays.

In sum, the isolation of EVs was accomplished under circumstances that are closely translatable to clinical settings. The quantity of EVs recovered may increase with the reduction in the MWCO of the amicon ultra centrifugal units used for EV UF. And the PPR was found to be in a similar magnitude to what was previously obtained using this experimental setup [188], and even higher, indicating a lower level of protein contamination. In addition, the EVs isolated were mostly below 200 nm, being considered small EVs.

3.1.3. MSC-EVs can be successfully labeled with Alexa Fluor™ 647 NHS Ester

After EV isolation the protocol of EV labeling is the following task when aiming to characterize possible improvements on cellular uptake. Separation of EVs from the unbounded dye after labeling is performed using SEC followed by concentration of EV-containing fractions by amicon-based UF. Figure 10A shows the chromatogram of the separation of the stained EVs and the unbound dye, Alexa Fluor 647 NHS Ester, in the BM EVs SEC 7 batch in which higher yields were obtained. Two ultraviolet light of wavelength 280 nm (UV280) absorbance peaks (blue line) are displayed in this chromatogram. The first corresponds to the elution of EVs and the second and most intense peak to the elution of the unbound dye as this substance has a lower molecular weight (MW) than EVs. All batches except BM EVs SEC 4 display an EV-associated UV280 absorbance peak (Figure 10A, and Supplementary figure 4). This, similarly to what is observed in the SEC firstly used to separate EVs from other conditioned medium (CM) substances can be associated with variability intrinsic to SEC and the samples. In such cases, the choice of fractions is done based on the most common fractions where EVs are usually eluted.

Besides the amount of starting material and SEC-induced loss of EVs, the MWCO of amicons ultracentrifugal unit also influences the EV quantity to be recovered. In fact, envisaging to improve the yield of the UF, which is often substantially low, amicons of different MWCO were tested. A yield of 14% was determined when using an MWCO of 10 kDa and an 18% EV recovery was associated with ultrafiltration performed with 3 kDa amicon ultracentrifugal units (Figure 10B). This suggests an increase

in EV recovery when lower MWCO are utilized. However. this conclusion is drawn from a limited number of experiments and as such should be confirmed in a more extensive evaluation. For instance, as this comparison is made between BM EVs SEC 6 and BM EVs SEC 7 the high discrepancy in the quantity of EVs yielded in both batches at the beginning of the process may also account for the variability observed in the ultrafiltration yields. Nonetheless, despite comparable, the recoveries here obtained are lower in comparison to what is reported in previous studies, where 4 mL 10 kDa amicons yielded a 26% (±4.4) particle recovery, even though the membrane material utilized is the same. As state previously, the quantity of particles loaded into the amicon ultra centrifugal filter may be a factor that influences these results [227].

As shown in Figure 10C the higher the quantity of isolated EVs the higher the maximum fluorescence intensity value displayed in the emission scans of the labeled EVs. For instance, in BM EVs SEC 7 higher intensities of fluorescence are observable in comparison with batches where lower amounts were isolated and were initially present at the beginning of labeling, e.g., BM EVs SEC 3, BM EVs SEC 4, and BM EVs SEC 5 and 6 (Pool).

A

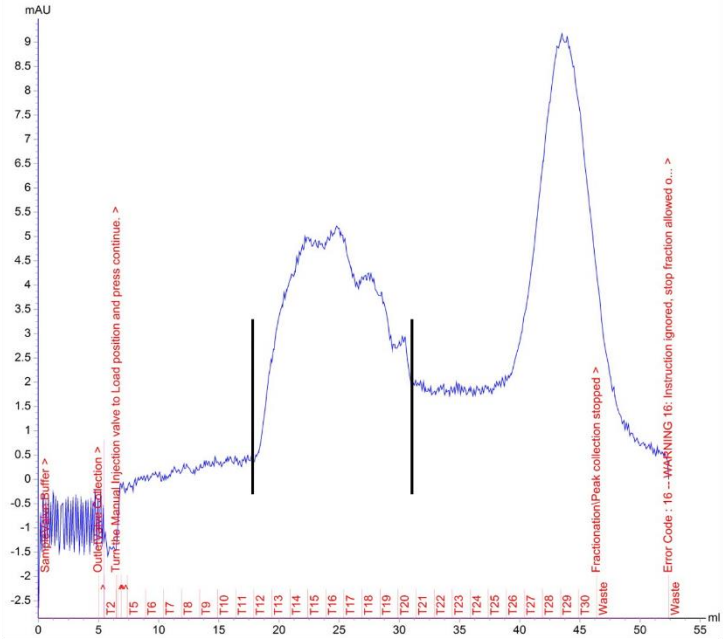

B

Samples	Total Particle no. Before Staining	Total Particle no. After Staining	Yield (%)	Amicon MWCO (kDa)
BM EVs SEC 5 and 6 (Pool)	$4{,}11 \times 10^{10}$	$5{,}85 \times 10^{9}$	14	10
BM EVs SEC 7	$9{,}06 \times 10^{11}$	$1{,}64 \times 10^{11}$	18	3

C

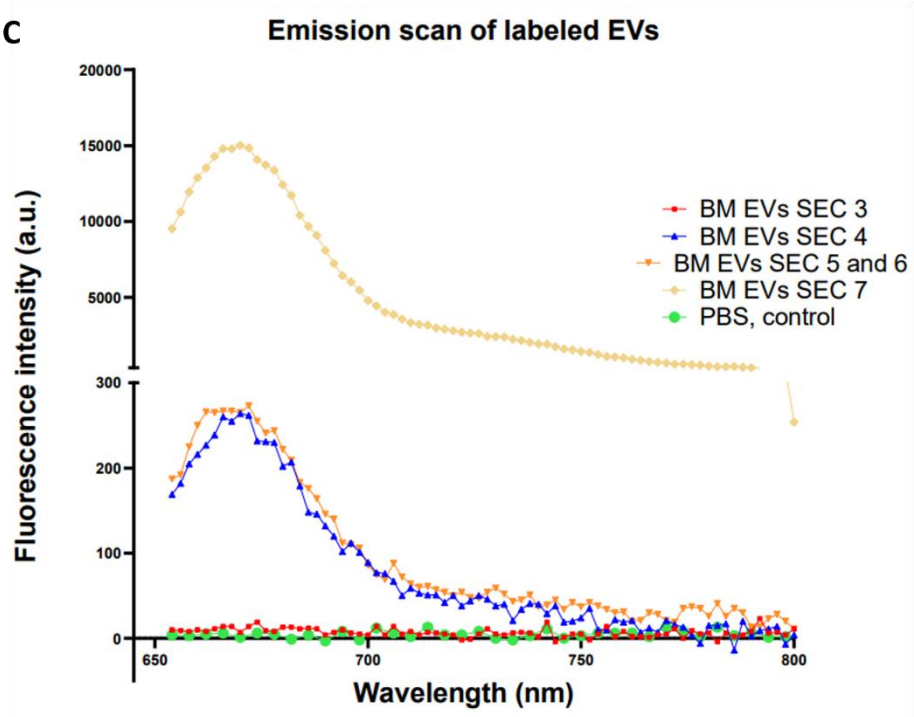

Figure 10 - **EV staining with Alexa Fluor™ 647 NHS Ester. A)** Representative fractionation of the labelled EVs (BM EVs SEC 7). The ultraviolet light of wavelength 280 nm (UV280) (blue line) was measured in the eluent. The fractions of the first peak area contain EVs, whereas the second peak

signals the fractions where the unbound dye (Alexa Fluor™ 647 NHS Ester) is being eluted. The y-axis represents the UV280 absorbance in milli-absorbance units and the x-axis represents the volume eluted through the column since the start of the sample elution. **B)** Comparison of MSC-EV yields in UF operation unit applied to labelled EVs. **C)** Comparison of the emission spectra of labelled MSC-EVs (excitation wavelength of 620 nm) of the different batches of MSC-EVs. MWCO - Molecular Weight Cut-Off

3.1.4. Decoration of EVs with CP05-p28 requires high quantities of starting EV material

A fusion peptide conjugating CP05 and p28 was used to functionalize the surface of EVs. CP05 interacts with the tetraspanins CD63 present at the surface of EVs remaining anchored. This peptide was firstly used in a study developed by Gao, X et al. (2018) to functionalize EVs for the treatment of muscular dystrophia [114].

The fusion of p28 with the rest of the peptide was performed in its C terminal because the 18 amino acid residues localized in the N terminal are identified as being the minimal motif for the internalization of p28 [207]. As such, being the most important peptide terminal for cancer cell uptake it should remain free of constraints to naturally interact with other biological structures. Additionally, a linker, $(GGGGS)_2$ was inserted in the middle of the peptide to prevent steric hindrance in this targeting moiety, which allows p28 to be freely exposed. And a c-Myc tag was also placed in between p28 and CP05 (and not in any of the terminals) in order not to create impairments in the interaction of p28 with biological structures such as cells as well as of CP05 with CD63 present at the surface of EVs. In sum, the final design of the peptide employed for EV functionalization, which was developed in previous work in the context of this study [188], consisted of CP05 - $(GGGGS)_2$ - c-Myc - p28 (Figure 11A and 11B).

Different batches of the CP05-p28 conjugation peptide were tested to assess their detectability through the Myc-tag by immunoblotting. With this purpose, different quantities of peptide, 10 µg, 5 µg, 2 µg, 1 µg, and 0,3 µg, were loaded into a dot blot apparatus. Additionally, a different peptide that consists of CP05 conjugated to a scrambled version of p28, CP05-p28Scrbl (UMC), was also tested for its detectability. This peptide consists of a version of p28 where the primary amino acid residues sequence of p28 is scrambled, which should alter the native secondary structure of the peptide as well. Moreover, CP05-p28Scrbl is intended to be used in the functionalization of EVs to serve as a control of EVs functionalized with the CP05-p28 in order to evaluate if it is the case that the mere presence of a peptide in the surface of EVs leads to their increased penetration into cancer cells, or if it is indeed the sequence and consequential 3D structure of p28 that play a role in this effect. Moreover, being able to detect the peptides used for EV functionalization through Myc-tag immunoblotting is crucial to have a rough estimative of the quantity of peptide that is bound on the surface of EVs as well as to determine if all the unbound peptide is washed out through ultrafiltration after its incubation with EVs. This guarantees that a purer EV-p28 product will be administered to cancer cells in uptake assays.

A

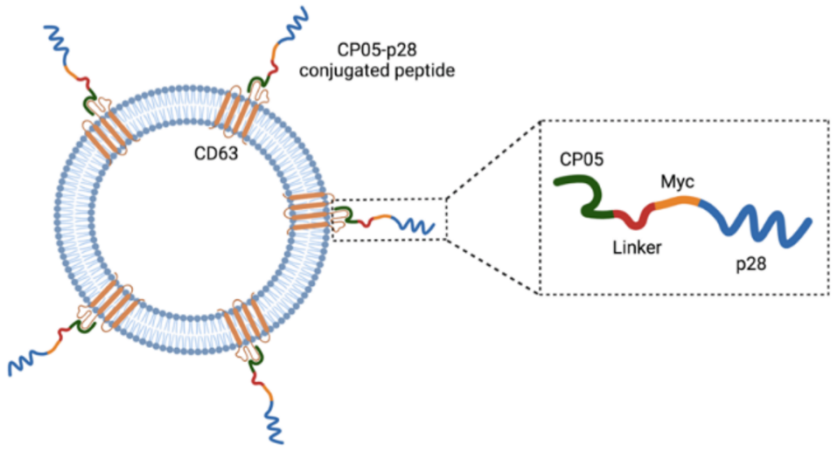

B

Nomenclature	Sequence
CP05	CRHSQMTVTSRL
p28	LSTAADMQGVVTDGMASGLDKDYLKPDD
Myc	EQKLISEEDL
Linker	$(GGGGS)_2$

Figure 11 - Design of the EV anchoring conjugated peptide CP05-p28. A) A diagram depicting the surface modification of EVs with a CP05-p28. A peptide sequence (CP05) that anchors to CD63 on the EV surface, a $(GGGGS)_2$ linker, a Myc-tag reporter, and the p28 peptide (i.e., the 28 amino acid sequence Leu^{50}-Asp^{77} from the protein azurin) comprise the final peptide design. From de Almeida Fuzeta M. et al. (2021) [188] (not to scale)**. B)** Description of the sequences that are present in the design of CP05-p28. The sequences of the peptides are presented from the N-terminal (left) to the C-terminal (right).

Of note, is that the CP05-p28 (UMC) and CP05-p28Scrbl (UMC) were stored for approximately 2 years, at -80 ºC. And CP05-p28 (2022) was freshly reconstituted, however, its purity is approximately 68%, being substantially lower than the purity of the other two peptides that is superior to 95%. These purities, however, were not considered when loading the peptide into the dot blot. This method was sensible to all the quantities of peptide-loaded, except for 0,3 µg of CP05-p28 (UMC) (Figure 12A and 12B). And, the intensity of the signal was proportional to the quantity of loaded peptide, suggesting that a longer period of storage may be more detrimental to the detection of the peptide in comparison to its purity, as the intensities of CP05-p28 (UMC) are significantly lower in comparison to CP05-p28 (2022). PBS and R2-C1C2, that was loaded at an amount of moles equivalent to 0,3 µg of CP05-p28, were used as a negative and positive control, respectively.

A

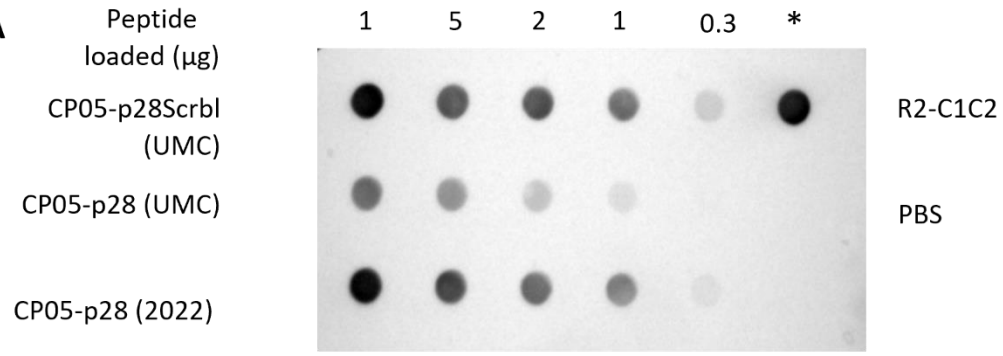

*Positive control: mol eq. to 0.3 µg of p28 peptides

B

Peptide (µg)	10	5	2	1	0.3
CP05-p28Scrbl (UMC)	103%	63%	61%	47%	12%
CP05-p28 (UMC)	50%	34%	16%	7%	1%
CP05-p28 (2022)	97%	67%	51%	39%	5%
R2-C1C2	100%				
PBS	0%				

C

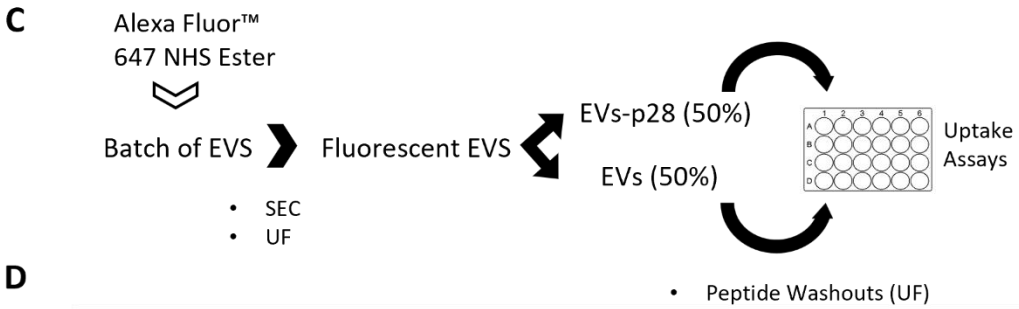

D

i)

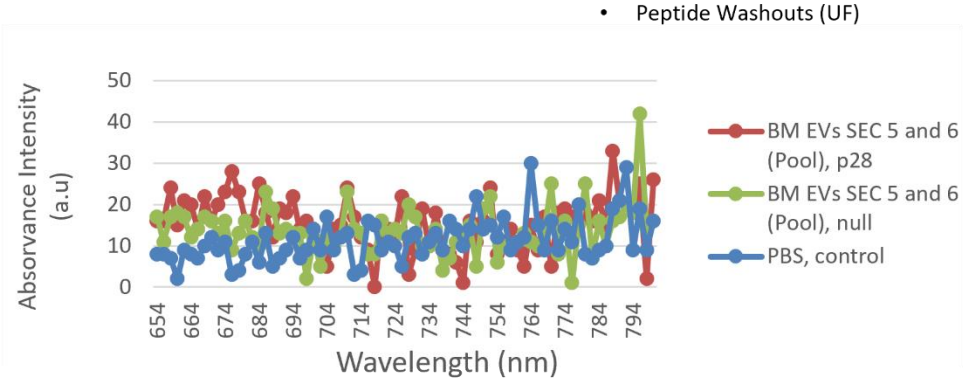

ii)

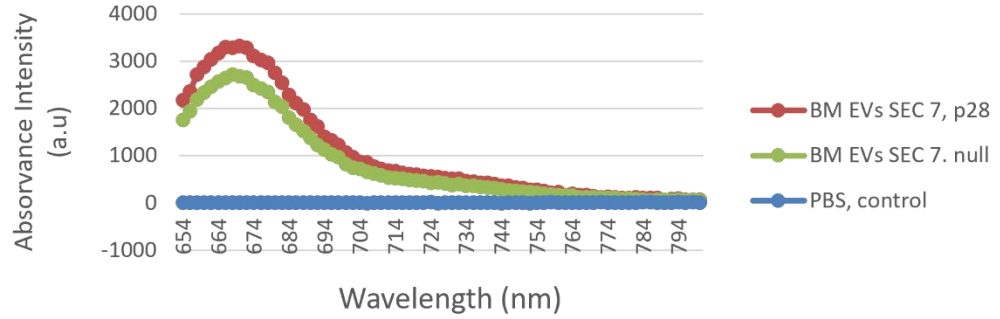

Figure 12 - Detection of CP05-p28 and functionalization of EVs with CP05-p28. A) Detection of CP05-p28 conjugation peptide through Myc-tag immunodetection in a dot blot. The peptide was loaded into the dot blot apparatus at different quantities, 10, 5, 2, 1, and 0.3 µg. PBS was utilized as a negative control and an already developed fusion protein, R2-C1C2, containing the same Myc-tag was used as a positive control. An equivalent amount of peptide molecules of R2-C1C2 as 0.3 µg of CP05-p28 conjugated peptide was loaded into the dot blot apparatus. The R2-C1C2 was generously provided by Sander Kooijmans (UMC Utrecht). **B)** Relative percentage of the signal intensity generated by the peptides loaded onto the dot blotting apparatus, considering the signal generated by R2-C1C2 as 100%. **C)** Scheme of the workflow employed for the labelling of each batch of EVs, as well as its functionalization and usage into assays of cell uptake. **D)** Emission spectrum (excitation wavelength of 620 nm) of functionalized and non-functionalized EVs. **i)** Batch where labelled functionalized and non-functionalized EVs did not display significant fluorescence in comparison with the negative control, PBS. **ii)** Batch where labelled, functionalized and non-functionalized, EVs displayed significant fluorescence in comparison with the negative control, PBS.

After the incubation of labeled EVs together with CP05-p28 (UMC) the unbound peptide was separated from the functionalized EVs through UF in either 100 kDa or 50 kDa MWCO amicon ultra centrifugal units. The number of washouts performed during this study was based on preliminary work [188] that showed that 3 washouts are sufficient for the unbound peptide to be eliminated (based on the detection of unbound peptide in amicon flowthrough by myc immunodetection)**.**

However, since the MWCO of the amicons used for this task was inferior to the 100 kDa previously used, an increased number of peptide washouts may be needed. This should be addressed in future work to guarantee that in uptake assays that follow there is no substantial contamination of EVs-p28 with unbound peptides, which could lead to a confounding effect, when both EVs-p28 and unbound p28 are administered together. For example, AFM demonstrated that azurin changed the membrane stiffness of lung cancer cells, increasing their permeability [231]. This can be the case for p28 in MDA-MB-231. The increase in the levels of unbound p28, because of their possible membrane modulation properties, can lead to increased membrane permeability and consequently to higher EV-p28 uptake, in comparison to pure EVs-p28. This does not allow a true assessment of how p28 EV functionalization impacts their uptake on target cancer cells.

After anchorage of CP05 to the surface of MSC(BM)-EVs, and separation of the unbound peptide, the batches that previously emitted substantial fluorescence intensity after the staining assays, at this stage do not show any fluorescence intensity signal except for BM EVs SEC 7. The loss of EVs imposed by the yields associated with the peptide washouts performed by UF leads to losses in the amount of stained EVs, which ultimately causes a decrease in the fluorescence intensity detected. Only with a high enough quantity of starting material, in the order of magnitude of 10^{10} to 10^{11} EVs, such as in BM EVs SEC 7**,** it was possible to recover enough quantities of EVs that displayed a substantial fluorescence intensity in comparison to negative controls of PBS, figure 12D.

Of note, is that the functionalization of EVs with CP05-p28 is only performed with half of the labeled EVs per batch. The other half of the EVs, the null condition, will be used as a non-functionalized control in the assays that follow (Figure 12C). However, both samples are subjected to the same procedure, except that the incubation of EVs in the null condition is made with PBS and not with CP05-p28.

The limitations associated with EV functionalization in this work are associated with the quantification of the number of CP05-p28 that is bound to the EVs, which is determined through Myc-tag immunoblotting and was not performed in the scope of this work. Nonetheless, it was already determined to be approximately 20 000, which appears to be unrealistic considering the amount of CD63 tetraspanins exposed on the surface of EVs. This is hypothesized to be caused by the NTA-associated underestimation of the number of particles [188].

In sum, we used a novel conjugation peptide CP05-p28, which remains anchored to EVs because of CP05 interaction with CD63 tetraspanins displayed on the EV's surface. We detected this peptide through Myc-tag immunoblotting, which revealed that CP05-p28 (2022) and CP05-p28Scrbl (UMC) but not CP05-p28 (UMC) (detected for all quantities except when 0.3 µg were loaded) where detected at all quantities loaded into the dot blot apparatus, implying that the peptides can be roughly estimated for their level of adherence to EVs. Additionally, the fluorescence of functionalized EVs was measured to assess their suitability for uptake assays, which suggested that only in high enough quantities of EVs their fluorescence can be detected.

3.1.5. EV uptake by breast cancer cells increases upon CP05-p28 anchorage to the surface of MSC-EVs

For batch BM EVs SEC 7, where fluorescence was detected after CP05-p28 functionalization, we performed uptake assays with all the experimental conditions. The treatment of breast cancer cells with EVs-p28 led to a 1,4-fold increase in the median intensity fluorescence (MFI) of cells in comparison to non-functionalized EVs (EVs) (Figure 13A), suggesting that the functionalization of EVs with p28 (EVs-p28) leads to an increase in their uptake by MDA-MB-231. The preliminary work done in the context of this study [188] demonstrated that breast cancer cells treated with EVs-p28 show an increase of 2,4-fold in comparison to non-functionalized EVs. Thus, EV functionalization through CP05-p28 anchorage may lead to values around a 1,4 - 2,4-fold increase in the uptake of EVs in triple-negative breast cancer cells.

The impact of the dosage of EVs-p28 on their uptake by breast cancer cells was also evaluated. With this aim, two conditions were tested, EVs-p28, high and low, where the low dosage consisted approximately in half of the higher dose, $1{,}40 \times 10^9$ and $2{,}95 \times 10^9$ total number of fluorescently-labeled EVs-p28, respectively. The oscillation of the MFI induced by the different dosages administered to cells was proportional to the amount of EVs administered, figure 13C. In the low dose regime (n=1) the MFI was approximately half of what was observed in the high dose (n=2, technical replicate).

As previously stated further studies making use of CP05-p28Scrbl, where a scrambled sequence of p28 is present instead of the original one, should be performed. The use of these functionalized EVs in uptake assays can confirm the impact p28 sequence and its consequential 3D structure in the increased uptake that is observed when EVs-p28 were administered to breast cancer cells. If p28 is responsible for the increased EV-p28 uptake by cancer cells, CP05-p28 functionalized EVs will display increased uptakes in comparison to EVs modified with CP05-p28 Scrbl.

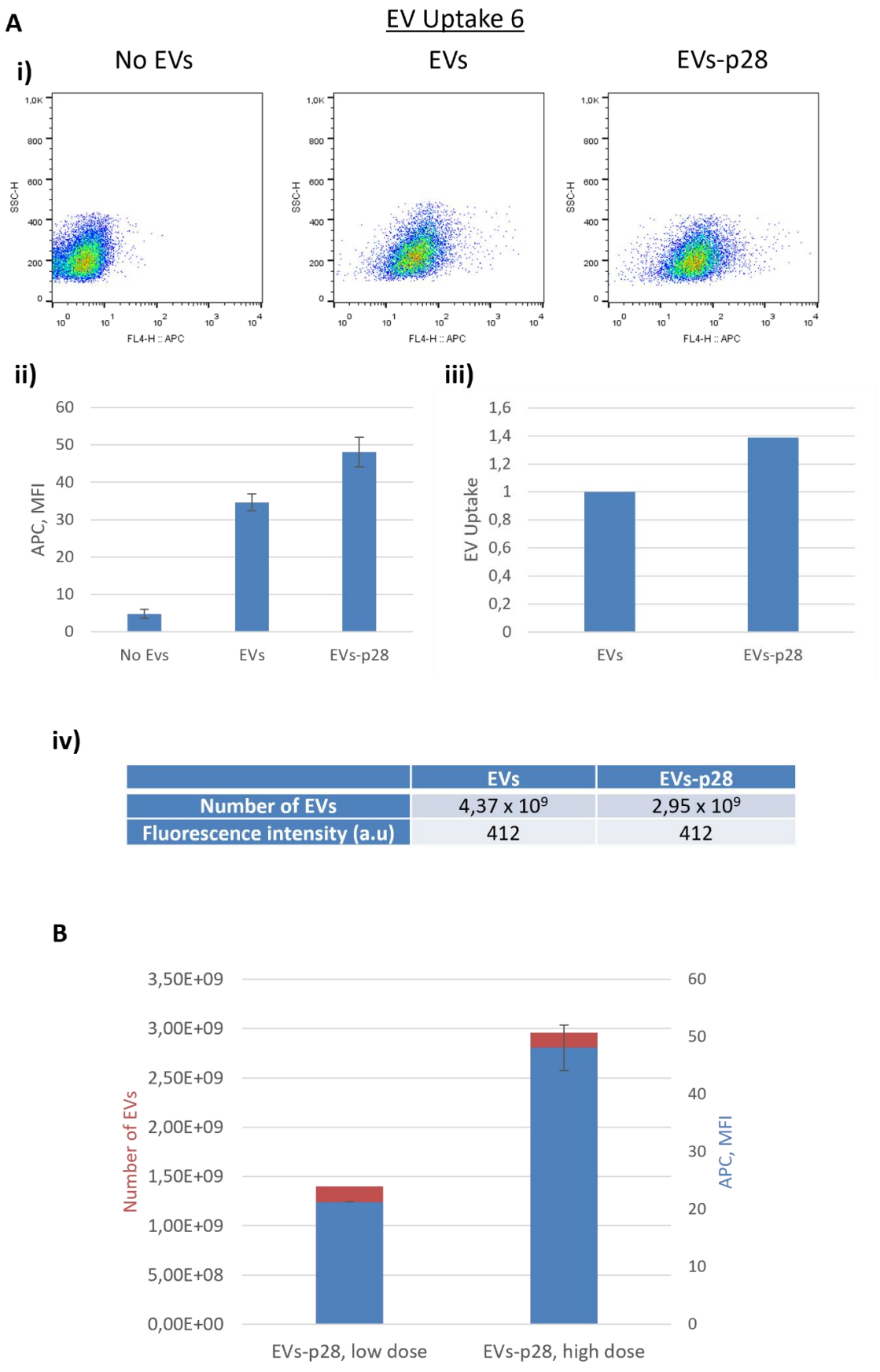

Figure 13 - Decoration of MSC-EVs with CP05-p28 increased the uptake of EVs by triple negative and metastatic breast cancer cells, MDA-MB-231. **A) i)** Flow Cytometry analysis of the EV uptake by

breast cancer cells, where EVs functionalized with CP05-p28 display an increase in the EV uptake into cells, the x-axis represents the EV fluorescence height and the y-axis represents the side scatter (n= 2 technical replicates). **ii)** Median fluorescence intensity (MFI) of flow cytometry (n= 2 technical replicates). **iii)** Relative EV uptake based on the MFI values. **iv)** Comparison between the quantity of EVs administered to breast cancer cells and their fluorescence intensity, in the different conditions tested, i.e. non-functionalized EVs (EVs) and CP05-p28 conjugation peptide-functionalized EVs (EVs-p28). **B)** Comparison between the Median fluorescence intensity (MFI) of flow cytometry when EVs are administered in different dosages to breast cancer cells (n=1, EVs-p28, low dose, and n=2 technical replicates, EVs-p28, high dose). MFI - median intensity fluorescence.

In this work, the functionalization of EVs was achieved through a direct approach, allowing for a fast establishment of EVs-p28, to achieve the proof of concept that p28 drives a preferential penetration of EVs into cancer cells when used as a targeting moiety. However, it will be interesting to investigate how the quantity of CP05-p28 anchored to EVs affects their increased targeting capabilities towards cancer cells. If there is a significant dependency, it can be hypothesized that alterations on the levels of CD63 present in the surface of EVs can shape their ability to be endowed with increased targeting abilities through CP05-p28 anchorage. And since it is the case that the abundance of CD63 can vary on EVs secreted by different cell types, trying to implement this mechanism of functionalization in EVs derived from other cells may also lead to increased targeting abilities.

Additionally, the decoration of EVs with CP05-p28 does not occur through a covalent interaction. As such it can lead to a detrimental degree of instability at the level of the anchorage of this targeting moiety, which can be detrimental for the use of EVs-p28 as a NDDS since it can cause the detachment of CP05-p28 from the surface of EVs. Therefore, in future studies, it may be valuable to investigate other approaches for the functionalization of EVs, that allow for stabler anchoring. In fact, it is also possible to achieve a direct surface modification of EVs established through covalent interactions through click chemistry, which was already used successfully in several studies [232], [233] for the enhancement of EV targeting abilities. And, recently, Pham TC *et al.* described a system of indirect EV engineering that through protein ligases permitted a covalent binding to be established between EGFR-targeting peptides or anti-EGFR targeting nanobodies which facilitated their accumulation in EGFR-positive cancers *in vivo* [234]. And this method is suitable for targeting other receptors such as HER2. One of the advantages of this method is that no harsh chemical treatments are necessary [235].

In terms of indirect approaches to the engineering of EVs, genetic engineering, which is based on the expression of transgenes or chimeric proteins that are known to be enriched into EVs, can be used for EV surface modification and drug loading. However, for surface engineering, this strategy is highly dependent on the degree of enrichment of these proteins into EVs, which can be a limitation. And it is a time-consuming technique that is hard to establish in primary cells [236]. However, once the cell engineering is successfully achieved it is substantially less laborious than direct interventions not requiring intense EV processing and separation from other substances (e.g., unbound targeting moieties aimed to be anchored on the surface of EVs) which not only severely impact the EV yield but can also affect EV biophysical properties and functional characteristics. In sum, both approaches (direct and indirect EV reconfigurations) may be advantageous depending on the final desired EV characteristics and their downstream application.

The optimization and reproducibility of EV surface engineering approaches aimed at improving EVs targeting abilities are crucially important for their clinical application since the systemic administration of naive EVs, i.e., non-functionalized EVs leads, mostly to their accumulation in organs such as the liver, spleen, and lungs [110], [113], [221], [237]. Consequently, EV decoration with targeting moieties may be an essential part of their clinical utilization.

When EV functionalization aims to achieve an increased target of cancer cells, several types of molecules were already utilized, such as peptides and aptamers. These moieties are generally targeted to specific overexpressed receptors on the surface of cancer cells, such as the HER2 [234] and EGFR, [113], [238].

Regarding p28, it is described to preferentially penetrate a variety of solid tumors. Thus, although this study was performed in breast cancer cells, it has the potential to be extended to different types of solid tumors. Studies testing this hypothesis can ultimately yield insights concerning an increased penetration efficiency of the NDDS towards specific tumors, showing the most suitable cancers to be treated with this system. Moreover, a polymeric nanocarrier was already decorated with p28 to increase its targeting ability toward A549 lung cancer cells. In fact, this NDDS that was loaded with Gefitinib reduced the primary and metastatic tumor burden in tumor-bearing mice [216]. Evidencing the ability of p28 to be employed as a targeting moiety of nanoparticles aimed at the treatment of cancer. Moreover, the functionalization of these polymeric nanoparticles, led to an increase of approximately 1,5-fold in lung cancer cell uptake in comparison to non-functionalized particles. This is a similar value to what was obtained in the present study, (1,4-fold to 2,4-fold increase) and it could demonstrate that p28 functionalization may lead to similar increases in nanoparticle penetration, despite the type of particle that is utilized. Overall, because of EVs' advantages over synthetic nanocarriers, such as increased biocompatibility, the use of EVs may be a safer choice when considering both options. Nonetheless, all things considered, two independent research studies investigating different types of nanoparticles and studying different types of solid tumors found similar results. When used as a targeting moiety, p28 was able to increase nanoparticle uptake by cancer cells.

Additionally, uptake assays comparing the uptake of EVs-p28 into normal cells and their cancerous counterparts will allow for the study of the specificity of the system.

Moreover, in a study developed by Ye Z. et al**.,** [239] EVs derived from L929, a fibroblast cell line, were functionalized with therapeutic and targeted peptides, the pro-apoptotic KLA peptide, combined with the low-density lipoprotein (LDL), respectively. This functionalization led to an increase in EV uptake by a human primary glioma cell line, U87, of approximately 2-fold in comparison to non-functionalized EVs and KLA-LDL-EVs. These EVs loaded with methotrexate were the most effective at extending the lives of glioma-bearing mice, showing the potential of EV based systems to improve cancer treatment outcomes in animal models.

In sum, in our work, it is the first time, to the best of our knowledge, that p28 is employed as a targeting moiety of EVs. And through this functionalization of EVs, which were produced in conditions that are readily translated to clinical settings using S/X-F conditions and the employment of the GMP-compatible scalable and selective isolation method comprised of TFF-SEC, it was shown that MSC(BM)-EVs-p28 are preferentially uptake by breast cancer cells in comparison to non-functionalized MSC(BM)-EVs.

Overall, the use of EVs-p28 as a new NDDS demonstrated to be a promising therapeutic approach that displays improved targeting of solid tumors.

3.2. Isolation of tumor cell – derived extracellular vesicles

3.2.1. Tumor Cells, a more proliferative but less productive cell type

MDA-MB-231 is a triple negative and metastatic breast cancer cell line that was also employed for EV production, CP05-p28 functionalization, and testing in uptake assays. The EVs from this cell source are also expected to present the same behavior in uptake assays as MSC-EVs after functionalization, i.e., MDA-MB-231 derived EVs-p28 are hypothesized to preferentially penetrate cancer cells. This cell line draws specific interest to be studied for EV production because a system that permits the evaluation of RNA functional transfer, denominated CROSS-FIRE [174], was developed in these cells. This allows for evaluating the impact of the p28 EV functionalization in the functional transfer of RNAs into cells. Additionally, cancer cell lines are very robust in cell culture conditions, including in periods of nutrient deficiency, e.g., caused by supplement depletion in the cell culture medium, and proliferate at a faster pace in comparison to primary MSC.Thus, it is valuable to establish the bioprocessing pipeline here employed for an immortalized cell line, since these may have interesting applications.

MDA-MB-231 cells grow to reach higher quantities per T-175 culture flask in comparison to MSC, comprising 2,37 x 10^7 – 2,93 x 10^7 cells per T-175 flask (Figure 14C and Figure 8B). However, the productivity of cells is significantly lower than that of MSC, in between 45 – 175 EVs released per cell (Figure 14B and Figure 8C). Moreover, the amount of EVs per T-175 varied considerably among the different batches changing between 1,07 x 10^9 and 4,47 x 10^9 EVs per T-175 culture flask (Figure 14A). Also, similarly to MSC, the quantity of EVs obtained after the downstream processing through TFF, SEC, and UF, appears to benefit from lowering the MWCO of the amicon ultra centrifugal units used during UF (Table 2 and Figure 9C).

A

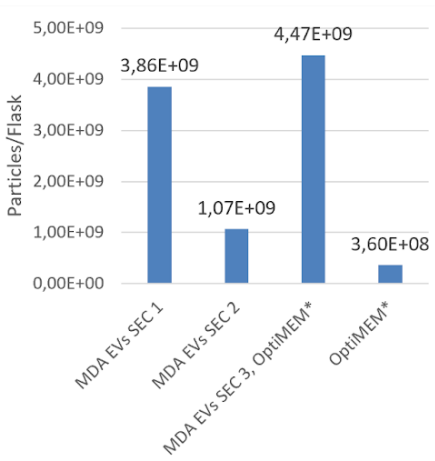

B

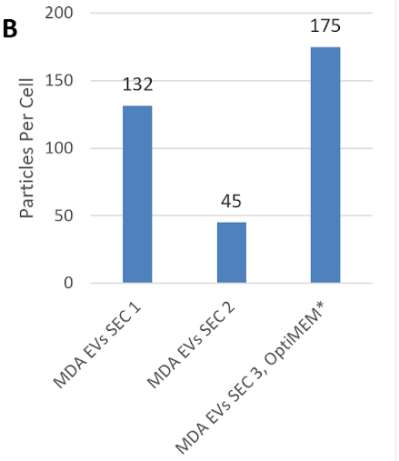

C

Assay No.	No. Cells/T-175	No. of T-175	Total No. Of EVs	MWCO of Amicons (kDa)
MDA EVs SEC 1	2,93 x 10^7	20	7,71 x 10^{10}	100
MDA EVs SEC 2	2,37 x 10^7	24	2,53 x 10^{10}	100
MDA EVs SEC 3, OptiMEM	2,55 x 10^7	20	8,94 x 10^{10}	50

D

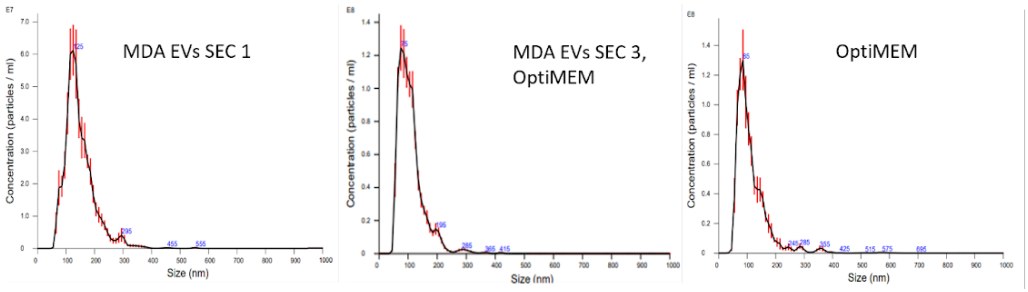

E

Samples	Average size (nm)	Mode of size (nm)
MDA EVs SEC 1	151,5	135
MDA EVs SEC 2	127,6	109,65
MDA EVs SEC 3, OptiMEM	113,55	87,35
OptiMEM	112,5	81

F

Samples	Total Particle no.
MDA EVs SEC 1	7,71 x 10^{10}
MDA EVs SEC 3, OptiMEM*	8,94 x 10^{10}
OptiMEM	7,20 x 10^9

14% increase

(1,23 x 10^{10} particles)

Figure 14- Production of MDA-MB-231 derived EVs and their characteristics. **A)** Number of TFF, SEC, and UF isolated particles per T-175 culture flask. **B)** Quantity of particles produced by each cell, quantified after CM was processed through TFF, SEC, and ultrafiltrated in amicons ultra centrifugal units. **C)** Comparison between batches considering the number of cells per T-culture flask at the end of the conditioning period, the size of each batch, i.e., the number of T-Flasks (20 mL of cell culture medium each), the total number of particles isolated through TFF, SEC and UF, and the MWCO of the amicons ultra centrifugal units used in UF of each batch. **D)** NTA size distribution curves of MDA-MB-231 derived EVs. **E)** Average size and mode of the size of MDA-MB-231 derived EVs. **F)** Comparison between the quantity of EVs obtained in MDA EVs SEC 1, produced in DMEM, MDA EVs SEC 3, OptiMEM, produced in OptiMEM, and OptiMEM that was processed through the whole isolation protocol, i.e., TFF, SEC, and

UF in amicon ultracentrifugal units.TFF- Tangential Flow Filtration. SEC - Size Exclusion Chromatography. UF - Ultrafiltration MWCO - molecular weight cut off. NTA - Nanoparticle Tracking Analysis.

In these cells, we also observed changes in cell behavior, e.g. substantial cell death and slower cell proliferation, when the complete cell culture medium utilized for cell expansion (i.e. DMEM with 10% FBS and 1% A/A) was switched to the basal DMEM (i.e. DMEM with 1% A/A, without the addition of a cell culture supplement, e.g. FBS or hPL), for a 24 hours conditioning period. Thus, to overcome this limitation, we performed the conditioning period using OptiMEM, an optimized formulation of Eagle's Minimal Essential Medium (MEM). In fact, Bost JP et al., described that using non-supplemented OptiMEM as an EV production medium can increase the quantity of EVs secreted by cells [240].
However, a rapid analysis on the total particle content of this medium by NTA revealed the presence of 1,54 x 10^9 particles / mL. Therefore, envisaging the use of OptiMEM as a production medium, we processed this medium only through the entire established isolation protocol (i.e. TFF combined with SEC) to evaluate if its utilization in cell conditioning leads to significant contamination of the sample with OptiMEM-derived particles, and if that is the case to further access the extent of the contamination and the characteristics of such particles. We discovered that 7,20 x 10^9 particles per 400 mL (equivalent to 20x T-175 culture flasks) are isolated from OptiMEM processed through the entire protocol. Hence, about 8% of the particles isolated in the MDA EVs SEC 3, OptiMEM can be considered OptiMEM-derived particles.
Additionally, comparing MDA EVs SEC 3 where OptiMEM was used for the conditioning period, with MDA EVs SEC 1, the isolation assay of MDA-MB-231 derived EVs with basal DMEM where more EVs were produced, we observe an increase of 14% in the number of particles isolated (Figure 14F). Of this 14%, 60% (7,20 x 10^9 particles) may correspond to OptiMEM-derived particles that were co-isolated with MDA-MB-231-derived EVs. The additional 40% of the particle increase may be caused by enhanced stabilization provided to cells by OptiMEM, in comparison to basal DMEM. In fact, the cell proliferation during conditioning periods was accelerated when OptiMEM was utilized rather than DMEM basal, which may account for the increase in the number of particles. However, this estimated 40% increase may also be caused by the fact that the UF of MDA EVs SEC 3, OptiMEM was performed in amicons with an MWCO of 50 kDa instead of 100 kDa that was used in MDA EVs SEC 1. Thus, more studies are required to determine the total increase in EVs when using this medium for the conditioning period.

Table 2 - Comparison of the MDA-MB-231 derived EVs recovery through the multiple operation units of the EV isolation protocol.

Samples	TFF Recovery (%)	SEC and Amicon Recovery (%)	Total Recovery (%)	MWCO of Amicons (kDa)
MDA EVs SEC 2	59	2,1	1,5	100
MDA EVs SEC 3 OptiMEM		10,8		50

Moreover, de Jong OG et al. reported obtaining a quantity of 2.2 x 10^{11} MDA-MB-231 derived EVs, with OptiMEM as an EV production medium, which corresponds to 1.1 x 10^{10} EVs per T-175 culture flask, [174]. The quantity of MDA-MB-231 derived EVs obtained in this study was greatly lower, corresponding to 35% for MDA EVs SEC 1 and to 11,5% for MDA EVs SEC 2 of the particles obtained by de Jong et al. And in MDA EVs 3, OptiMEM, the batch where similar conditions to those employed in this study were utilized, the value was still lower corresponding to 40% of the EVs obtained by de Jong OG et al. Such differences may be attributed to instrument variability, as well as the passage number of the cells that were inoculated for final EV production.

The average size and mode of EVs produced in OptiMEM, MDA EVs SEC 3 are in accordance to small EVs (i.e. EVs bellow 200 nm). Additionally, in the size distribution curve relative to OptiMEM only (Figure 14D) one peak is similar to one of the peaks present in the size distribution curve referent to the MDA EVs SEC 3 both in shape and placement in the graph (Figure 14D) However, in MDA EVs SEC 3 a shoulder in this peak correspondent to another EV sub-population is displayed. This one, however, does not overlap with the OptiMEM size distribution curve and as such, it likely is generated by particles derived from cells. Overall, such findings reflect the degree of contamination of OptiMEM-derived particles in MDA EVs SEC 3.

All things considered, OptiMEM as an EV production medium may or may not be ideal depending on the downstream application of EVs and even though it may lead to an increase in the quantity of EVs produced in a determined batch, it comes with the sacrifice of reduced purity.

Additionally, the average size and mode of MDA-MB-231-derived EVs, that were produced in DMEM, i.e., MDA EVs SEC 1 and MDA EVs SEC 2, were also in accordance to small EVs (Figure 14D), being slightly higher than those produced in OptiMEM.

Overall, there are not as many EV sub-populations above 200 nm in the NTA size distribution curves referent to the MDA-MD-231 derived EVs (Figure 14D and Supplementary figure 3) in comparison to what is observed for MSC-EVs (Figure 9F and Supplementary figure 3).

In sum, it was concluded that MDA-MB-231 cells are substantially less productive (i.e. the quantity of EVs secreted by each cell) in comparison to MSC. However, the quantity of EVs per T-flask is increased when utilizing these cells for EV production in comparison with most of MSC batches (except BM EVs SEC 7, where the fine tune of the EV production conditions led to a substantially higher quantity of EVs being produced, and also not considering the batch MDA EVs SEC 2, where an atypical low quantity of EVs was isolated in comparison to other MDA-MB-231 batches), mainly because of the higher quantities of cells present in each of the T-flasks. Additionally, apart from the usual EV production medium used in this work, OptiMEM was utilized for EV production, and in this batch, MDA EVs SEC 3, OptiMEM yielded increased quantities of EVs. However, OptiMEM-derived particle contamination accounts for a substantial amount of that increase in EV production. Finally, MDA-MB-231 derived EVs average size and mode were below 200 nm, being in the range of small EVs.

3.2.2. Amicon ultra centrifugal units MWCO decrease from 100 kDa to 10 kDa doubles the yield of the ultrafiltration of EVs

The evaluation of the labeled EVs fluorescence determined this procedure to be a success (Figure 15B). As in the case of labeled MSC-EVs (Figure 10C), the quantity of the fluorescence intensity appears to be proportional to the amount of starting EV material available to be labeled by the Alexa Fluor™ 647 NHS Ester. Another factor that also impacts the EV recovery at this stage is the MWCO of amicon ultra centrifugal units. The yield of MDA-MB-231 derived EVs at least doubled when a lower MWCO amicon was used for concentration after SEC separation of EVs and the dye (Figure 15A). Combined with the assays performed with MSC-EVs (Figure 10B), the results point out that it is advantageous to decrease the MWCO during the UF of EVs as it decreases the losses of particles. This however requires further testing to consolidate more significant conclusions.

However, when using MDA-MB-231 derived EVs, the quantity of functionalized EVs obtained after EV incubation with CP05-p28 was not sufficient to yield significant fluorescence intensity (Figure 15C), in comparison to the negative control, suggesting that low amounts of EVs were obtained, possibly approximately to the order of magnitude $1x10^8$ EVs or less (per each condition, i.e., functionalized and non-functionalized EVs). This is likely caused by the three washouts that are performed with amicon ultra centrifugal filtering units to obtain EVs-p28 devoid of unbound peptides, as well as because of the splitting of each EV batch into two conditions of functionalization (Figure 12C) which results in only half of the EVs being measured for fluorescence intensity, decreasing the signal in comparison to the signal measured immediately after labeling (Figure 15B and Figure 15C.)

A

Samples	Total Particle no. Before Staining	Total Particle no. After Staining	Yield (%)	Amicon MWCO (kDa)
MDA EVs SEC 1	7,71 x 10^{10}	3,85 x 10^{9}	6	100
MDA EVs SEC 2	2,53 x 10^{10}	3,42 x 10^{9}	13	100
MDA EVs SEC 3, OptiMEM	8,94 x 10^{10}	2,33 x 10^{10}	26	10

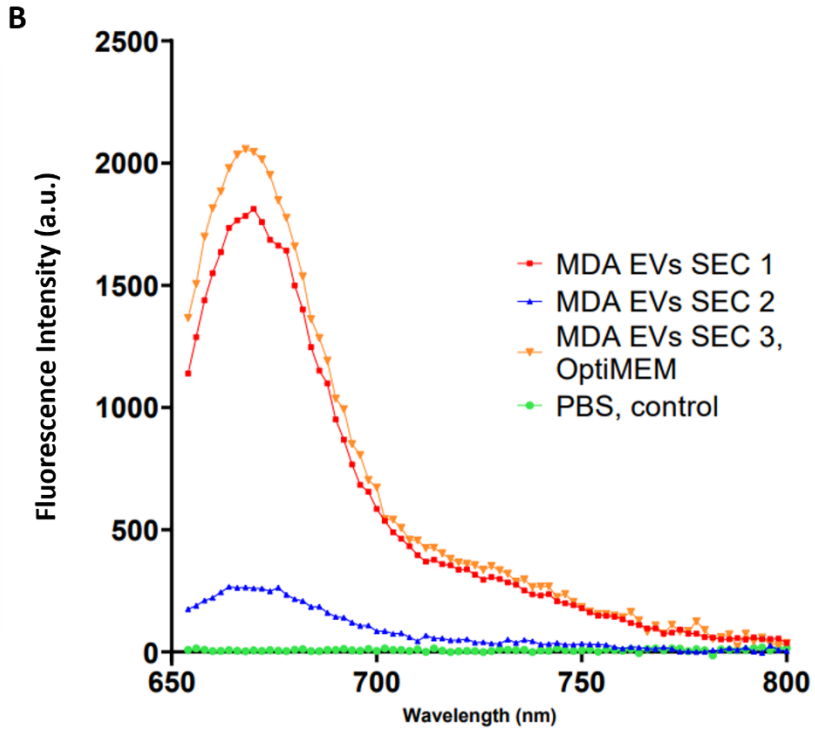

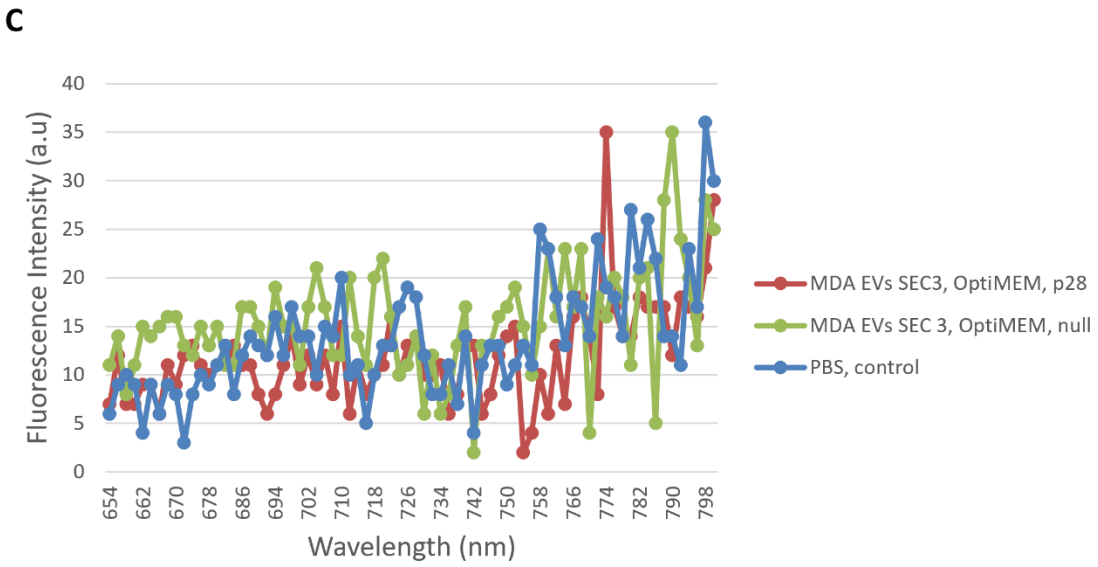

Figure 15 - EV staining with Alexa Fluor™ 647 NHS Ester. A) Comparison of EV yields in UF operation unit performed for stained MDA-MB-231 derived EVs. **B)** Comparison between the emission spectra (excitation wavelength of 620 nm) of the different batches of MDA-MB-231 derived EVs. **C)** Representative emission spectrum (excitation wavelength of 620 nm) of a batch where labelled

functionalized and non-functionalized EVs did not display significant fluorescence in comparison with the negative control, PBS.

3.2.3. Low quantities of EVs are detrimental for successful uptake assays

When using non-functionalized MDA-MB-231 derived EVs that display fluorescence after labeling, a 2,5-fold increase in the MFI is detected compared to conditions where no EVs where administered to cells.

The similarity in the increase of the MFI using EVs derived from MSC (2-fold) and MDA-MB-231 (2,5-fold) (Supplementary figure 5 and 6) suggests that both EVs display similar behaviors in terms of cellular uptake.

However, when breast cancer cells, MDA-MB-231, were treated with CP05-p28 functionalized MDA-MB-231 derived EVs, no differences in the MFI in comparison to the non-functionalized EVs and no EVs controls were observed (Figure 16A and 16B and Supplementary figure 8). Overall, the splitting of the total quantity of EVs and UF performed for unbound peptide removal causes detrimental reduction in the number of EVs which abrogates the chances of a successful uptake experiment. Together with the results observed for MSC-EVs, the MDA-MB-231 derived EVs assays also point that there is a minimum value of EVs that is necessary to be administered to cells if fluorescence through flow cytometry is to be detected in the target cells after the incubation time. Considering the successful EV uptake experience, where the batch BM EVs SEC 7 was employed, the minimum value that is needed to be administered to target cancer cells is in the order of magnitude 1,5 x 10^9 EVs. Scaling up the production as well as maintaining the low MWCO of amicon ultra centrifugal units used during ultrafiltration, identically to what was experimented with MSC-EVs should also allow for the accomplishment of a successful MDA-MB-231 derived EVs uptake assay that achieves conclusive findings.

Further implementations that may facilitate the production of more higher EV quantities, in the order of magnitude of 10^{11}, after isolation, as discussed for MSC-EVs are for instance EV production cell stimuli such as hypoxia or shear stress, or the likely the most significant change the implementation of 3D dynamic culture conditions. And additionally, the pre-treatment of amicon ultra centrifugal unit membranes may also be explored to reduce the non-specific adsorption of EVs to the regenerated cellulose membrane.

It may also be advantageous to adopt alternative EV labelling and functionalization, as they may be more effective and require a smaller amount of EV UF, preventing the substantial losses of material here experienced. Such methods could involve creating hybrid particles by fusing labelled and p28 functionalized liposomes with EVs. This would enable the achievement of all EV reconfigurations required for this proof of concept. And it would also enable the loading of therapeutic cargoes into EVs-p28 since the liposomes used for fusion can also be loaded with therapeutic agents.

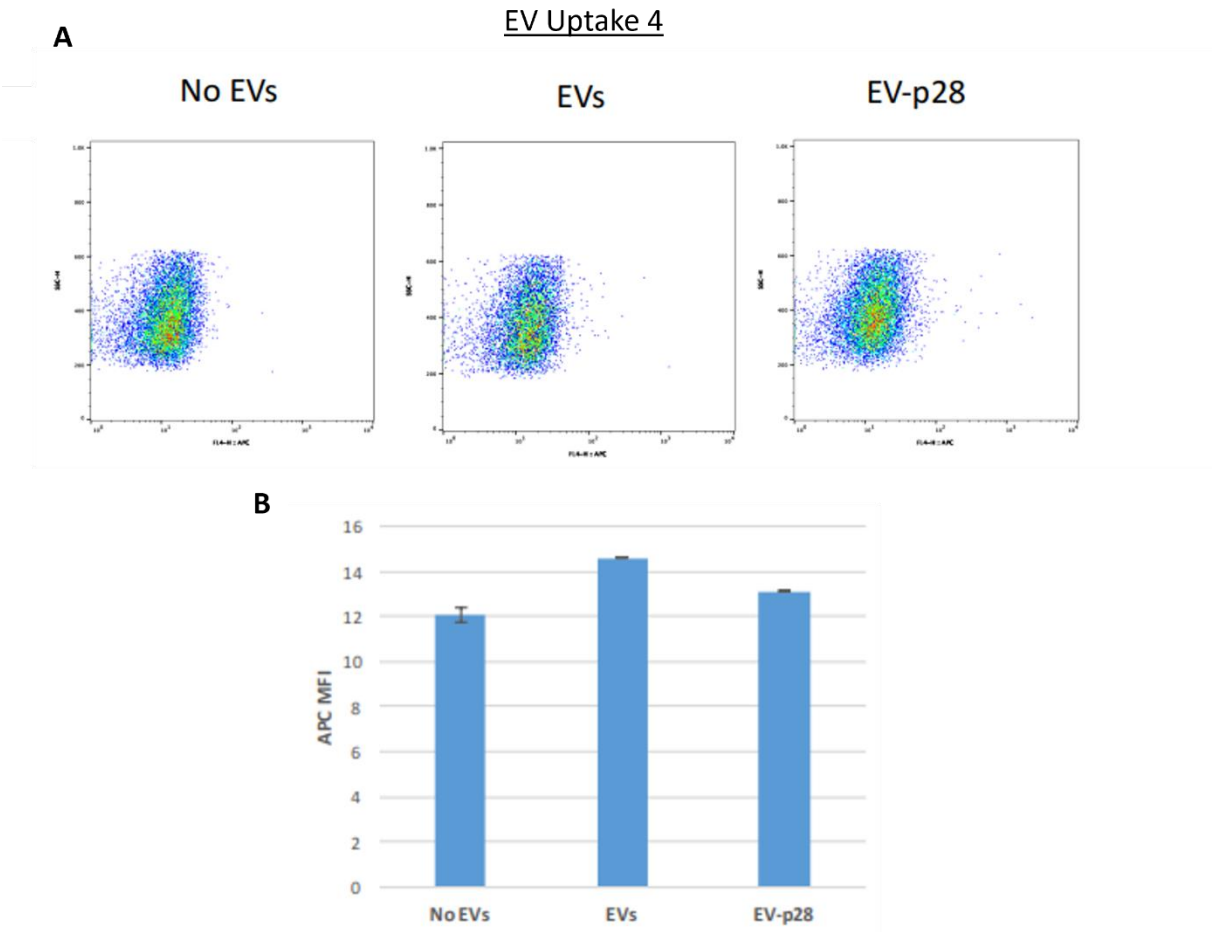

Figure 16 - Uptake assay with CP05-p28 functionalized MDA-MB-231 derived EVs. **A)** Representative flow cytometry analysis of the MDA-MB-231 derived EV uptake by breast cancer cells, MDA-MB-231. The x-axis represents the EV florescence height, and the y-axis represents the side scatter. **B)** Median fluorescence intensity (MFI) of flow cytometry measurements. (n=2 technical replicates for no EVs, and n=1 for EVs and EVs-p28). MFI - Median Fluorescence Intensity.

All things considered, tumor cells may be a valuable source of EVs to be used in basic and translational research, especially when envisaging scalability, considering their rapid proliferation and robustness in cell culture conditions. However, here, their use for EV production, although superior in terms of the quantity of EVs produced (except for the batch MDA EVs SEC 2), in comparison to most MSC batches, did not lead to the significant increases that would be necessary for the use of one EV batch in uptake assays, as such the results that we found were inconclusive in terms of the ability of the cancer cell derived EVs to be engineered with CP05-p28 and for its impact on EV by cancer cells. Possibly if the quantity of T-flasks used, 20 - 24 x T-175 culture flasks was increased to a number similar to what was used for MSC-EVs productions, 30 - 48 x T-175 culture flasks, the production of the necessary quantity of EVs to achieve conclusive results in assays of uptake would have been achieved.

Moreover, as a NDDS for targeted cancer therapies the use of tumor-derived EVs may present several advantages [121]–[123]. For instance, tumor-derived EVs may display a particularly enhanced ability to target their parent tumor cells [121], and as such their efficiency in delivering therapeutic cargoes to these cells can be enhanced, serving as a Trojan horse. However, intercellular signaling messengers, such as nucleic acids, enzymes, and proteins, linked with tumor growth, progression, and metastasis,

which may trigger tumorigenesis, are possibly present in tumor-derived EVs. Therefore, comprehensive safety evaluations are required. Additionally, it is still unclear how cancer cell-derived EVs interact with the immune system and whether they act as immune system inhibitors or activators. Depending on the type of tumor being considered, this may change. Overall, these are the factors that should be considered when planning to use tumor-derived EVs as NDDS.

4. Conclusions and Future Perspectives

In the present work, with the aim of developing an EV-based NDDS for targeted cancer therapy, p28, a peptide from the bacterial protein azurin that preferentially penetrates multiple solid tumors, was anchored to the surface of EVs, to test the hypothesis that it would improve EV uptake by cancer cells. For this purpose, a novel conjugation peptide, CP05-p28, previously developed by our group was utilized for this functionalization.

Moreover, we employed S/X-F cell culture conditions to produce human MSC(BM)-EVs and isolated the EVs from the cell culture-conditioned medium through TFF combined with SEC, a GMP-compatible scalable and selective isolation procedure. Since this method was not yet fully implemented in our lab facilities, it was established during the time of the present work. Of note is that these production conditions render this bioprocessing pipeline closely translatable to clinical practice. Additionally, this EV isolation method was established not only for primary cells but also for the immortalized cell line, MDA-MB-231, a breast cancer cell line.

The major finding of the study was that MSC(BM)-EVs-p28 uptake by triple-negative breast cancer cells was increased by 40% in comparison to its non-functionalized counterparts. Based on preliminary studies [188], it can be concluded that the increase of MSC-EVs-p28 uptake by breast cancer cells should range between 40% and 140% suggesting that this novel system could be valuable in efficiently delivering anticancer agents that have associated off-target effects.

The functionalization of MDA-MB-231-derived EVs was also tested, however, the low yields, similarly to what was observed in multiple batches of MSC-EVs, ultimately prevented conclusive findings, when exploring the functionalization of these EVs.

In fact, low EV yields were a major challenge faced in this study as well as a limitation because restricted conclusive technical replicates were performed in assays of EV-p28 uptake by cancer cells. This could have rendered the findings of the study substantially more robust.

Importantly, a suggestion concerning the number of EVs that should be present at the start of each procedure, such as EV labeling as well as EV functionalization, and how to proceed accordingly is shown in Figure 17A. The main objective is to ensure the success of the entire procedure and avoid wasting resources on experiences that will likely yield inconclusive findings. Briefly, it is suggested that it is preferable to store an EV batch when the quantity of EVs does not meet the minimum requirements, pool it with another batch, and only then follow the normal EV labeling and functionalization protocol, rather than following the protocol of EV labeling and functionalization with a batch with low quantities of EVs, which will probably yield inconclusive results and lead to the waste of valuable biological material.

Additionally, a suggestion of the MWCO of amicons ultra centrifugal units to be used in each procedure of the protocol is made in figure 17B. Although a size of 4 mL was used for the labeled EV concentration post SEC and for the peptide washout of labelled and functionalized EVs, a recent study demonstrated that 15 mL amicons give higher particle recoveries. Therefore, in the future it may be of value testing with larger amicons.

Moreover, although EV yields were significantly increased in the last MSC-EV production, BM EVs SEC 7, mainly caused by the fine-tuning of cell culture conditions such as the achievement of high cell

densities before conditioning, that led to higher amounts of EVs being produced and the use of MWCO amicons inferior to 100 kDa, that were advantageous for EV recovery (Figure 17B), the implementation of a more efficient upstream processing could render EV production substantially more efficient and cost-effective.

A

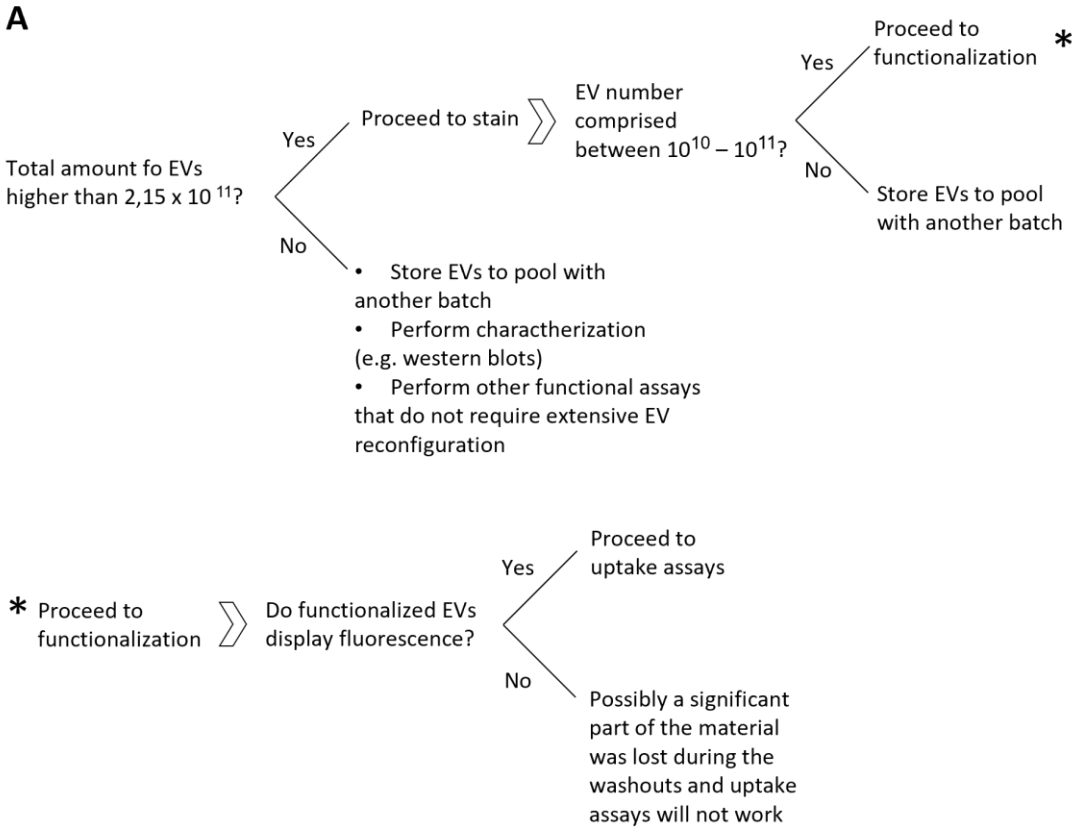

B

Stage of the protocol	Before	After
EV concentration post SEC	100 kDa	10 kDa - 30 kDa
Labelled EV concentration post SEC	100 kDa	10 kDa
Labelled and functionalized EVs, unbound peptide washout	100 kDa	30 kDa - 50 kDa

Figure 17 – Suggestions for future studies. A) Suggestions on how to navigate the EV manipulation protocols according to the quantity of EVs isolated and the fluorescence of EVs in each batch. The quantity of EVs suggested is aimed for the performance of assay uptakes comprising one technical replicate in each condition, i.e., functionalized, and non-functionalized EVs, with approximately $2x10^9$ EVs. **B)** Contrast of the MWCO of amicon ultra centrifugal units necessary for EV UF at the different stages of the study. The "After" column comprises the suggestions made for future work following a similar workflow.

Improvements in the process could rely on changing the expansion platform to multilayer T-flasks or 3D dynamic platforms, e.g., hollow-fiber, stirred tank, and the Vertical-Wheel™ bioreactor (Figure 18), which are described to increase EV yields by several folds [223]–[225], as reviewed in the Introduction, (section 1.2.8). Chemical or mechanical cell stimuli can also cause cells to produce more EVs [241]–[244], and, additionally, the impact of different production mediums can be studied to this end. In fact, we evaluated the effect of using OptiMEM (i.e., an optimized formulation of Eagle's Minimal Essential Medium (MEM)) as an EV production medium and determined that although it can lead to an increase in EV production and cell robustness during periods of conditioning it leads to the contamination of the cell-derived EVs. Nonetheless, other promising options are available as well. For instance, RoosterBio® offers the EV production medium RoosterCollect™-EV, which was already shown to increase EV production by cells, without substantial contamination [245], [246]. This could therefore be also tested using our experimental setup.

Overall, such strategies can likely lead not only to changes in the EV number but also in EV's biophysical and functional characteristics and investigation concerning this subject should follow such implementations. It should be noted as well that the conditions used in the upstream processing should be GMP compatible to operate in conditions that are more meaningful to clinical settings. Additionally, the MSC cell sources that are more productive such as the WJ can be adopted [224], [226].

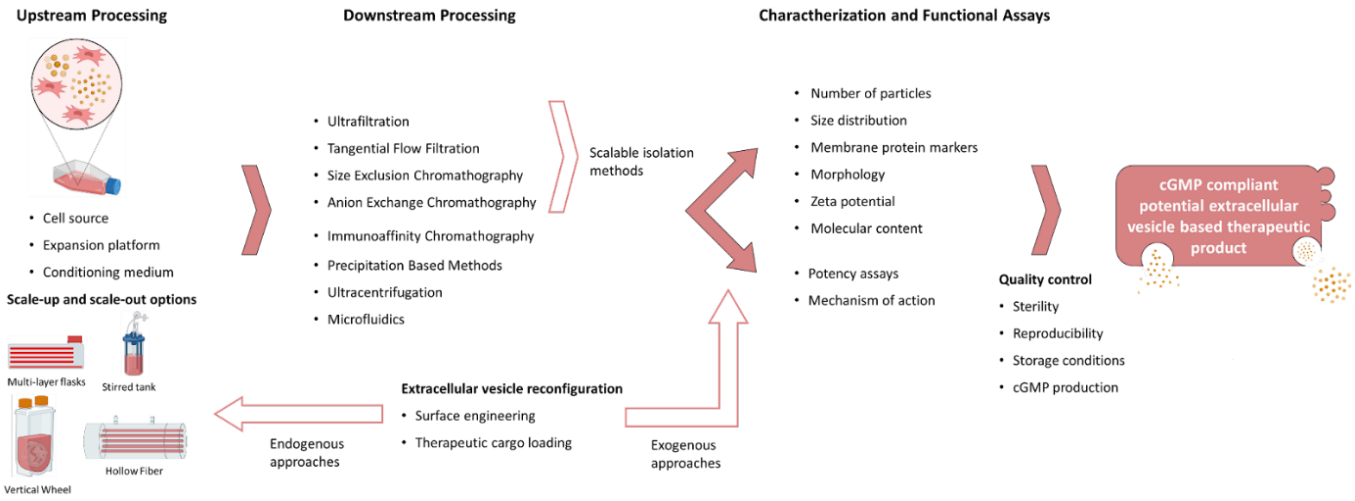

Figure 18 - Important aspects for the translation of extracellular vesicle (EV) - based therapies into clinical settings.

Moreover, in addition to the optimization of the upstream processing conditions, several challenges still must be overcome in the field of EVs to harness their full potential as therapeutic options. For instance, drug loading techniques available are still considered to have low efficiencies. And certain strategies such as genetic engineering, employed both for cargo loading and EV functionalization are difficult to implement especially in primary cells [247]. Importantly drug loading techniques as well as strategies aimed at EV surface modification should seek to be as efficient and reproducible as possible while maintaining EV integrity.

In addition, the selection of an appropriate cell source is also important. It should especially consider the downstream application of the EVs since their characteristics, such as the intraluminal molecules carried, are intrinsically related to the parent cell phenotype [130]. Moreover, additional variables such as cell availability, expandability, and EV productivity are also important to consider when choosing a parent cell source.

Concerning EV isolation, methods should be reproducible and efficient, as well as GMP-compatible and scalable. The balance between yield and purity should also be considered, and future EV-focused research will possibly solve this compromise. Interestingly, there is an increase in alternatives to the gold standard EV isolation technique, ultracentrifugation, [149] and this trend may continue to overcome ultracentrifugation's limitations. It is worth noting that filtration techniques, e.g. TFF and ultrafiltration, and SEC are a growing trend in the field [248].

Other challenges are that the EV characterization criteria as well as potency assays must be standardized to allow the comparison of findings throughout multiple laboratories. This will ultimately validate findings and thus prompt the clinical translation of EVs.

Additionally, more research will be needed to definitively determine ideal EV storage conditions, which could allow for their adoption as off-the-shelf products. Important discoveries have already been made in this area, such as the prevention of EV aggregation and cryodamage by the addition of trehalose, a non-toxic natural sugar commonly used in the food and pharmaceutical industries [249]. Tween 20, which is vastly used nonionic surfactant, was also demonstrated to be an interesting excipient to be used for EV storage. It is able to modulate the stability of colloidal particles and to cover solid liquid interfaces limiting biologicals' adherence to tubes, therefore it was able to decrease EV loss during storage, while not compromising EV function [227]. Moreover, it has been also demonstrated that freeze-drying keeps the qualities of EV cargo intact and can be a suitable strategy for EV preservation [185].

Furthermore, a greater understanding of EV biology, such as the processes governing endosomal escape following EV internalization and the attribution of specific traits to EV subpopulations can lead to the development of more effective EV-based therapeutic options.

In conclusion, the EV field is still in its infancy, and despite the significant obstacles that remain, there is now vast research output that highlights their outstanding features and therapeutic qualities, when compared to synthetic nanocarriers and cell therapies, which will hopefully be leveraged for the effective treatment of several pathological conditions in the future.

5. References

[1] Pecorino Lauren, *Molecular Biology of Cancer: Mechanisms, Targets, and Therapeutics, 5th Edition*. Accessed: Aug. 31, 2022. [Online]. Available: https://books.google.pt/books?hl=pt-PT&lr=&id=n8owEAAAQBAJ&oi=fnd&pg=PP1&dq=molecular+biology+of+cancer+mechanisms+targets+and+therapeutics+5th+edition&ots=X7bpCEb5vJ&sig=8pq2ubrSKCbh-u69L0E6dsKF4zs&redir_esc=y#v=onepage&q=molecular%20biology%20of%20cancer%20mechanisms%20targets%20and%20therapeutics%205th%20edition&f=false

[2] "Cancer, Facts Sheet." https://www.who.int/en/news-room/fact-sheets/detail/cancer (accessed Aug. 31, 2022).

[3] D. Hanahan and R. A. Weinberg, "The Hallmarks of Cancer," *Cell*, vol. 100, no. 1, pp. 57–70, Jan. 2000, doi: 10.1016/S0092-8674(00)81683-9.

[4] D. Hanahan and R. A. Weinberg, "Hallmarks of cancer: The next generation," *Cell*, vol. 144, no. 5, pp. 646–674, Mar. 2011, doi: 10.1016/J.CELL.2011.02.013/ATTACHMENT/3F528E16-8B3C-4D8D-8DE5-43E0C98D8475/MMC1.PDF.

[5] D. Hanahan, "Hallmarks of Cancer: New Dimensions," *Cancer Discov*, vol. 12, no. 1, pp. 31–46, Jan. 2022, doi: 10.1158/2159-8290.CD-21-1059.

[6] L. Sapio and S. Naviglio, "Innovation through Tradition: The Current Challenges in Cancer Treatment," *Int J Mol Sci*, vol. 23, no. 10, May 2022, doi: 10.3390/IJMS23105296.

[7] A. K. Mitra *et al.*, "Novel delivery approaches for cancer therapeutics," *J Control Release*, vol. 219, pp. 248–268, Dec. 2015, doi: 10.1016/J.JCONREL.2015.09.067.

[8] H. Nakamura and H. Maeda, "Cancer Chemotherapy," *Fundamentals of Pharmaceutical Nanoscience*, pp. 401–427, Mar. 2022, doi: 10.1007/978-1-4614-9164-4_15.

[9] O. M. Elsharkasy *et al.*, "Extracellular vesicles as drug delivery systems: Why and how?," *Advanced Drug Delivery Reviews*, vol. 159. Elsevier B.V., pp. 332–343, Jan. 01, 2020. doi: 10.1016/j.addr.2020.04.004.

[10] C. Massaro, G. Sgueglia, V. Frattolillo, S. R. Baglio, L. Altucci, and C. Dell'aversana, "Extracellular Vesicle-Based Nucleic Acid Delivery: Current Advances and Future Perspectives in Cancer Therapeutic Strategies," *Pharmaceutics*, vol. 12, no. 10, pp. 1–19, Oct. 2020, doi: 10.3390/PHARMACEUTICS12100980.

[11] X.-M. Xi, "Drug loading techniques for exosome-based drug delivery systems," p. 7, 2021, [Online]. Available: files/208/Xi - 2021 - Drug loading techniques for exosome-based drug del.pdf

[12] M. Richter, P. Vader, and G. Fuhrmann, "Approaches to surface engineering of extracellular vesicles," *Adv Drug Deliv Rev*, vol. 173, pp. 416–426, 2021, doi: 10.1016/j.addr.2021.03.020.

[13] E. Woith, G. Fuhrmann, and M. F. Melzig, “Extracellular Vesicles—Connecting Kingdoms,” *International Journal of Molecular Sciences 2019, Vol. 20, Page 5695*, vol. 20, no. 22, p. 5695, Nov. 2019, doi: 10.3390/IJMS20225695.

[14] E. Chargaff and R. West, “THE BIOLOGICAL SIGNIFICANCE OF THE THROMBOPLASTIC PROTEIN OF BLOOD*,” *Journal of Biological Chemistry*, vol. 166, pp. 189–197, 1946, doi: 10.1016/S0021-9258(17)34997-9.

[15] P. Wolf, “The nature and significance of platelet products in human plasma,” *Br J Haematol*, vol. 13, no. 3, pp. 269–288, 1967, doi: 10.1111/J.1365-2141.1967.TB08741.X.

[16] E. R. Abels and X. O. Breakefield, “Introduction to Extracellular Vesicles: Biogenesis, RNA Cargo Selection, Content, Release, and Uptake,” *Cell Mol Neurobiol*, vol. 36, no. 3, pp. 301–312, Apr. 2016, doi: 10.1007/S10571-016-0366-Z.

[17] C. R. Harrell, N. Jovicic, V. Djonov, N. Arsenijevic, and V. Volarevic, “Mesenchymal Stem Cell-Derived Exosomes and Other Extracellular Vesicles as New Remedies in the Therapy of Inflammatory Diseases,” *Cells*, vol. 8, no. 12, Dec. 2019, doi: 10.3390/CELLS8121605.

[18] C. Williams *et al.*, “Assessing the role of surface glycans of extracellular vesicles on cellular uptake,” *Sci Rep*, vol. 9, no. 1, Dec. 2019, doi: 10.1038/S41598-019-48499-1.

[19] P. Lara, A. B. Chan, L. J. Cruz, A. F. G. Quest, and M. J. Kogan, “Exploiting the natural properties of extracellular vesicles in targeted delivery towards specific cells and tissues,” *Pharmaceutics*, vol. 12, no. 11. MDPI AG, pp. 1–25, Nov. 01, 2020. doi: 10.3390/pharmaceutics12111022.

[20] G. van Niel, G. D’Angelo, and G. Raposo, “Shedding light on the cell biology of extracellular vesicles,” *Nature Reviews Molecular Cell Biology*, vol. 19, no. 4. Nature Publishing Group, pp. 213–228, Apr. 01, 2018. doi: 10.1038/nrm.2017.125.

[21] S. Keerthikumar *et al.*, “Proteogenomic analysis reveals exosomes are more oncogenic than ectosomes,” *Oncotarget*, vol. 6, no. 17, pp. 15375–15396, Apr. 2015, doi: 10.18632/ONCOTARGET.3801.

[22] R. M. Johnstone, M. Adam, J. R. Hammonds, L. Orro, and C. Turbide, “THE JOURNAL OF BIOLOGICAL CHEMISTRY Vesicle Formation during Reticulocyte Maturation ASSOCIATION OF PLASMA MEMBRANE ACTIVITIES WITH RELEASED VESICLES (EXOSOMES)*,” vol. 262, pp. 9412–9420, 1987, doi: 10.1016/S0021-9258(18)48095-7.

[23] S. el Andaloussi, I. Mäger, X. O. Breakefield, and M. J. A. Wood, “Extracellular vesicles: biology and emerging therapeutic opportunities,” *Nature Reviews Drug Discovery 2013 12:5*, vol. 12, no. 5, pp. 347–357, Apr. 2013, doi: 10.1038/nrd3978.

[24] G. Palmisano *et al.*, “Characterization of Membrane-shed Microvesicles from Cytokine-stimulated β-Cells Using Proteomics Strategies,” *Mol Cell Proteomics*, vol. 11, no. 8, p. 230, Aug. 2012, doi: 10.1074/MCP.M111.012732.

[25] R. C. Piper and D. J. Katzmann, “Biogenesis and Function of Multivesicular Bodies,” *Annu Rev Cell Dev Biol*, vol. 23, p. 519, 2007, doi: 10.1146/ANNUREV.CELLBIO.23.090506.123319.

[26] G. Raposo and W. Stoorvogel, “Extracellular vesicles: Exosomes, microvesicles, and friends,” *J Cell Biol*, vol. 200, no. 4, p. 373, Feb. 2013, doi: 10.1083/JCB.201211138.

[27] Y. Sun, A. C. Hedman, X. Tan, N. J. Schill, and R. A. Anderson, “Endosomal Type Iγ PIP 5-Kinase Controls EGF Receptor Lysosomal Sorting,” *Dev Cell*, vol. 25, no. 2, p. 144, Apr. 2013, doi: 10.1016/J.DEVCEL.2013.03.010.

[28] P. Majumder and O. Chakrabarti, “Mahogunin regulates fusion between amphisomes/MVBs and lysosomes via ubiquitination of TSG101,” *Cell Death Dis*, vol. 6, no. 11, Nov. 2015, doi: 10.1038/CDDIS.2015.257.

[29] C. Villarroya-Beltri *et al.*, “ISGylation controls exosome secretion by promoting lysosomal degradation of MVB proteins,” *Nat Commun*, vol. 7, Nov. 2016, doi: 10.1038/NCOMMS13588.

[30] X. Peng, L. Yang, Y. Ma, Y. Li, and H. Li, “Focus on the morphogenesis, fate and the role in tumor progression of multivesicular bodies,” *Cell Communication and Signaling*, vol. 18, no. 1, pp. 1–15, Aug. 2020, doi: 10.1186/S12964-020-00619-5/TABLES/1.

[31] M. Colombo *et al.*, “Analysis of ESCRT functions in exosome biogenesis, composition and secretion highlights the heterogeneity of extracellular vesicles,” *J Cell Sci*, vol. 126, no. Pt 24, pp. 5553–5565, Dec. 2013, doi: 10.1242/JCS.128868.

[32] M. F. Baietti *et al.*, “Syndecan-syntenin-ALIX regulates the biogenesis of exosomes,” *Nat Cell Biol*, vol. 14, no. 7, pp. 677–685, Jul. 2012, doi: 10.1038/NCB2502.

[33] K. Trajkovic *et al.*, “Ceramide triggers budding of exosome vesicles into multivesicular endosomes,” *Science*, vol. 319, no. 5867, pp. 1244–1247, Feb. 2008, doi: 10.1126/SCIENCE.1153124.

[34] G. van Niel *et al.*, “The Tetraspanin CD63 Regulates ESCRT-Independent and -Dependent Endosomal Sorting during Melanogenesis,” *Dev Cell*, vol. 21, no. 4, pp. 708–721, Oct. 2011, doi: 10.1016/J.DEVCEL.2011.08.019/ATTACHMENT/48737DD0-122F-4D5A-A46B-F45FFB263E31/MMC1.PDF.

[35] S. I. Buschow *et al.*, “MHC II in dendritic cells is targeted to lysosomes or T cell-induced exosomes via distinct multivesicular body pathways,” *Traffic*, vol. 10, no. 10, pp. 1528–1542, Oct. 2009, doi: 10.1111/J.1600-0854.2009.00963.X.

[36] R. Jahn and R. H. Scheller, “SNAREs — engines for membrane fusion,” *Nature Reviews Molecular Cell Biology 2006 7:9*, vol. 7, no. 9, pp. 631–643, Aug. 2006, doi: 10.1038/nrm2002.

[37] M. Ostrowski *et al.*, “Rab27a and Rab27b control different steps of the exosome secretion pathway,” *Nat Cell Biol*, vol. 12, no. 1, pp. 19–30, Jan. 2010, doi: 10.1038/NCB2000.

[38] C. Hsu *et al.*, “Regulation of exosome secretion by Rab35 and its GTPase-activating proteins TBC1D10A-C,” *J Cell Biol*, vol. 189, no. 2, pp. 223–232, Apr. 2010, doi: 10.1083/JCB.200911018.

[39] C. Tricarico, J. Clancy, and C. D’Souza-Schorey, “Biology and biogenesis of shed microvesicles,” *Small GTPases*, vol. 8, no. 4, pp. 220–232, Oct. 2017, doi: 10.1080/21541248.2016.1215283.

[40] D. Perez-Hernandez *et al.*, “The intracellular interactome of tetraspanin-enriched microdomains reveals their function as sorting machineries toward exosomes,” *J Biol Chem*, vol. 288, no. 17, pp. 11649–11661, Apr. 2013, doi: 10.1074/JBC.M112.445304.

[41] B. R. Lee *et al.*, “Ascorbate peroxidase-mediated in situ labelling of proteins in secreted exosomes,” *J Extracell Vesicles*, vol. 11, no. 6, p. e12239, Jun. 2022, doi: 10.1002/JEV2.12239.

[42] N. Bahram Sangani, A. R. Gomes, L. M. G. Curfs, and C. P. Reutelingsperger, “The role of Extracellular Vesicles during CNS development,” *Prog Neurobiol*, vol. 205, p. 102124, 2021, doi: 10.1016/j.pneurobio.2021.102124.

[43] A. Hoshino *et al.*, “Tumour exosome integrins determine organotropic metastasis,” *Nature 2015 527:7578*, vol. 527, no. 7578, pp. 329–335, Oct. 2015, doi: 10.1038/nature15756.

[44] S. Rana, S. Yue, D. Stadel, and M. Zöller, “Toward tailored exosomes: The exosomal tetraspanin web contributes to target cell selection,” *Int J Biochem Cell Biol*, vol. 44, no. 9, pp. 1574–1584, Sep. 2012, doi: 10.1016/J.BIOCEL.2012.06.018.

[45] B. H. Sung, T. Ketova, D. Hoshino, A. Zijlstra, and A. M. Weaver, “Directional cell movement through tissues is controlled by exosome secretion.,” *Nat Commun*, vol. 6, pp. 7164–7164, May 2015, doi: 10.1038/NCOMMS8164.

[46] L. A. Mulcahy, R. C. Pink, and D. R. F. Carter, “Routes and mechanisms of extracellular vesicle uptake,” *J Extracell Vesicles*, vol. 3, no. 1, 2014, doi: 10.3402/JEV.V3.24641.

[47] McPherson Peter S., Ritter Brigitte, and Wendland Beverly, “Clathrin-Mediated Endocytosis - Madame Curie Bioscience Database - NCBI Bookshelf,” Accessed: Jun. 26, 2022. [Online]. Available: https://www.ncbi.nlm.nih.gov/books/NBK6479/

[48] J. A. Swanson, “Shaping cups into phagosomes and macropinosomes,” *Nat Rev Mol Cell Biol*, vol. 9, no. 8, p. 639, Aug. 2008, doi: 10.1038/NRM2447.

[49] B. S. Joshi, M. A. de Beer, B. N. G. Giepmans, and I. S. Zuhorn, “Endocytosis of Extracellular Vesicles and Release of Their Cargo from Endosomes,” *ACS Nano*, vol. 14, no. 4, pp. 4444–4455, Apr. 2020, doi: 10.1021/ACSNANO.9B10033/ASSET/IMAGES/LARGE/NN9B10033_0005.JPEG.

[50] M. de Almeida Fuzeta, P. P. Gonçalves, A. Fernandes-Platzgummer, J. M. S. Cabral, N. Bernardes, and Cláudia Lobato da Silva, “From Promise to Reality: Bioengineering Strategies to Enhance the Therapeutic Potential of Extracellular Vesicles,” *Bioengineering*, 2022.

[51] C. Wen, R. C. Seeger, M. Fabbri, L. Wang, A. S. Wayne, and A. Y. Jong, “Biological roles and potential applications of immune cell-derived extracellular vesicles,” *J Extracell Vesicles*, vol. 6, no. 1, p. 1400370, 2017, doi: 10.1080/20013078.2017.1400370.

[52] A. G. Yates *et al.*, “In sickness and in health: The functional role of extracellular vesicles in physiology and pathology in vivo,” *J Extracell Vesicles*, vol. 11, no. 1, p. e12190, 2022, doi: 10.1002/jev2.12190.

[53] G. Raposo *et al.*, “B lymphocytes secrete antigen-presenting vesicles,” *J Exp Med*, vol. 183, no. 3, pp. 1161–1172, Mar. 1996, doi: 10.1084/JEM.183.3.1161.

[54] C. Théry, L. Duban, E. Segura, P. Væron, O. Lantz, and S. Amigorena, “Indirect activation of naïve CD4+ T cells by dendritic cell-derived exosomes,” *Nat Immunol*, vol. 3, no. 12, pp. 1156–1162, Dec. 2002, doi: 10.1038/NI854.

[55] S. Wan *et al.*, “CD8α + CD11c + Extracellular Vesicles in the Lungs Control Immune Homeostasis of the Respiratory Tract via TGF-β1 and IL-10,” *J Immunol*, vol. 200, no. 5, p. ji1701447, Jan. 2018, doi: 10.4049/JIMMUNOL.1701447.

[56] E. Lopez *et al.*, “Platelet-derived- Extracellular Vesicles Promote Hemostasis and Prevent the Development of Hemorrhagic Shock,” *Scientific Reports 2019 9:1*, vol. 9, no. 1, pp. 1–10, Nov. 2019, doi: 10.1038/s41598-019-53724-y.

[57] G. Tans *et al.*, “Comparison of anticoagulant and procoagulant activities of stimulated platelets and platelet-derived microparticles,” *Blood*, vol. 77, no. 12, pp. 2641–2648, Jun. 1991, doi: 10.1182/BLOOD.V77.12.2641.2641.

[58] Y. Miyazawa *et al.*, “AQP2 in human urine is predominantly localized to exosomes with preserved water channel activities,” *Clin Exp Nephrol*, vol. 22, no. 4, pp. 782–788, Aug. 2018, doi: 10.1007/S10157-018-1538-6/FIGURES/5.

[59] E. Hergenreider *et al.*, “Atheroprotective communication between endothelial cells and smooth muscle cells through miRNAs,” *Nat Cell Biol*, vol. 14, no. 3, pp. 249–256, Mar. 2012, doi: 10.1038/NCB2441.

[60] Y. Tanaka, Y. Okada, and N. Hirokawa, “FGF-induced vesicular release of Sonic hedgehog and retinoic acid in leftward nodal flow is critical for left–right determination,” *Nature 2005 435:7039*, vol. 435, no. 7039, pp. 172–177, May 2005, doi: 10.1038/nature03494.

[61] M. A. Lopez-Verrilli, F. Picou, and F. A. Court, “Schwann cell-derived exosomes enhance axonal regeneration in the peripheral nervous system,” *Glia*, vol. 61, no. 11, pp. 1795–1806, Nov. 2013, doi: 10.1002/GLIA.22558.

[62] C. S. Alvarez, J. Badia, M. Bosch, R. Giménez, and L. Baldomà, “Outer membrane vesicles and soluble factors released by probiotic escherichia coli nissle 1917 and commensal ECOR63

enhance barrier function by regulating expression of tight junction proteins in intestinal epithelial cells," *Front Microbiol*, vol. 7, no. DEC, 2016, doi: 10.3389/FMICB.2016.01981/FULL.

[63] N. Díaz-Garrido, J. Badia, and L. Baldomà, "Microbiota-derived extracellular vesicles in interkingdom communication in the gut," *J Extracell Vesicles*, vol. 10, no. 13, Nov. 2021, doi: 10.1002/JEV2.12161.

[64] K. Miyado *et al.*, "The fusing ability of sperm is bestowed by CD9-containing vesicles released from eggs in mice," *Proc Natl Acad Sci U S A*, vol. 105, no. 35, p. 12921, Sep. 2008, doi: 10.1073/PNAS.0710608105.

[65] K. H. Park *et al.*, "Ca2+ signaling tools acquired from prostasomes are required for progesterone-induced sperm motility," *Sci Signal*, vol. 4, no. 173, May 2011, doi: 10.1126/SCISIGNAL.2001595.

[66] M. Guescini *et al.*, "Muscle Releases Alpha-Sarcoglycan Positive Extracellular Vesicles Carrying miRNAs in the Bloodstream," *PLoS One*, vol. 10, no. 5, p. e0125094, May 2015, doi: 10.1371/JOURNAL.PONE.0125094.

[67] C. S. Fry, T. J. Kirby, K. Kosmac, J. J. McCarthy, and C. A. Peterson, "Myogenic Progenitor Cells Control Extracellular Matrix Production by Fibroblasts during Skeletal Muscle Hypertrophy," *Cell Stem Cell*, vol. 20, no. 1, pp. 56–69, Jan. 2017, doi: 10.1016/J.STEM.2016.09.010.

[68] C. Gomes, S. Keller, P. Altevogt, and J. Costa, "Evidence for secretion of Cu,Zn superoxide dismutase via exosomes from a cell model of amyotrophic lateral sclerosis," *Neurosci Lett*, vol. 428, no. 1, pp. 43–46, Nov. 2007, doi: 10.1016/J.NEULET.2007.09.024.

[69] C. Quek and A. F. Hill, "The role of extracellular vesicles in neurodegenerative diseases," *Biochem Biophys Res Commun*, vol. 483, no. 4, pp. 1178–1186, Feb. 2017, doi: 10.1016/J.BBRC.2016.09.090.

[70] C. Falker *et al.*, "Exosomal cellular prion protein drives fibrillization of amyloid beta and counteracts amyloid beta-mediated neurotoxicity," *J Neurochem*, vol. 137, no. 1, pp. 88–100, Apr. 2016, doi: 10.1111/JNC.13514.

[71] A. Schober, M. Nazari-Jahantigh, and C. Weber, "MicroRNA-mediated mechanisms of the cellular stress response in atherosclerosis," *Nat Rev Cardiol*, vol. 12, no. 6, pp. 361–374, Jun. 2015, doi: 10.1038/NRCARDIO.2015.38.

[72] L. Lyu *et al.*, "A critical role of cardiac fibroblast-derived exosomes in activating renin angiotensin system in cardiomyocytes," *J Mol Cell Cardiol*, vol. 89, no. Pt B, pp. 268–279, Dec. 2015, doi: 10.1016/J.YJMCC.2015.10.022.

[73] C. Bang *et al.*, "Cardiac fibroblast–derived microRNA passenger strand-enriched exosomes mediate cardiomyocyte hypertrophy," *J Clin Invest*, vol. 124, no. 5, p. 2136, May 2014, doi: 10.1172/JCI70577.

[74] L. Yang *et al.*, “Extracellular Vesicles Regulated by Viruses and Antiviral Strategies,” *Front Cell Dev Biol*, vol. 9, p. 2842, Oct. 2021, doi: 10.3389/FCELL.2021.722020/XML/NLM.

[75] Y. Jiang *et al.*, “Role of Extracellular Vesicles in Influenza Virus Infection,” *Front Cell Infect Microbiol*, vol. 10, p. 366, Jul. 2020, doi: 10.3389/FCIMB.2020.00366/XML/NLM.

[76] M. Hassanpour, J. Rezaie, M. Nouri, and Y. Panahi, “The role of extracellular vesicles in COVID-19 virus infection,” *Infection, Genetics and Evolution*, vol. 85, p. 104422, Nov. 2020, doi: 10.1016/J.MEEGID.2020.104422.

[77] P. Kucharzewska *et al.*, “Exosomes reflect the hypoxic status of glioma cells and mediate hypoxia-dependent activation of vascular cells during tumor development,” *Proc Natl Acad Sci U S A*, vol. 110, no. 18, pp. 7312–7317, Apr. 2013, doi: 10.1073/PNAS.1220998110/-/DCSUPPLEMENTAL/PNAS.201220998SI.PDF.

[78] E. Y. Yen, S. C. Miaw, J. S. Yu, and I. R. Lai, “Exosomal TGF-β1 is correlated with lymphatic metastasis of gastric cancers,” *Am J Cancer Res*, vol. 7, no. 11, p. 2199, 2017, Accessed: Aug. 30, 2022. [Online]. Available: /pmc/articles/PMC5714749/

[79] A. Hoshino *et al.*, “Tumour exosome integrins determine organotropic metastasis,” *Nature*, vol. 527, no. 7578, pp. 329–335, Nov. 2015, doi: 10.1038/NATURE15756.

[80] V. Muralidharan-Chari *et al.*, “Microvesicle removal of anticancer drugs contributes to drug resistance in human pancreatic cancer cells,” *Oncotarget*, vol. 7, no. 31, pp. 50365–50379, Jul. 2016, doi: 10.18632/ONCOTARGET.10395.

[81] R. W. Y. Yeo, R. C. Lai, K. H. Tan, and S. K. Lim, “Exosome: A Novel and Safer Therapeutic Refinement of Mesenchymal Stem Cell:,” *http://dx.doi.org/10.5772/57460*, p. 1, Jan. 2013, doi: 10.5772/57460.

[82] S. G. Ong and J. C. Wu, “Exosomes as Potential Alternatives to Stem Cell Therapy in Mediating Cardiac Regeneration,” *Circ Res*, vol. 117, no. 1, p. 7, Jun. 2015, doi: 10.1161/CIRCRESAHA.115.306593.

[83] R. C. Lai *et al.*, “Exosome secreted by MSC reduces myocardial ischemia/reperfusion injury,” *Stem Cell Res*, vol. 4, no. 3, pp. 214–222, May 2010, doi: 10.1016/J.SCR.2009.12.003.

[84] S. Bruno *et al.*, “Mesenchymal stem cell-derived microvesicles protect against acute tubular injury,” *J Am Soc Nephrol*, vol. 20, no. 5, pp. 1053–1067, May 2009, doi: 10.1681/ASN.2008070798.

[85] A. I. Caplan and J. E. Dennis, “Mesenchymal stem cells as trophic mediators,” *J Cell Biochem*, vol. 98, no. 5, pp. 1076–1084, Aug. 2006, doi: 10.1002/JCB.20886.

[86] A. Klimczak and U. Kozlowska, “Mesenchymal Stromal Cells and Tissue-Specific Progenitor Cells: Their Role in Tissue Homeostasis,” *Stem Cells Int*, vol. 2016, 2016, doi: 10.1155/2016/4285215.

[87] J. Wu *et al.*, “miR-100-5p-abundant exosomes derived from infrapatellar fat pad MSCs protect articular cartilage and ameliorate gait abnormalities via inhibition of mTOR in osteoarthritis,” *Biomaterials*, vol. 206, pp. 87–100, Jun. 2019, doi: 10.1016/J.BIOMATERIALS.2019.03.022.

[88] Y. Nakamura *et al.*, “Mesenchymal-stem-cell-derived exosomes accelerate skeletal muscle regeneration,” *FEBS Lett*, vol. 589, no. 11, pp. 1257–1265, May 2015, doi: 10.1016/J.FEBSLET.2015.03.031.

[89] S. Gatti *et al.*, “Microvesicles derived from human adult mesenchymal stem cells protect against ischaemia–reperfusion-induced acute and chronic kidney injury,” *Nephrology Dialysis Transplantation*, vol. 26, no. 5, pp. 1474–1483, May 2011, doi: 10.1093/NDT/GFR015.

[90] Q. Luo *et al.*, “Antioxidant activity of mesenchymal stem cell-derived extracellular vesicles restores hippocampal neurons following seizure damage,” *Theranostics*, vol. 11, no. 12, p. 5986, 2021, doi: 10.7150/THNO.58632.

[91] F. Arslan *et al.*, “Mesenchymal stem cell-derived exosomes increase ATP levels, decrease oxidative stress and activate PI3K/Akt pathway to enhance myocardial viability and prevent adverse remodeling after myocardial ischemia/reperfusion injury,” *Stem Cell Res*, vol. 10, no. 3, pp. 301–312, May 2013, doi: 10.1016/J.SCR.2013.01.002.

[92] K. Clark *et al.*, “Placental Mesenchymal Stem Cell-Derived Extracellular Vesicles Promote Myelin Regeneration in an Animal Model of Multiple Sclerosis,” *Cells*, vol. 8, no. 12, Dec. 2019, doi: 10.3390/CELLS8121497.

[93] P. Vader, X. O. Breakefield, and M. J. A. Wood, “Extracellular vesicles: Emerging targets for cancer therapy,” *Trends Mol Med*, vol. 20, no. 7, p. 385, 2014, doi: 10.1016/J.MOLMED.2014.03.002.

[94] G. Szabo and F. Momen-Heravi, “Extracellular vesicles in liver disease and potential as biomarkers and therapeutic targets,” *Nat Rev Gastroenterol Hepatol*, vol. 14, no. 8, pp. 455–466, Aug. 2017, doi: 10.1038/NRGASTRO.2017.71.

[95] F. Urabe, N. Kosaka, K. Ito, T. Kimura, S. Egawa, and T. Ochiya, “Extracellular vesicles as biomarkers and therapeutic targets for cancer,” *Am J Physiol Cell Physiol*, vol. 318, no. 1, pp. C29–C39, 2020, doi: 10.1152/AJPCELL.00280.2019/ASSET/IMAGES/LARGE/ZH00012085970003.JPEG.

[96] N. Kosaka, H. Iguchi, K. Hagiwara, Y. Yoshioka, F. Takeshita, and T. Ochiya, “Neutral sphingomyelinase 2 (nSMase2)-dependent exosomal transfer of angiogenic micrornas regulate cancer cell metastasis,” *Journal of Biological Chemistry*, vol. 288, no. 15, pp. 10849–10859, Apr. 2013, doi: 10.1074/JBC.M112.446831.

[97] A. G. Thompson *et al.*, “Extracellular vesicles in neurodegenerative disease - pathogenesis to biomarkers,” *Nat Rev Neurol*, vol. 12, no. 6, pp. 346–357, Jun. 2016, doi: 10.1038/NRNEUROL.2016.68.

[98] T. Katsuda, N. Kosaka, and T. Ochiya, “The roles of extracellular vesicles in cancer biology: toward the development of novel cancer biomarkers,” *Proteomics*, vol. 14, no. 4–5, pp. 412–425, Mar. 2014, doi: 10.1002/PMIC.201300389.

[99] O. G. de Jong *et al.*, “Drug Delivery with Extracellular Vesicles: From Imagination to Innovation,” *Acc Chem Res*, vol. 52, no. 7, pp. 1761–1770, Jul. 2019, doi: 10.1021/ACS.ACCOUNTS.9B00109/ASSET/IMAGES/LARGE/AR-2019-00109Z_0003.JPEG.

[100] J. Skog *et al.*, “Glioblastoma microvesicles transport RNA and proteins that promote tumour growth and provide diagnostic biomarkers,” *Nat Cell Biol*, vol. 10, no. 12, pp. 1470–1476, 2008, doi: 10.1038/NCB1800.

[101] J. Liu *et al.*, “Extracellular Vesicles in Liquid Biopsies: Potential for Disease Diagnosis,” *Biomed Res Int*, vol. 2021, 2021, doi: 10.1155/2021/6611244.

[102] M. Mehanny, C. M. Lehr, and G. Fuhrmann, “Extracellular vesicles as antigen carriers for novel vaccination avenues,” *Adv Drug Deliv Rev*, vol. 173, pp. 164–180, Jun. 2021, doi: 10.1016/J.ADDR.2021.03.016.

[103] L. Zitvogel *et al.*, “Eradication of established murine tumors using a novel cell-free vaccine: dendritic cell-derived exosomes,” *Nat Med*, vol. 4, no. 5, pp. 594–600, May 1998, doi: 10.1038/NM0598-594.

[104] S. Adepu and S. Ramakrishna, “Controlled Drug Delivery Systems: Current Status and Future Directions,” *Molecules*, vol. 26, no. 19, Oct. 2021, doi: 10.3390/MOLECULES26195905.

[105] M. K. Jayasinghe *et al.*, “New approaches in extracellular vesicle engineering for improving the efficacy of anti-cancer therapies,” *Semin Cancer Biol*, vol. 74, pp. 62–78, Sep. 2021, doi: 10.1016/j.semcancer.2021.02.010.

[106] S. Kamerkar *et al.*, “Exosomes facilitate therapeutic targeting of oncogenic KRAS in pancreatic cancer,” *Nature 2017 546:7659*, vol. 546, no. 7659, pp. 498–503, Jun. 2017, doi: 10.1038/nature22341.

[107] L. Alvarez-Erviti, Y. Seow, H. Yin, C. Betts, S. Lakhal, and M. J. A. Wood, “Delivery of siRNA to the mouse brain by systemic injection of targeted exosomes,” *Nat Biotechnol*, vol. 29, no. 4, pp. 341–345, Apr. 2011, doi: 10.1038/NBT.1807.

[108] T. R. Damase, R. Sukhovershin, C. Boada, F. Taraballi, R. I. Pettigrew, and J. P. Cooke, “The Limitless Future of RNA Therapeutics,” *Front Bioeng Biotechnol*, vol. 9, p. 161, Mar. 2021, doi: 10.3389/FBIOE.2021.628137/BIBTEX.

[109] J. A. Kulkarni *et al.*, “The current landscape of nucleic acid therapeutics,” *Nature Nanotechnology 2021 16:6*, vol. 16, no. 6, pp. 630–643, May 2021, doi: 10.1038/s41565-021-00898-0.

[110] T. Smyth, M. Kullberg, N. Malik, P. Smith-Jones, M. W. Graner, and T. J. Anchordoquy, “Biodistribution and delivery efficiency of unmodified tumor-derived exosomes,” *Journal of Controlled Release*, vol. 199, pp. 145–155, Feb. 2015, doi: 10.1016/J.JCONREL.2014.12.013.

[111] A. Akbarzadeh *et al.*, “Liposome: classification, preparation, and applications,” *Nanoscale Res Lett*, vol. 8, no. 1, p. 102, 2013, doi: 10.1186/1556-276X-8-102.

[112] L. van der Koog, T. B. Gandek, and A. Nagelkerke, “Liposomes and Extracellular Vesicles as Drug Delivery Systems: A Comparison of Composition, Pharmacokinetics, and Functionalization,” *Adv Healthc Mater*, vol. 11, no. 5, p. 2100639, Mar. 2022, doi: 10.1002/ADHM.202100639.

[113] S. A. A. Kooijmans *et al.*, “PEGylated and targeted extracellular vesicles display enhanced cell specificity and circulation time,” *Journal of Controlled Release*, vol. 224, pp. 77–85, Feb. 2016, doi: 10.1016/J.JCONREL.2016.01.009.

[114] X. Gao *et al.*, “Anchor peptide captures, targets, and loads exosomes of diverse origins for diagnostics and therapy,” *Sci Transl Med*, vol. 10, no. 444, p. eaat0195, 2018, doi: 10.1126/scitranslmed.aat0195.

[115] G. Jia *et al.*, “NRP-1 targeted and cargo-loaded exosomes facilitate simultaneous imaging and therapy of glioma in vitro and in vivo,” *Biomaterials*, vol. 178, pp. 302–316, Sep. 2018, doi: 10.1016/J.BIOMATERIALS.2018.06.029.

[116] R. Tamura, S. Uemoto, and Y. Tabata, “Augmented liver targeting of exosomes by surface modification with cationized pullulan,” *Acta Biomater*, vol. 57, pp. 274–284, Jul. 2017, doi: 10.1016/J.ACTBIO.2017.05.013.

[117] D. E. Murphy *et al.*, “Extracellular vesicle-based therapeutics: natural versus engineered targeting and trafficking,” *Exp Mol Med*, vol. 51, no. 3, p. 32, 2019, doi: 10.1038/s12276-019-0223-5.

[118] N. Kosaka, H. Iguchi, Y. Yoshioka, F. Takeshita, Y. Matsuki, and T. Ochiya, “Secretory Mechanisms and Intercellular Transfer of MicroRNAs in Living Cells,” *J Biol Chem*, vol. 285, no. 23, p. 17442, Jun. 2010, doi: 10.1074/JBC.M110.107821.

[119] P. Vader, E. A. Mol, G. Pasterkamp, and R. M. Schiffelers, “Extracellular vesicles for drug delivery,” *Adv Drug Deliv Rev*, vol. 106, no. Pt A, pp. 148–156, Nov. 2016, doi: 10.1016/J.ADDR.2016.02.006.

[120] B. György, M. E. H. #3, X. O. Breakefield, and J. N. Leonard, “Therapeutic Applications of Extracellular Vesicles: Clinical Promise and Open Questions HHS Public Access,” *Annu Rev Pharmacol Toxicol*, vol. 55, pp. 439–464, 2015, doi: 10.1146/annurev-pharmtox-010814-124630.

[121] L. Qiao *et al.*, “Tumor cell-derived exosomes home to their cells of origin and can be used as Trojan horses to deliver cancer drugs,” *Theranostics*, vol. 10, no. 8, pp. 3474–3487, 2020, doi: 10.7150/THNO.39434.

[122] M. Guo *et al.*, “Autologous tumor cell-derived microparticle-based targeted chemotherapy in lung cancer patients with malignant pleural effusion,” *Sci Transl Med*, vol. 11, no. 474, Jan. 2019, doi: 10.1126/SCITRANSLMED.AAT5690.

[123] T. Yong *et al.*, “Tumor exosome-based nanoparticles are efficient drug carriers for chemotherapy,” *Nature Communications 2019 10:1*, vol. 10, no. 1, pp. 1–16, Aug. 2019, doi: 10.1038/s41467-019-11718-4.

[124] J. Ma *et al.*, “Reversing drug resistance of soft tumor-repopulating cells by tumor cell-derived chemotherapeutic microparticles,” *Cell Research 2016 26:6*, vol. 26, no. 6, pp. 713–727, May 2016, doi: 10.1038/cr.2016.53.

[125] N. Chaput and C. Théry, “Exosomes: immune properties and potential clinical implementations,” *Semin Immunopathol*, vol. 33, no. 5, pp. 419–440, Jan. 2011, doi: 10.1007/S00281-010-0233-9.

[126] S. Walker *et al.*, “Extracellular vesicle-based drug delivery systems for cancer treatment,” *Theranostics*, vol. 9, no. 26, p. 8001, 2019, doi: 10.7150/THNO.37097.

[127] S. Kalimuthu *et al.*, “In Vivo therapeutic potential of mesenchymal stem cell-derived extracellular vesicles with optical imaging reporter in tumor mice model,” *Sci Rep*, vol. 6, Jul. 2016, doi: 10.1038/SREP30418.

[128] Y. Zhou, Y. Yamamoto, F. Takeshita, T. Yamamoto, Z. Xiao, and T. Ochiya, “Delivery of miR-424-5p via extracellular vesicles promotes the apoptosis of MDA-MB-231 TNBC cells in the tumor microenvironment,” *Int J Mol Sci*, vol. 22, no. 2, pp. 1–17, Jan. 2021, doi: 10.3390/IJMS22020844.

[129] R. Kim *et al.*, “Exosomes derived from microRNA-584 transfected mesenchymal stem cells: novel alternative therapeutic vehicles for cancer therapy,” *BMB Rep*, vol. 51, no. 8, p. 406, 2018, doi: 10.5483/BMBREP.2018.51.8.105.

[130] C. Paganini, U. Capasso Palmiero, G. Pocsfalvi, N. Touzet, A. Bongiovanni, and P. Arosio, “Scalable Production and Isolation of Extracellular Vesicles: Available Sources and Lessons from Current Industrial Bioprocesses,” *Biotechnol J*, vol. 14, no. 10, p. 1800528, Oct. 2019, doi: 10.1002/BIOT.201800528.

[131] M. J. A. WSamir EL Andaloussi, Imre Mäger, Xandra O. Breakefield and Matthew J. A. Woodood, “Extracellular vesicles: biology and emerging therapeutic opportunities,” *Nature Publishing Group*, vol. 12, no. 5, pp. 347–357, 2013, doi: 10.1038/nrd3978.

[132] A. Grangier *et al.*, “Technological advances towards extracellular vesicles mass production,” *Adv Drug Deliv Rev*, vol. 176, 2021, doi: 10.1016/J.ADDR.2021.113843.

[133] R. J. Madel *et al.*, “Independent human mesenchymal stromal cell-derived extracellular vesicle preparations differentially affect symptoms in an advanced murine Graft-versus-Host-Disease model,” *bioRxiv*, p. 2020.12.21.423658, Dec. 2020, doi: 10.1101/2020.12.21.423658.

[134] D. B. Patel, K. M. Gray, Y. Santharam, T. N. Lamichhane, K. M. Stroka, and S. M. Jay, “Impact of cell culture parameters on production and vascularization bioactivity of mesenchymal stem cell-derived extracellular vesicles,” *Bioeng Transl Med*, vol. 2, no. 2, pp. 170–179, 2017, doi: 10.1002/BTM2.10065.

[135] J. Cao *et al.*, “Three-dimensional culture of MSCs produces exosomes with improved yield and enhanced therapeutic efficacy for cisplatin-induced acute kidney injury,” *Stem Cell Res Ther*, vol. 11, no. 1, pp. 1–13, May 2020, doi: 10.1186/S13287-020-01719-2/FIGURES/7.

[136] R. A. Haraszti *et al.*, “Exosomes Produced from 3D Cultures of MSCs by Tangential Flow Filtration Show Higher Yield and Improved Activity,” *Mol Ther*, vol. 26, no. 12, pp. 2838–2847, Dec. 2018, doi: 10.1016/J.YMTHE.2018.09.015.

[137] M. de Almeida Fuzeta *et al.*, “Scalable Production of Human Mesenchymal Stromal Cell-Derived Extracellular Vesicles Under Serum-/Xeno-Free Conditions in a Microcarrier-Based Bioreactor Culture System,” *Front Cell Dev Biol*, vol. 8, p. 553444, 2020, doi: 10.3389/fcell.2020.553444.

[138] M. S. Croughan, D. Giroux, D. Fang, and B. Lee, “Novel Single-Use Bioreactors for Scale-Up of Anchorage-Dependent Cell Manufacturing for Cell Therapies,” *Stem Cell Manufacturing*. Elsevier, pp. 105–139, Sep. 2016. doi: 10.1016/B978-0-444-63265-4.00005-4.

[139] J. P. Bost *et al.*, “Growth Media Conditions Influence the Secretion Route and Release Levels of Engineered Extracellular Vesicles,” *Adv Healthc Mater*, vol. 11, no. 5, Mar. 2022, doi: 10.1002/ADHM.202101658.

[140] M. Lu and Y. Huang, “Bioinspired exosome-like therapeutics and delivery nanoplatforms,” *Biomaterials*, vol. 242, Jun. 2020, doi: 10.1016/J.BIOMATERIALS.2020.119925.

[141] Y. Zhang *et al.*, “Systemic administration of cell-free exosomes generated by human bone marrow derived mesenchymal stem cells cultured under 2D and 3D conditions improves functional recovery in rats after traumatic brain injury,” *Neurochem Int*, vol. 111, pp. 69–81, Dec. 2017, doi: 10.1016/J.NEUINT.2016.08.003.

[142] S. C. Jang *et al.*, “ExoSTING, an extracellular vesicle loaded with STING agonists, promotes tumor immune surveillance,” *Commun Biol*, vol. 4, no. 1, p. 497, 2021, doi: 10.1038/s42003-021-02004-5.

[143] A. Grangier *et al.*, “Technological advances towards extracellular vesicles mass production,” *Adv Drug Deliv Rev*, vol. 176, Sep. 2021, doi: 10.1016/J.ADDR.2021.113843.

[144] K. Rekker *et al.*, “Comparison of serum exosome isolation methods for microRNA profiling,” *Clin Biochem*, vol. 47, no. 1–2, pp. 135–138, Jan. 2014, doi: 10.1016/J.CLINBIOCHEM.2013.10.020.

[145] J. Stam, S. Bartel, R. Bischoff, and J. C. Wolters, “Isolation of extracellular vesicles with combined enrichment methods,” *Journal of Chromatography B*, vol. 1169, p. 122604, 2021, doi: https://doi.org/10.1016/j.jchromb.2021.122604.

[146] K. Brennan *et al.*, “A comparison of methods for the isolation and separation of extracellular vesicles from protein and lipid particles in human serum,” *Sci Rep*, vol. 10, no. 1, p. 1039, 2020, doi: 10.1038/s41598-020-57497-7.

[147] M. Zhang *et al.*, “Methods and Technologies for Exosome Isolation and Characterization,” *Small Methods*, vol. 2, no. 9, p. 1800021, Sep. 2018, doi: 10.1002/SMTD.201800021.

[148] F. Zhang *et al.*, “Application of engineered extracellular vesicles for targeted tumor therapy,” *J Biomed Sci*, vol. 29, no. 1, Dec. 2022, doi: 10.1186/S12929-022-00798-Y.

[149] F. Royo, C. Théry, J. M. Falcón-Pérez, R. Nieuwland, and K. W. Witwer, “Methods for Separation and Characterization of Extracellular Vesicles: Results of a Worldwide Survey Performed by the ISEV Rigor and Standardization Subcommittee,” *Cells*, vol. 9, no. 9, Aug. 2020, doi: 10.3390/CELLS9091955.

[150] C. Théry *et al.*, “Minimal information for studies of extracellular vesicles 2018 (MISEV2018): a position statement of the International Society for Extracellular Vesicles and update of the MISEV2014 guidelines,” *J Extracell Vesicles*, vol. 7, no. 1, Jan. 2018, doi: 10.1080/20013078.2018.1535750.

[151] Z. Zhao, H. Wijerathne, A. K. Godwin, and S. A. Soper, “Isolation and analysis methods of extracellular vesicles (EVs),” *Extracell Vesicles Circ Nucl Acids*, vol. 2, p. 80, 2021, doi: 10.20517/EVCNA.2021.07.

[152] S. Otsuru *et al.*, “Extracellular vesicles released from mesenchymal stromal cells stimulate bone growth in osteogenesis imperfecta,” *Cytotherapy*, vol. 20, no. 1, pp. 62–73, Jan. 2018, doi: 10.1016/J.JCYT.2017.09.012.

[153] C. lo Sicco *et al.*, “Mesenchymal Stem Cell-Derived Extracellular Vesicles as Mediators of Anti-Inflammatory Effects: Endorsement of Macrophage Polarization,” *Stem Cells Transl Med*, vol. 6, no. 3, pp. 1018–1028, Mar. 2017, doi: 10.1002/SCTM.16-0363.

[154] T. Han *et al.*, “MSC secreted extracellular vesicles carrying TGF-beta upregulate Smad 6 expression and promote the regrowth of neurons in spinal cord injured rats,” *Stem Cell Rev Rep*, vol. 18, no. 3, p. 1078, Mar. 2022, doi: 10.1007/S12015-021-10219-6.

[155] Y. Lu *et al.*, “Bone Mesenchymal Stem Cell-Derived Extracellular Vesicles Promote Recovery Following Spinal Cord Injury via Improvement of the Integrity of the Blood-Spinal Cord Barrier,” *Front Neurosci*, vol. 13, Mar. 2019, doi: 10.3389/FNINS.2019.00209.

[156] K. M. Luther *et al.*, “Exosomal miR-21a-5p mediates cardioprotection by mesenchymal stem cells,” *J Mol Cell Cardiol*, vol. 119, pp. 125–137, Jun. 2018, doi: 10.1016/J.YJMCC.2018.04.012.

[157] S. Mardpour *et al.*, “Extracellular vesicles derived from human embryonic stem cell-MSCs ameliorate cirrhosis in thioacetamide-induced chronic liver injury,” *J Cell Physiol*, vol. 233, no. 12, pp. 9330–9344, Dec. 2018, doi: 10.1002/JCP.26413.

[158] S. Varderidou-Minasian and M. J. Lorenowicz, “Mesenchymal stromal/stem cell-derived extracellular vesicles in tissue repair: challenges and opportunities,” *Theranostics*, vol. 10, no. 13, p. 5979, 2020, doi: 10.7150/THNO.40122.

[159] J. D. McBride, L. Rodriguez-Menocal, W. Guzman, A. Candanedo, M. Garcia-Contreras, and E. v. Badiavas, “Bone Marrow Mesenchymal Stem Cell-Derived CD63+ Exosomes Transport Wnt3a Exteriorly and Enhance Dermal Fibroblast Proliferation, Migration, and Angiogenesis In Vitro,” *Stem Cells Dev*, vol. 26, no. 19, pp. 1384–1398, Oct. 2017, doi: 10.1089/SCD.2017.0087.

[160] L. Paolini *et al.*, “Residual matrix from different separation techniques impacts exosome biological activity,” *undefined*, vol. 6, Mar. 2016, doi: 10.1038/SREP23550.

[161] C. Xue *et al.*, “Exosomes Derived from Hypoxia-Treated Human Adipose Mesenchymal Stem Cells Enhance Angiogenesis Through the PKA Signaling Pathway,” *Stem Cells Dev*, vol. 27, no. 7, pp. 456–465, Apr. 2018, doi: 10.1089/SCD.2017.0296.

[162] Y. Zhu *et al.*, “Comparison of exosomes secreted by induced pluripotent stem cell-derived mesenchymal stem cells and synovial membrane-derived mesenchymal stem cells for the treatment of osteoarthritis,” *Stem Cell Res Ther*, vol. 8, no. 1, Mar. 2017, doi: 10.1186/S13287-017-0510-9.

[163] S. Busatto *et al.*, “Tangential Flow Filtration for Highly Efficient Concentration of Extracellular Vesicles from Large Volumes of Fluid,” *Cells*, vol. 7, no. 12, Jan. 2018, doi: 10.3390/CELLS7120273.

[164] C. H. Woo *et al.*, “Small extracellular vesicles from human adipose-derived stem cells attenuate cartilage degeneration,” *J Extracell Vesicles*, vol. 9, no. 1, Jan. 2020, doi: 10.1080/20013078.2020.1735249.

[165] A. Porzionato *et al.*, “Intratracheal administration of clinical-grade mesenchymal stem cell-derived extracellular vesicles reduces lung injury in a rat model of bronchopulmonary dysplasia,” *Am J Physiol Lung Cell Mol Physiol*, vol. 316, no. 1, pp. L6–L19, Jan. 2019, doi: 10.1152/AJPLUNG.00109.2018.

[166] M. Monguió-Tortajada *et al.*, “Nanosized UCMSC-derived extracellular vesicles but not conditioned medium exclusively inhibit the inflammatory response of stimulated T cells: implications for nanomedicine,” *Theranostics*, vol. 7, no. 2, p. 270, 2017, doi: 10.7150/THNO.16154.

[167] S. S. Kanwar, C. J. Dunlay, D. M. Simeone, and S. Nagrath, “Microfluidic device (ExoChip) for on-chip isolation, quantification and characterization of circulating exosomes,” *Lab Chip*, vol. 14, no. 11, pp. 1891–1900, Jun. 2014, doi: 10.1039/C4LC00136B.

[168] H. Shao *et al.*, “Chip-based analysis of exosomal mRNA mediating drug resistance in glioblastoma,” *Nature Communications 2015 6:1*, vol. 6, no. 1, pp. 1–9, May 2015, doi: 10.1038/ncomms7999.

[169] S. Varderidou-Minasian and M. J. Lorenowicz, “Mesenchymal stromal/stem cell-derived extracellular vesicles in tissue repair: challenges and opportunities,” *Theranostics*, vol. 10, no. 13, p. 5979, 2020, doi: 10.7150/THNO.40122.

[170] S. C. Guo, S. C. Tao, and H. Dawn, “Microfluidics-based on-a-chip systems for isolating and analysing extracellular vesicles,” *J Extracell Vesicles*, vol. 7, no. 1, Jan. 2018, doi: 10.1080/20013078.2018.1508271.

[171] N. Heath *et al.*, “Rapid isolation and enrichment of extracellular vesicle preparations using anion exchange chromatography,” *Scientific Reports 2018 8:1*, vol. 8, no. 1, pp. 1–12, Apr. 2018, doi: 10.1038/s41598-018-24163-y.

[172] T. Shigemoto-Kuroda *et al.*, “MSC-derived Extracellular Vesicles Attenuate Immune Responses in Two Autoimmune Murine Models: Type 1 Diabetes and Uveoretinitis,” *Stem Cell Reports*, vol. 8, no. 5, p. 1214, May 2017, doi: 10.1016/J.STEMCR.2017.04.008.

[173] D. C. Watson *et al.*, “Scalable, cGMP-compatible purification of extracellular vesicles carrying bioactive human heterodimeric IL-15/lactadherin complexes,” *J Extracell Vesicles*, vol. 7, no. 1, Jan. 2018, doi: 10.1080/20013078.2018.1442088/SUPPL_FILE/ZJEV_A_1442088_SM6568.ZIP.

[174] O. G. de Jong *et al.*, “A CRISPR-Cas9-based reporter system for single-cell detection of extracellular vesicle-mediated functional transfer of RNA,” *Nature Communications 2020 11:1*, vol. 11, no. 1, pp. 1–13, Feb. 2020, doi: 10.1038/s41467-020-14977-8.

[175] Y. You *et al.*, “Human neural cell type-specific extracellular vesicle proteome defines disease-related molecules associated with activated astrocytes in Alzheimer’s disease brain,” *J Extracell Vesicles*, vol. 11, no. 1, p. e12183, Jan. 2022, doi: 10.1002/JEV2.12183.

[176] Y. Chen and L. Yu, “Extracellular vesicles: from bench to bedside,” *Current Medicine 2022 1:1*, vol. 1, no. 1, pp. 1–12, May 2022, doi: 10.1007/S44194-022-00001-2.

[177] A. Nagelkerke *et al.*, “Extracellular vesicles for tissue repair and regeneration: Evidence, challenges and opportunities,” *Adv Drug Deliv Rev*, vol. 175, p. 113775, Aug. 2021, doi: 10.1016/J.ADDR.2021.04.013.

[178] W. Meng, C. He, Y. Hao, L. Wang, L. Li, and G. Zhu, “Prospects and challenges of extracellular vesicle-based drug delivery system: considering cell source,” *Drug Deliv*, vol. 27, no. 1, pp. 585–598, Jan. 2020, doi: 10.1080/10717544.2020.1748758.

[179] G. E. Melling, E. Carollo, R. Conlon, J. C. Simpson, and D. R. F. Carter, “The Challenges and Possibilities of Extracellular Vesicles as Therapeutic Vehicles,” *Eur J Pharm Biopharm*, vol. 144, pp. 50–56, Nov. 2019, doi: 10.1016/J.EJPB.2019.08.009.

[180] M. I. Ramirez *et al.*, “Technical challenges of working with extracellular vesicles,” *Nanoscale*, vol. 10, no. 3, pp. 881–906, Jan. 2018, doi: 10.1039/C7NR08360B.

[181] I. K. Herrmann, M. J. A. Wood, and G. Fuhrmann, “Extracellular vesicles as a next-generation drug delivery platform,” *Nature Nanotechnology 2021 16:7*, vol. 16, no. 7, pp. 748–759, Jul. 2021, doi: 10.1038/s41565-021-00931-2.

[182] V. Agrahari, V. Agrahari, P. A. Burnouf, C. H. Chew, and T. Burnouf, “Extracellular Microvesicles as New Industrial Therapeutic Frontiers,” *Trends Biotechnol*, vol. 37, no. 7, pp. 707–729, Jul. 2019, doi: 10.1016/J.TIBTECH.2018.11.012.

[183] M. Tkach and C. Théry, “Communication by Extracellular Vesicles: Where We Are and Where We Need to Go,” *Cell*, vol. 164, no. 6, pp. 1226–1232, Mar. 2016, doi: 10.1016/J.CELL.2016.01.043.

[184] Y. Xu, K. Feng, H. Zhao, L. Di, L. Wang, and R. Wang, “Tumor-derived extracellular vesicles as messengers of natural products in cancer treatment,” *Theranostics*, vol. 12, no. 4, p. 1683, 2022, doi: 10.7150/THNO.67775.

[185] J. Frank, M. Richter, C. de Rossi, C. M. Lehr, K. Fuhrmann, and G. Fuhrmann, “Extracellular vesicles protect glucuronidase model enzymes during freeze-drying,” *Sci Rep*, vol. 8, no. 1, Dec. 2018, doi: 10.1038/S41598-018-30786-Y.

[186] T. Burnouf, V. Agrahari, and V. Agrahari, “Extracellular Vesicles As Nanomedicine: Hopes And Hurdles In Clinical Translation,” *Int J Nanomedicine*, vol. 14, p. 8847, 2019, doi: 10.2147/IJN.S225453.

[187] A. I. Caplan, “Mesenchymal stem cells,” *J Orthop Res*, vol. 9, no. 5, pp. 641–650, 1991, doi: 10.1002/JOR.1100090504.

[188] M. de Almeida Fuzeta, “Scalable Production of Extracellular Vesicles Derived from Mesenchymal Stromal Cells for Cancer-Targeted Drug Delivery,” 2021.

[189] S. Viswanathan *et al.*, “Mesenchymal stem versus stromal cells: International Society for Cell & Gene Therapy (ISCT®) Mesenchymal Stromal Cell committee position statement on nomenclature,” *Cytotherapy*, vol. 21, no. 10, pp. 1019–1024, Oct. 2019, doi: 10.1016/J.JCYT.2019.08.002.

[190] L. da Silva Meirelles, A. M. Fontes, D. T. Covas, and A. I. Caplan, “Mechanisms involved in the therapeutic properties of mesenchymal stem cells,” *Cytokine Growth Factor Rev*, vol. 20, no. 5–6, pp. 419–427, Oct. 2009, doi: 10.1016/J.CYTOGFR.2009.10.002.

[191] D. Macrin, J. P. Joseph, A. A. Pillai, and A. Devi, “Eminent Sources of Adult Mesenchymal Stem Cells and Their Therapeutic Imminence,” *Stem Cell Rev Rep*, vol. 13, no. 6, pp. 741–756, Dec. 2017, doi: 10.1007/S12015-017-9759-8.

[192] U. Kozlowska *et al.*, “Similarities and differences between mesenchymal stem/progenitor cells derived from various human tissues,” *World J Stem Cells*, vol. 11, no. 6, p. 347, Jun. 2019, doi: 10.4252/WJSC.V11.I6.347.

[193] M. Strioga, S. Viswanathan, A. Darinskas, O. Slaby, and J. Michalek, “Same or Not the Same? Comparison of Adipose Tissue-Derived Versus Bone Marrow-Derived Mesenchymal Stem and Stromal Cells,” *https://home.liebertpub.com/scd*, vol. 21, no. 14, pp. 2724–2752, Apr. 2012, doi: 10.1089/SCD.2011.0722.

[194] Y. Petrenko *et al.*, “A Comparative Analysis of Multipotent Mesenchymal Stromal Cells derived from Different Sources, with a Focus on Neuroregenerative Potential,” *Scientific Reports 2020 10:1*, vol. 10, no. 1, pp. 1–15, Mar. 2020, doi: 10.1038/s41598-020-61167-z.

[195] H. M. Lazarus, S. E. Haynesworth, S. L. Gerson, N. S. Rosenthal, and A. I. Caplan, “Ex vivo expansion and subsequent infusion of human bone marrow-derived stromal progenitor cells (mesenchymal progenitor cells): implications for therapeutic use.,” *Bone Marrow Transplant*, vol. 16, no. 4, pp. 557–564, Oct. 1995, Accessed: Aug. 31, 2022. [Online]. Available: https://europepmc.org/article/med/8528172

[196] J. Galipeau and L. Sensébé, “Mesenchymal Stromal Cells: Clinical Challenges and Therapeutic Opportunities,” *Cell Stem Cell*, vol. 22, no. 6, pp. 824–833, Jun. 2018, doi: 10.1016/J.STEM.2018.05.004.

[197] N. Bernardes and A. M. Fialho, “Perturbing the Dynamics and Organization of Cell Membrane Components: A New Paradigm for Cancer-Targeted Therapies,” *Int J Mol Sci*, vol. 19, no. 12, Dec. 2018, doi: 10.3390/IJMS19123871.

[198] N. Bernardes *et al.*, “The bacterial protein azurin impairs invasion and FAK/Src signaling in P-cadherin-overexpressing breast cancer cell models,” *PLoS One*, vol. 8, no. 7, Jul. 2013, doi: 10.1371/JOURNAL.PONE.0069023.

[199] V. Punj *et al.*, “Bacterial cupredoxin azurin as an inducer of apoptosis and regression in human breast cancer,” *Oncogene*, vol. 23, no. 13, pp. 2367–2378, Mar. 2004, doi: 10.1038/SJ.ONC.1207376.

[200] T. Yamada *et al.*, “Bacterial redox protein azurin, tumor suppressor protein p53, and regression of cancer,” *Proc Natl Acad Sci U S A*, vol. 99, no. 22, p. 14098, Oct. 2002, doi: 10.1073/PNAS.222539699.

[201] N. Bernardes, S. Abreu, F. A. Carvalho, F. Fernandes, N. C. Santos, and A. M. Fialho, “Modulation of membrane properties of lung cancer cells by azurin enhances the sensitivity to

EGFR-targeted therapy and decreased β1 integrin-mediated adhesion," *Cell Cycle*, vol. 15, no. 11, pp. 1415–1424, Jun. 2016, doi: 10.1080/15384101.2016.1172147.

[202] T. Yamada, A. M. Fialho, V. Punj, L. Bratescu, T. K. das Gupta, and A. M. Chakrabarty, "Internalization of bacterial redox protein azurin in mammalian cells: entry domain and specificity," *Cell Microbiol*, vol. 7, no. 10, pp. 1418–1431, Oct. 2005, doi: 10.1111/J.1462-5822.2005.00567.X.

[203] R. R. Lulla *et al.*, "Phase I trial of p28 (NSC745104), a non-HDM2-mediated peptide inhibitor of p53 ubiquitination in pediatric patients with recurrent or progressive central nervous system tumors: A Pediatric Brain Tumor Consortium Study," *Neuro Oncol*, vol. 18, no. 9, pp. 1319–1325, Sep. 2016, doi: 10.1093/NEUONC/NOW047.

[204] R. R. Mehta *et al.*, "A 28-amino-acid peptide fragment of the cupredoxin azurin prevents carcinogen-induced mouse mammary lesions," *Cancer Prev Res (Phila)*, vol. 3, no. 10, pp. 1351–1360, Oct. 2010, doi: 10.1158/1940-6207.CAPR-10-0024.

[205] M. A. Warso *et al.*, "A first-in-class, first-in-human, phase I trial of p28, a non-HDM2-mediated peptide inhibitor of p53 ubiquitination in patients with advanced solid tumours," *Br J Cancer*, vol. 108, no. 5, pp. 1061–1070, Mar. 2013, doi: 10.1038/BJC.2013.74.

[206] T. Yamada *et al.*, "A peptide fragment of azurin induces a p53-mediated cell cycle arrest in human breast cancer cells," *Mol Cancer Ther*, vol. 8, no. 10, pp. 2947–2958, Oct. 2009, doi: 10.1158/1535-7163.MCT-09-0444.

[207] B. N. Taylor *et al.*, "Noncationic peptides obtained from azurin preferentially enter cancer cells," *Cancer Res*, vol. 69, no. 2, pp. 537–546, Jan. 2009, doi: 10.1158/0008-5472.CAN-08-2932.

[208] F. Cantini, P. Gianni', P. Savarin, A. R. Bizzarri, and M. Sette, "Solution structure of the anticancer p28 peptide in biomimetic medium," *J Pept Sci*, vol. 27, no. 11, Nov. 2021, doi: 10.1002/PSC.3357.

[209] A. R. Bizzarri *et al.*, "Interaction of an anticancer peptide fragment of azurin with p53 and its isolated domains studied by atomic force spectroscopy," *Int J Nanomedicine*, vol. 6, no. 1, pp. 3011–3019, 2011, doi: 10.2147/IJN.S26155.

[210] T. Yamada *et al.*, "p28, A first in class peptide inhibitor of cop1 binding to p53," *Br J Cancer*, vol. 108, no. 12, p. 2495, Jun. 2013, doi: 10.1038/BJC.2013.266.

[211] T. Yamada *et al.*, "Apoptosis or growth arrest: Modulation of tumor suppressor p53's specificity by bacterial redox protein azurin," *Proc Natl Acad Sci U S A*, vol. 101, no. 14, pp. 4770–4775, Apr. 2004, doi: 10.1073/PNAS.0400899101.

[212] R. R. Mehta *et al.*, "A cell penetrating peptide derived from azurin inhibits angiogenesis and tumor growth by inhibiting phosphorylation of VEGFR-2, FAK and Akt," *Angiogenesis*, vol. 14, no. 3, pp. 355–369, Sep. 2011, doi: 10.1007/S10456-011-9220-6.

[213] T. Yamada, T. K. das Gupta, and C. W. Beattie, “p28-Mediated Activation of p53 in G2-M Phase of the Cell Cycle Enhances the Efficacy of DNA Damaging and Antimitotic Chemotherapy,” *Cancer Res*, vol. 76, no. 8, pp. 2354–2365, Apr. 2016, doi: 10.1158/0008-5472.CAN-15-2355.

[214] N. Bernardes *et al.*, “High-throughput molecular profiling of a P-cadherin overexpressing breast cancer model reveals new targets for the anti-cancer bacterial protein azurin,” *Int J Biochem Cell Biol*, vol. 50, no. 1, pp. 1–9, May 2014, doi: 10.1016/J.BIOCEL.2014.01.023.

[215] M. Goto *et al.*, “Image-guided surgery with a new tumour-targeting probe improves the identification of positive margins,” *EBioMedicine*, vol. 76, Feb. 2022, doi: 10.1016/J.EBIOM.2022.103850.

[216] A. R. Garizo *et al.*, “p28-functionalized PLGA nanoparticles loaded with gefitinib reduce tumor burden and metastases formation on lung cancer,” *J Control Release*, vol. 337, pp. 329–342, Sep. 2021, doi: 10.1016/J.JCONREL.2021.07.035.

[217] E. v. Batrakova and M. S. Kim, “Using exosomes, naturally-equipped nanocarriers, for drug delivery,” *J Control Release*, vol. 219, pp. 396–405, Dec. 2015, doi: 10.1016/J.JCONREL.2015.07.030.

[218] D. E. Murphy, O. G. de Jong, M. J. W. Evers, M. Nurazizah, R. M. Schiffelers, and P. Vader, “Natural or Synthetic RNA Delivery: A Stoichiometric Comparison of Extracellular Vesicles and Synthetic Nanoparticles,” *Nano Lett*, vol. 21, no. 4, pp. 1888–1895, 2021, doi: 10.1021/acs.nanolett.1c00094.

[219] C. Chakraborty, A. R. Sharma, G. Sharma, and S. S. Lee, “Therapeutic advances of miRNAs: A preclinical and clinical update,” *J Adv Res*, vol. 28, pp. 127–138, Feb. 2021, doi: 10.1016/J.JARE.2020.08.012.

[220] V. Wang and W. Wu, “MicroRNA-Based Therapeutics for Cancer.”

[221] M. Kang, V. Jordan, C. Blenkiron, and L. W. Chamley, “Biodistribution of extracellular vesicles following administration into animals: A systematic review,” *J Extracell Vesicles*, vol. 10, no. 8, Jun. 2021, doi: 10.1002/JEV2.12085.

[222] F. dos Santos, P. Z. Andrade, J. S. Boura, M. M. Abecasis, C. L. da Silva, and J. M. S. Cabral, “Ex vivo expansion of human mesenchymal stem cells: a more effective cell proliferation kinetics and metabolism under hypoxia,” *J Cell Physiol*, vol. 223, no. 1, pp. 27–35, Apr. 2010, doi: 10.1002/JCP.21987.

[223] A. Rutt, K. Bio, and J. J. Cadwell, “Clinical Scale Production and Wound Healing Activity of Human Adipose Derived Mesenchymal Stem Cell Extracellular Vesicles from a Hollow Fiber Bioreactor”.

[224] R. A. Haraszti *et al.*, “Exosomes Produced from 3D Cultures of MSCs by Tangential Flow Filtration Show Higher Yield and Improved Activity,” *Mol Ther*, vol. 26, no. 12, pp. 2838–2847, Dec. 2018, doi: 10.1016/J.YMTHE.2018.09.015.

[225] M. de Almeida Fuzeta *et al.*, “Scalable Production of Human Mesenchymal Stromal Cell-Derived Extracellular Vesicles Under Serum-/Xeno-Free Conditions in a Microcarrier-Based Bioreactor Culture System,” *Front Cell Dev Biol*, vol. 8, p. 553444, 2020, doi: 10.3389/fcell.2020.553444.

[226] M. de Almeida Fuzeta *et al.*, “Scalable Production of Human Mesenchymal Stromal Cell-Derived Extracellular Vesicles Under Serum-/Xeno-Free Conditions in a Microcarrier-Based Bioreactor Culture System,” *Front Cell Dev Biol*, vol. 8, Nov. 2020, doi: 10.3389/FCELL.2020.553444.

[227] S. I. van de Wakker *et al.*, “Influence of short term storage conditions, concentration methods and excipients on extracellular vesicle recovery and function,” *European Journal of Pharmaceutics and Biopharmaceutics*, vol. 170, pp. 59–69, Jan. 2022, doi: 10.1016/j.ejpb.2021.11.012.

[228] G. Vergauwen *et al.*, “Confounding factors of ultrafiltration and protein analysis in extracellular vesicle research”, doi: 10.1038/s41598-017-02599-y.

[229] K. J. Lee *et al.*, “Modulation of Nonspecific Binding in Ultrafiltration Protein Binding Studies,” *Pharmaceutical Research 2003 20:7*, vol. 20, no. 7, pp. 1015–1021, Jul. 2003, doi: 10.1023/A:1024406221962.

[230] D. Gupta, A. M. Zickler, and S. el Andaloussi, “Dosing extracellular vesicles,” *Adv Drug Deliv Rev*, vol. 178, p. 113961, Nov. 2021, doi: 10.1016/J.ADDR.2021.113961.

[231] N. Bernardes, S. Abreu, F. A. Carvalho, F. Fernandes, N. C. Santos, and A. M. Fialho, “Modulation of membrane properties of lung cancer cells by azurin enhances the sensitivity to EGFR-targeted therapy and decreased β1 integrin-mediated adhesion,” *Cell Cycle*, vol. 15, no. 11, p. 1415, Jun. 2016, doi: 10.1080/15384101.2016.1172147.

[232] T. Smyth *et al.*, “Surface functionalization of exosomes using click chemistry,” *Bioconjug Chem*, vol. 25, no. 10, pp. 1777–1784, Oct. 2014, doi: 10.1021/BC500291R/SUPPL_FILE/BC500291R_SI_001.PDF.

[233] W. Nan, C. Zhang, H. Wang, H. Chen, and S. Ji, “Direct Modification of Extracellular Vesicles and Its Applications for Cancer Therapy: A Mini-Review,” *Front Chem*, vol. 10, p. 538, May 2022, doi: 10.3389/FCHEM.2022.910341/BIBTEX.

[234] T. C. Pham *et al.*, “Covalent conjugation of extracellular vesicles with peptides and nanobodies for targeted therapeutic delivery,” *J Extracell Vesicles*, vol. 10, no. 4, p. e12057, Feb. 2021, doi: 10.1002/JEV2.12057.

[235] E. Lallana, E. Fernandez-Megia, and R. Riguera, “Surpassing the use of copper in the click functionalization of polymeric nanostructures: a strain-promoted approach,” *J Am Chem Soc*, vol. 131, no. 16, pp. 5748–5750, Apr. 2009, doi: 10.1021/JA8100243.

[236] S. A. A. Kooijmans, R. M. Schiffelers, N. Zarovni, and R. Vago, “Modulation of tissue tropism and biological activity of exosomes and other extracellular vesicles: New nanotools for cancer treatment,” *Pharmacol Res*, vol. 111, pp. 487–500, Sep. 2016, doi: 10.1016/J.PHRS.2016.07.006.

[237] C. P. Lai *et al.*, “Dynamic biodistribution of extracellular vesicles in vivo using a multimodal imaging reporter,” *ACS Nano*, vol. 8, no. 1, pp. 483–494, Jan. 2014, doi: 10.1021/NN404945R/SUPPL_FILE/NN404945R_SI_001.PDF.

[238] S. A. A. Kooijmans, J. J. J. M. Gitz-Francois, R. M. Schiffelers, and P. Vader, “Recombinant phosphatidylserine-binding nanobodies for targeting of extracellular vesicles to tumor cells: a plug-and-play approach,” *Nanoscale*, vol. 10, no. 5, pp. 2413–2426, Feb. 2018, doi: 10.1039/C7NR06966A.

[239] Z. Ye *et al.*, “Methotrexate-Loaded Extracellular Vesicles Functionalized with Therapeutic and Targeted Peptides for the Treatment of Glioblastoma Multiforme,” *ACS Appl Mater Interfaces*, vol. 10, no. 15, pp. 12341–12350, Apr. 2018, doi: 10.1021/ACSAMI.7B18135.

[240] J. P. Bost *et al.*, “Growth Media Conditions Influence the Secretion Route and Release Levels of Engineered Extracellular Vesicles,” *Adv Healthc Mater*, vol. 11, no. 5, Mar. 2022, doi: 10.1002/ADHM.202101658.

[241] J. Zhu *et al.*, “Myocardial reparative functions of exosomes from mesenchymal stem cells are enhanced by hypoxia treatment of the cells via transferring microRNA-210 in an nSMase2-dependent way,” *Artif Cells Nanomed Biotechnol*, vol. 46, no. 8, pp. 1659–1670, Nov. 2018, doi: 10.1080/21691401.2017.1388249.

[242] D. B. Patel, C. R. Luthers, M. J. Lerman, J. P. Fisher, and S. M. Jay, “Enhanced extracellular vesicle production and ethanol-mediated vascularization bioactivity via a 3D-printed scaffold-perfusion bioreactor system,” *Acta Biomater*, vol. 95, p. 236, Sep. 2019, doi: 10.1016/J.ACTBIO.2018.11.024.

[243] Y. Wen *et al.*, “Factors influencing the measurement of the secretion rate of extracellular vesicles,” *Analyst*, vol. 145, no. 17, pp. 5870–5877, Aug. 2020, doi: 10.1039/D0AN01199A.

[244] S. E. Headland, H. R. Jones, A. S. V. D’Sa, M. Perretti, and L. v. Norling, “Cutting-edge analysis of extracellular microparticles using ImageStream(X) imaging flow cytometry,” *Sci Rep*, vol. 4, Jun. 2014, doi: 10.1038/SREP05237.

[245] “Low particle media, RoosterCollect-EV, and RoosterCollect-EV-CC support a seamless transition from hMSC expansion to EV collection”.

[246] “Cell Number Total EV Production Cell Expan-sion Phase EV Collection Phase EXTRACELLULAR VESICLE (EV) PRODUCTION HIGH VOLUME hMSCs | BIOPROCESS MEDIA COLLECTION MEDIA & REAGENTS A Standardized System Drives Massive Yields. Tunable at Multiple Scales. REVOLUTIONIZING EXTRACELLULAR VESICLE PRODUCTION Transition from hMSC expansion to dependable EV collection During collection, EV Boost crosses you over to the Boost Zone TM”, Accessed: Oct. 22, 2022. [Online]. Available: www.roosterbio.com.

[247] S. A. A. Kooijmans, R. M. Schiffelers, N. Zarovni, and R. Vago, “Modulation of tissue tropism and biological activity of exosomes and other extracellular vesicles: New nanotools for cancer treatment,” *Pharmacol Res*, vol. 111, pp. 487–500, Sep. 2016, doi: 10.1016/J.PHRS.2016.07.006.

[248] T. Liangsupree, E. Multia, and M. L. Riekkola, “Modern isolation and separation techniques for extracellular vesicles,” *J Chromatogr A*, vol. 1636, p. 461773, Jan. 2021, doi: 10.1016/J.CHROMA.2020.461773.

[249] S. Bosch *et al.*, “Trehalose prevents aggregation of exosomes and cryodamage,” *Scientific Reports 2016 6:1*, vol. 6, no. 1, pp. 1–11, Nov. 2016, doi: 10.1038/srep36162.

6. Supplementary material

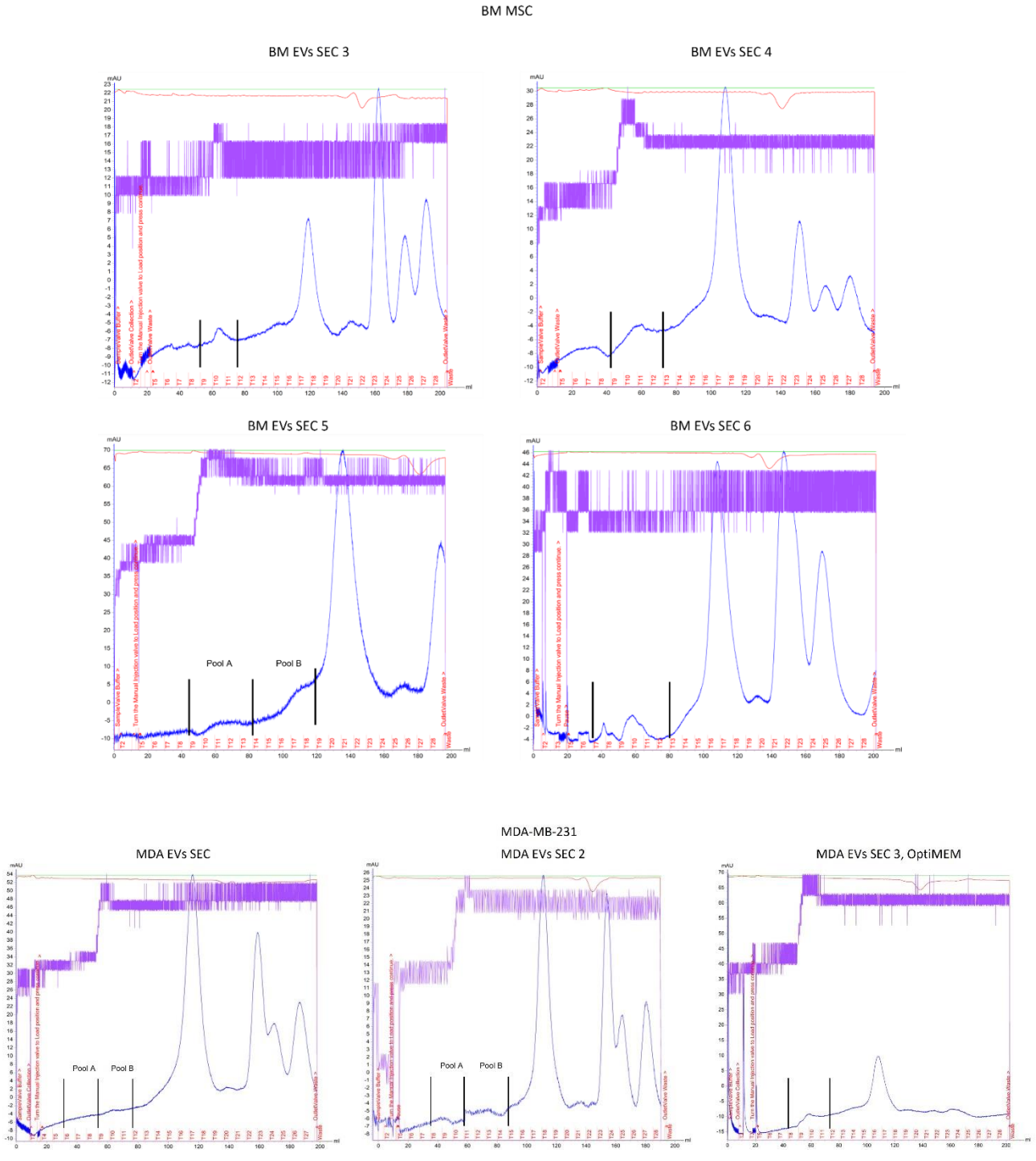

Supplementary figure 1 - MSC-EV and MDA-MB-231 derived EVs isolation chromatograms. Fractionation of the TFF concentrated cell conditioning medium of MSC(BM), MDA-MB-231. The ultraviolet light of wavelength 280 nm (UV280) (blue line) was measured in the eluent. The y-axis represents the UV280 absorbance in milli-absorbance units and the x-axis represents the volume eluted through the column since the start of the sample elution. The fractions of the first UV280 peak area

contain EVs, whereas smaller constituents of the cell conditioning medium, such as contaminating proteins are contained in later fractions. The two vertical lines indicate the fractions that were collected. When two intervals of fractions, pool A and pool B are displayed both were collected, however, in all cases, only one of those fractions was maintained for labelling and functionalization. BM EVs SEC - Pool A, MDA EVs SEC 1, and MDA EVs SEC 3 - Pool B. The purple line indicates the pressure of the system.

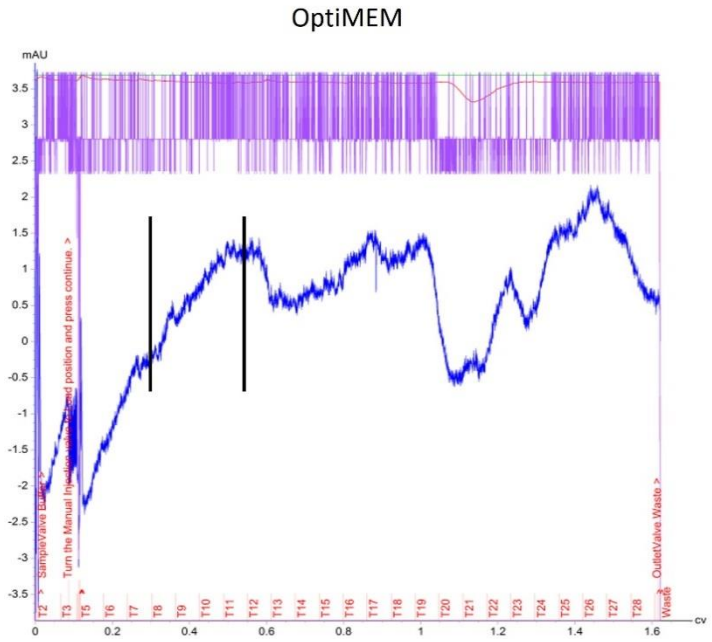

Supplementary Figure 2 - TFF concentrated OptiMEM chromatogram. The ultraviolet light of wavelength 280 nm (UV280) (blue line) was measured in the eluent. The two vertical lines indicate the fractions that were collected And, the purple line indicates the pressure. The y-axis represents the UV280 absorbance in milli-absorbance units and the x-axis represents the volume eluted through the column since the start of the sample elution.

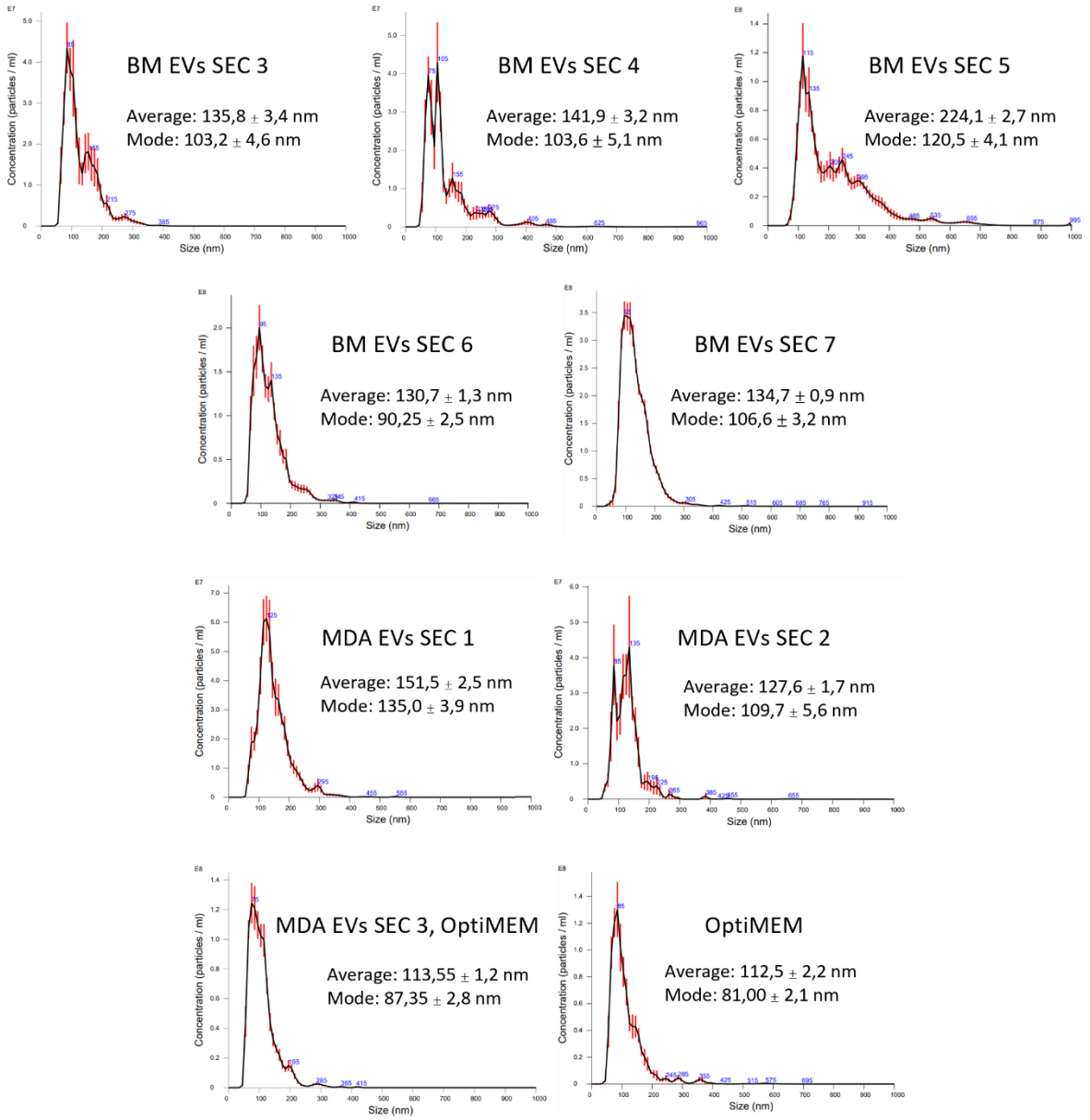

Supplementary figure 3 - NTA size distribution curves, average and mode of the size of TFF and SEC processed MSC(BM)-EVs, MDA-MB-231 derived EVs, and OptiMEM isolated particles.

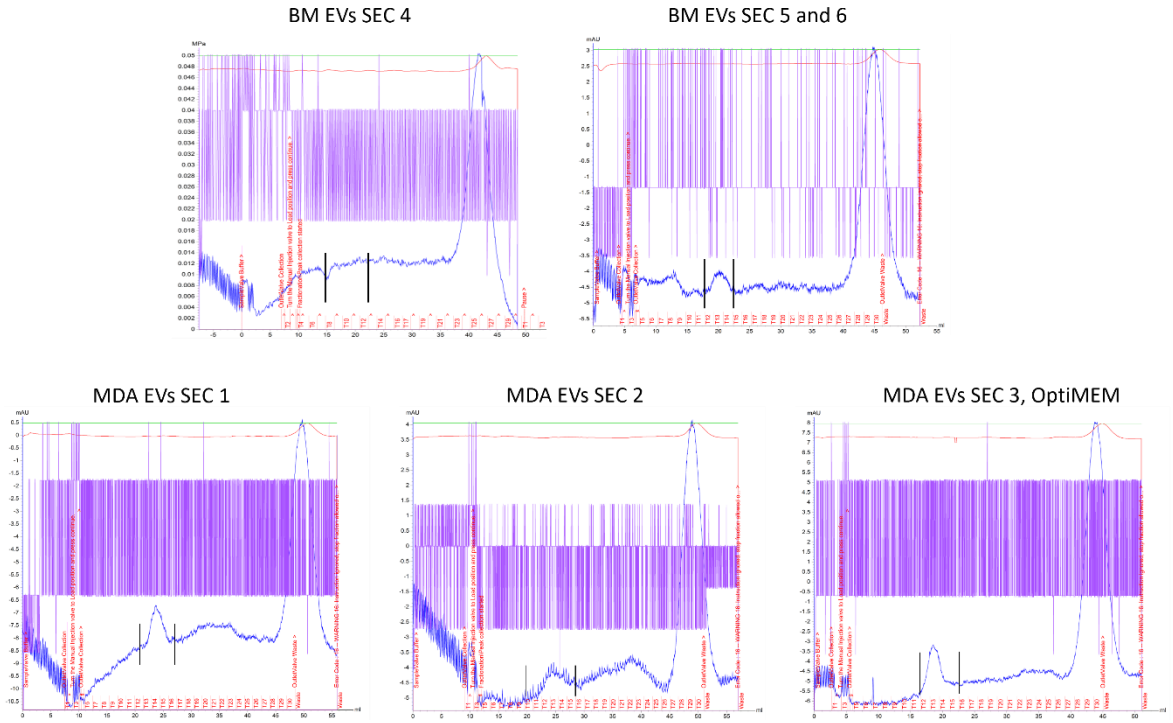

Supplementary figure 4 - Chormathograms referent to the separation of the unbound dye (Alexa Fluor™ 647 NHS Ester) and EVs, derived from MSC(BM) and MDA-MB-231. Fractionation of the labeled EVs. The ultraviolet light of wavelength 280 nm (UV280) (blue line) was measured in the eluent. The y-axis represents the UV280 absorbance in milli-absorbance units and the x-axis represents the volume eluted through the column since the start of the sample elution. The fractions of the first peak area contain EVs, whereas the second peak signals the fractions where the unbound dye (Alexa Fluor™ 647 NHS Ester) is being eluted. The two vertical lines indicate the fractions that were collected And, the purple line indicates the pressure.

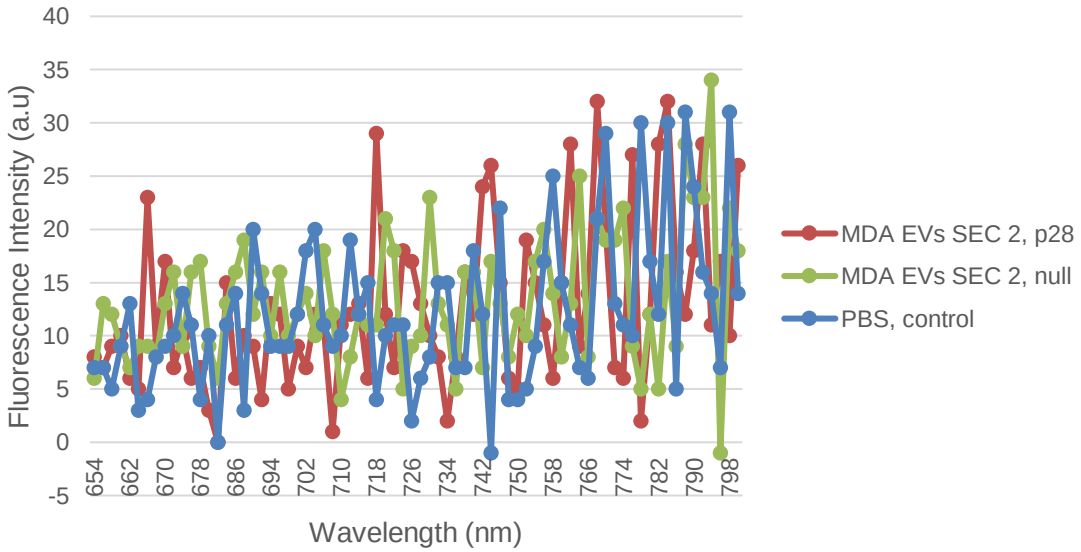

Supplementary figure 5 - CP05-p28 functionalized MDA-MB-231 derived EVs emission scan. Emission scans (excitation wavelength of 620 nm) of functionalized and non-functionalized EVs in a batch where no significant fluorescence was displayed by EVs in comparison with the negative control, PBS.

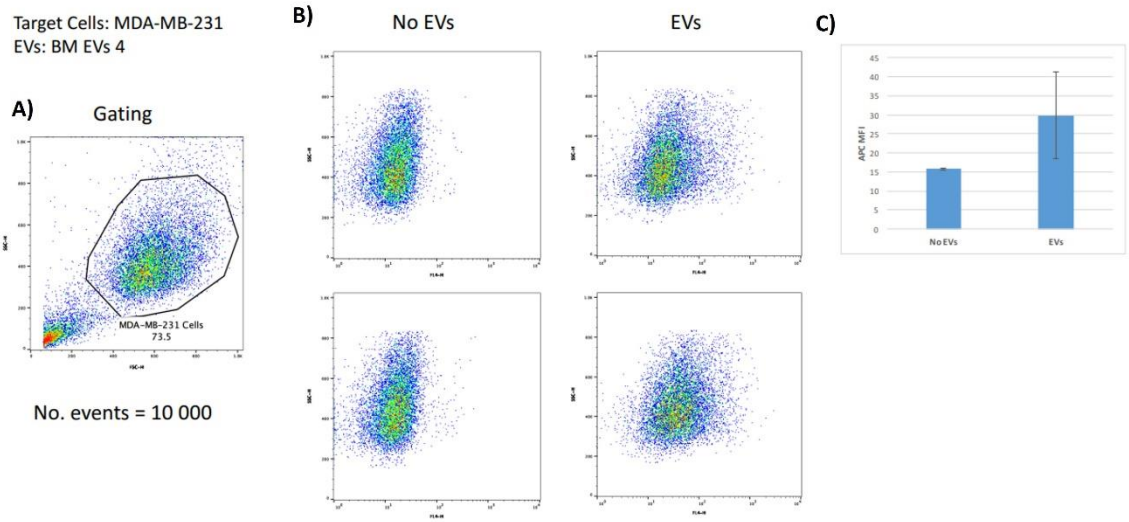

Supplementary figure 6 - Flow cytometry analysis of the MSC-EVs uptake by breast cancer cells (EV uptake 1). A) Cell gating, the x-axis represents the forward scatter and the y-axis represents the side scatter **B)** Comparison of flow cytometry analysis of the EV uptake by breast cancer cells among the different conditions, i.e., when no EVs and non-functionalized EVs (EVs) were administered to cells, the x-axis represents the EV florescence height and the y-axis represents the side scatter. **C)** Median fluorescence intensity (MFI) of flow cytometry (n=2, technical replicates).

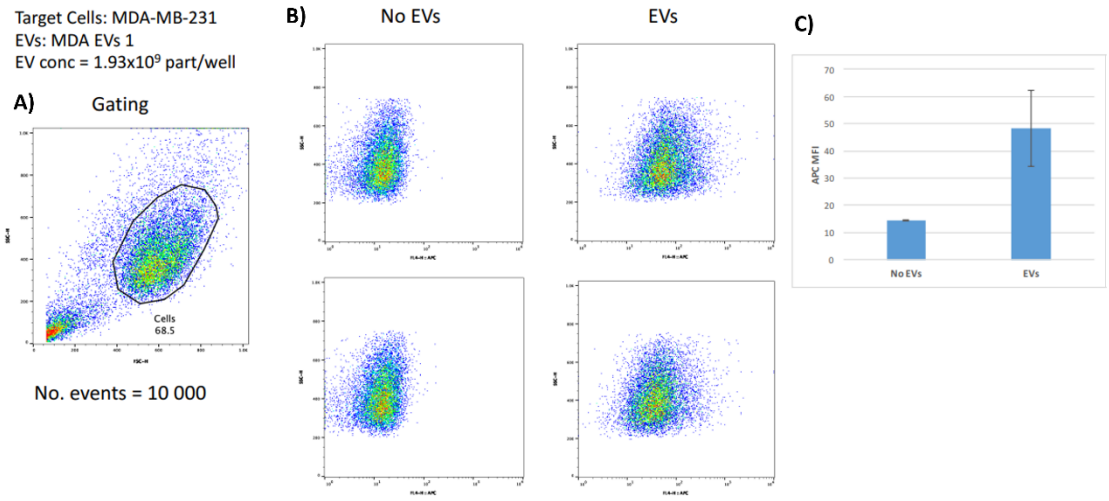

Supplementary figure 7 - Flow cytometry analysis of the MDA-MB-231 derived EVs uptake by breast cancer cells (EV uptake 2). A) Cell gating, the x-axis represents the forward scatter and the y-axis represents the side scatter **B)** Comparison of flow cytometry analysis of the EV uptake by breast cancer cells among the different conditions, i.e., when no EVs and non-functionalized EVs (EVs) were administered to cells, the x-axis represents the EV florescence height and the y-axis represents the side scatter. **C)** Median fluorescence intensity (MFI) of flow cytometry (n=2, technical replicates).

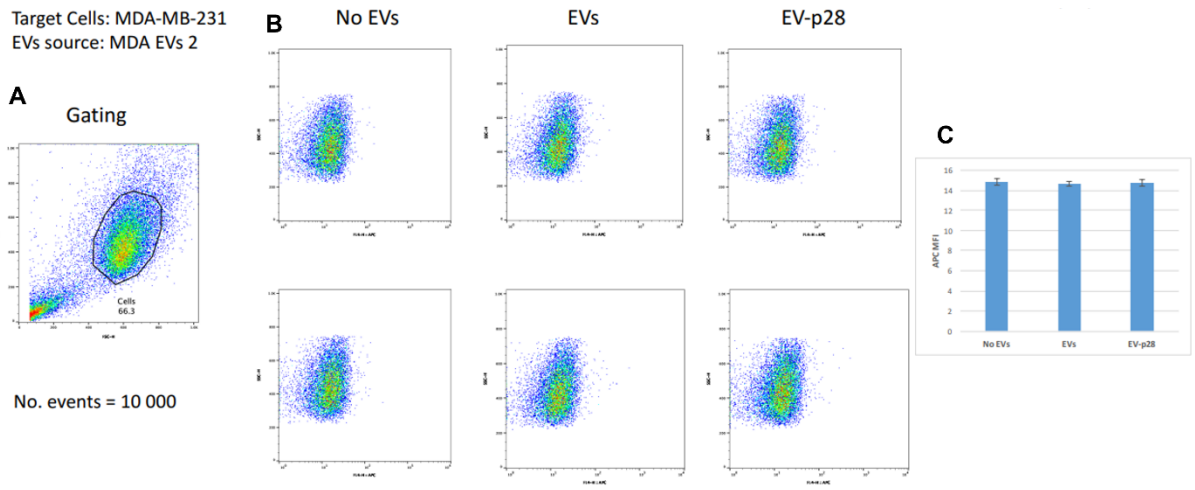

Supplementary figure 8 - Flow cytometry analysis of CP05-p28 functionalized MDA-MB-231 derived EVs uptake by breast cancer cells (EV uptake 3). A) Cell gating, the x-axis represents the forward scatter and the y-axis represents the side scatter **B)** Comparison of flow cytometry analysis of the EV uptake by breast cancer cells among the different conditions, i.e., when no EVs, as well as, CP05-p28 functionalized EVs and non-functionalized EVs (EVs) were administered to cells, the x-axis represents the EV florescence height and the y-axis represents the side scatter. **C)** Median fluorescence intensity (MFI) of flow cytometry (n=2, technical replicates, for no EVs, n=1 for EVs and EVs-p28).

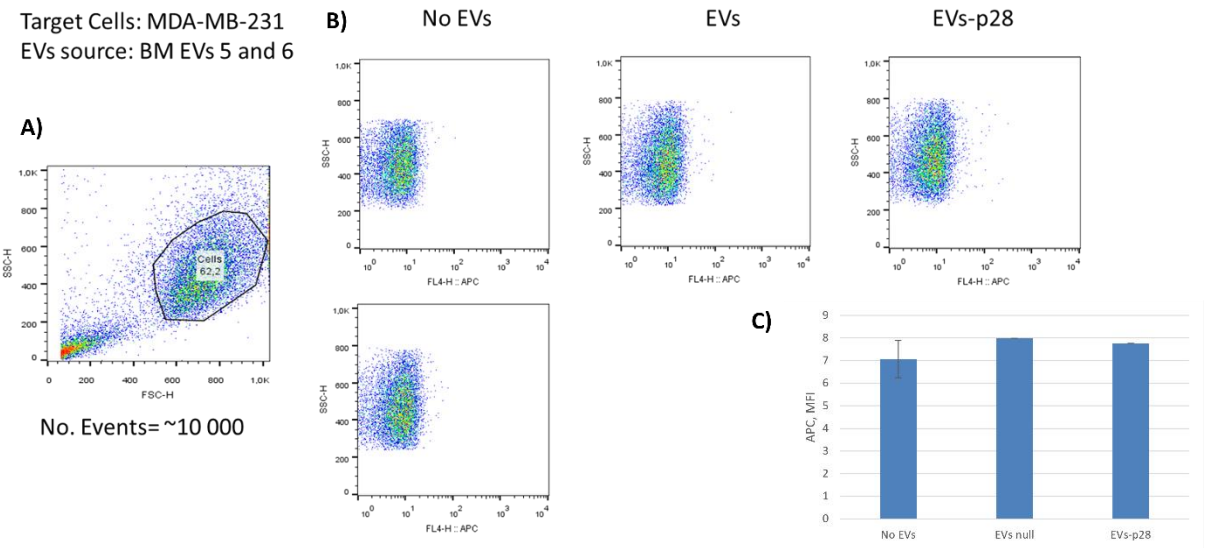

Supplementary figure 9 - Flow cytometry analysis of CP05-p28 functionalized MSC-EVs uptake by breast cancer cells (EV uptake 5). A) Cell gating, the x-axis represents the forward scatter and the y-axis represents the side scatter **B)** Comparison of flow cytometry analysis of the EV uptake by breast cancer cells among the different conditions, i.e., when no EVs, as well as, CP05-p28 functionalized EVs and non-functionalized EVs (EVs) were administered to cells, the x-axis represents the EV florescence height and the y-axis represents the side scatter. **C)** Median fluorescence intensity (MFI) of flow cytometry (n=2, technical replicates, for no EVs, n=1 for EVs and EVs-p28).